AD-A167 672 CORRELATION OF NONDESTRUCTIVE PAVEMENT EVALUATION TEST RESULTS WITH RESUL..(U) ARMY ENGINEER WATERWAYS EXPERIMENT STATION VICKSBURG MS GEOTE.. D R ALEXANDER 1/2

UNCLASSIFIED FEB 86 WES/TR/GL-86-1-VOL-1 F/G 14/2 NL

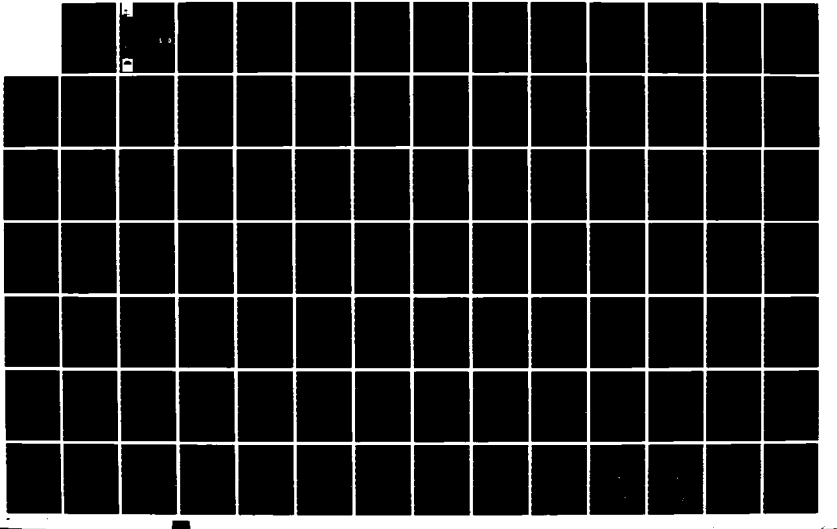

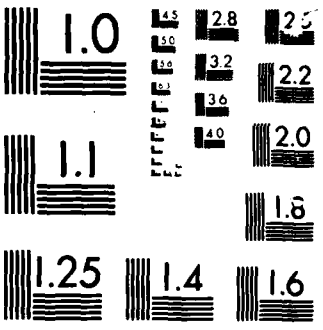

MICROCOPY CHART

US Army Corps of Engineers

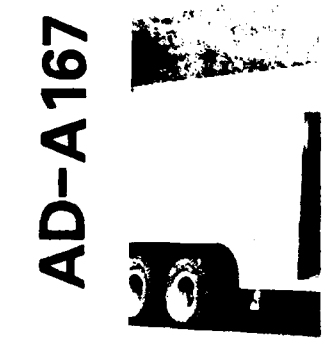

GEOTECHNICAL LABORATORY

TECHNICAL REPORT GL-86-1

CORRELATION OF NONDESTRUCTIVE PAVEMENT EVALUATION TEST RESULTS WITH RESULTS OF CONVENTIONAL QUALITY CONTROL AND IN-SITU STRENGTH TESTS ON AN MX ROAD TEST SECTION

VOLUME I: MAIN TEXT

by

Don R. Alexander

Geotechnical Laboratory

DEPARTMENT OF THE ARMY
Waterways Experiment Station, Corps of Engineers
PO Box 631, Vicksburg, Mississippi 39180-0631

February 1986
Final Report

Prepared for

DEPARTMENT OF THE ARMY
US Army Corps of Engineers
Washington, DC 20314-1000

Unclassified

SECURITY CLASSIFICATION OF THIS PAGE *(When Data Entered)*

REPORT DOCUMENTATION PAGE

READ INSTRUCTIONS BEFORE COMPLETING FORM

1. REPORT NUMBER Technical Report GL-86-1	2. GOVT ACCESSION NO.
3. RECIPIENT'S CATALOG NUMBER	
4. TITLE *(and Subtitle)* CORRELATION OF NONDESTRUCTIVE PAVEMENT EVALUATION TEST RESULTS WITH RESULTS OF CONVENTIONAL QUALITY CONTROL AND IN-SITU STRENGTH TESTS ON AN MX ROAD TEST SECTION; VOLUME I: MAIN TEXT	
5. TYPE OF REPORT & PERIOD COVERED Final report (in two volumes)	
6. PERFORMING ORG. REPORT NUMBER	
7. AUTHOR(s) Don R. Alexander	
8. CONTRACT OR GRANT NUMBER(s)	
9. PERFORMING ORGANIZATION NAME AND ADDRESS US Army Engineer Waterways Experiment Station Geotechnical Laboratory PO Box 631, Vicksburg, Mississippi 39180-0631	
10. PROGRAM ELEMENT, PROJECT, TASK AREA & WORK UNIT NUMBERS	
11. CONTROLLING OFFICE NAME AND ADDRESS DEPARTMENT OF THE ARMY US Army Corps of Engineers Washington, DC 20314-1000	
12. REPORT DATE February 1986	
13. NUMBER OF PAGES Volume I--143, Volume II--468	
14. MONITORING AGENCY NAME & ADDRESS *(if different from Controlling Office)*	
15. SECURITY CLASS. *(of this report)* Unclassified	
15a. DECLASSIFICATION/DOWNGRADING SCHEDULE	

16. DISTRIBUTION STATEMENT *(of this Report)*

Approved for public release; distribution unlimited.

17. DISTRIBUTION STATEMENT *(of the abstract entered in Block 20, if different from Report)*

18. SUPPLEMENTARY NOTES

Appendix A is published separately in Volume II. Both volumes are available from National Technical Information Service, 5285 Port Royal Road, Springfield, Virginia 22161.

19. KEY WORDS *(Continue on reverse side if necessary and identify by block number)*

20. ABSTRACT *(Continue on reverse side if necessary and identify by block number)*

An investigation was performed to develop and study relationships between nondestructive test (NDT) results and various pavement parameters such as layer thickness, density, and strength. The use of NDT devices has proven viable for evaluation of conventionally designed rigid and flexible pavements and is seen as a great advance over costly and time-consuming destructive evaluation techniques. These same principles can perhaps be effectively applied to include the evaluation of in-situ soil conditions, unsurfaced design or design verification, and construction quality control. Data for this study were obtained during the construction and traffic testing of a test section built for the purpose of obtaining data to validate and possibly reduce present criteria or develop new criteria for design of roads subjected to the heavy wheel loads associated with a proposed MX missile transporter.

(Continued)

DD FORM 1 JAN 73 1473 EDITION OF 1 NOV 65 IS OBSOLETE

Unclassified

SECURITY CLASSIFICATION OF THIS PAGE *(When Data Entered)*

20. ABSTRACT (Continued).

The test section measured 250 ft long by 50 ft wide by 6 ft deep and consisted of three traffic lanes with five items per lane. Materials used in constructing the test section included limestone, buckshot clay, silt, Blend I, and Blend II. The blended soils were put together at the Waterways Experiment Station (WES) to simulate gradations anticipated in the proposed construction area.

Types of surfacing included unsurfaced blended soils, crushed limestone and silt, cement-stabilized blended soils, lean mix concrete batched from blended soil, and single- and double-bituminous surface treatments.

Soil instrumentation was provided in three items for measurement of vertical deflection, vertical stress, and pore pressures.

Nondestructive tests were performed during construction and traffic with the WES 16-kip vibrator, a Dynatest falling weight deflectometer, and a Road Rater 2008.

The test section was trafficked with a two-wheel (single tandem) load cart representing two axles of the transporter. A total of 2,600 load cart passes were applied to each lane.

Due to inherent limitations of the data set, results of this study were inconclusive with respect to the feasibility of NDT for pavement construction quality control and design verification. However, some useful direct comparisons between NDT results and conventional test parameters were obtained. A brief summary of the significant findings is as follows:

a. Dynamic stiffness modulus (DSM) versus thickness relationships can be determined for any soil type, and a limiting stiffness for each material does exist. Once sufficient thickness has been added to achieve this limiting value, no change in DSM can be realized by further addition of the same quality material.

b. DSM, although a function of thickness as well as strength, is a potentially good indicator of inplace strength with respect to performance; it is perhaps better than the conventional California Bearing Ratio (CBR) test.

c. Good correlation was observed between in-place density and surface DSM, layer thickness, and subgrade DSM.

d. Efforts to directly correlate NDT test results to the conventional strength parameters of CBR and k were relatively unsuccessful.

e. It was determined statistically that high levels of confidence can be achieved for the 16-kip vibrator and falling weight deflectometer test results by performing a reasonable number of tests.

f. Modulus values computed using the layered elastic computer program BISDEF and WES 16-kip vibrator deflection data appeared reasonable for subsurface layers and surface layers greater than about 15 in. thick and compared relatively well with laboratory resilient modulus test results.

g. Favorable comparison was observed between vertical displacements measured by linear variable differential transformer gages installed in the test section and deflections predicted using layered elastic theory (computer programs BISAR and BISDEF) and falling weight deflectometer surface deflection data.

h. It was not determined how or to what extent NDT test results would be affected by the approach of failure, and very little performance data were gained since traffic on the test section was stopped after 2,600 passes.

i. Relatively good correlation was found to exist between 16 kip and falling weight deflectometer DSM's.

PREFACE

The investigation of nondestructive test results and their potential applicability to pavement design and construction quality control described in this report was sponsored by the Office, Chief of Engineers, US Army, under the Operations and Maintenance, Army (O&MA) program. The data used in this investigation were obtained under another program, MX Road Design Criteria Studies, sponsored by the US Air Force Ballistics Missile Office (BMO), Air Force Regional Civil Engineer (AFRCE-MX), Norton Air Force Base, Calif.

The fieldwork was conducted at the US Army Engineer Waterways Experiment Station (WES) during the period March 1980 to July 1981. Mr. D. R. Alexander, Pavement Systems Division (PSD), Geotechnical Laboratory (GL), WES, was the engineer directing the field testing. Laboratory testing was performed under the supervision of Mr. J. C. Oldham, Chief, Soils Testing Facility, WES.

Personnel of the PSD, WES, actively engaged in the planning and execution of the work that led to the preparation of this report were Messrs. J. W. Hall, Jr., R. W. Grau, and D. R. Alexander. The project was under the general supervision of Mr. A. H. Joseph, Chief, PSD (Retired), Dr. T. D. White, Former Chief, PSD, Mr. H. H. Ulery, Jr., Chief, PSD, and Dr. W. F. Marcuson III, Chief, GL. This report was prepared by Mr. Alexander. Ms. Odell F. Allen Publications and Graphic Arts Division, edited this report.

COL Allen F. Grum, USA, was Director of WES during the preparation and publication of this report. Dr. Robert W. Whalin was Technical Director.

CONTENTS

* Published separately in Volume II.

LIST OF TABLES

* Main text tables are grouped following the last page of main text and Appendix A tables are grouped after the last page of the appendix.

LIST OF FIGURES

*Figures in the main text are grouped after the main text tables.

LIST OF PHOTOS

* Photographs in the appendix are grouped following the last page of appendix tables.

Photo No.	
A35	Model 2008 Road Rater
A36	Falling Weight Deflectometer
A37	MX test vehicle (modified prime mover, test wheels loaded to 62,500 lb)
A38	MX test vehicle (shown from behind)
A39	Side-view of tires used on the MX load cart
A40	Smooth tires used on the MX load cart
A41	Lane 1, Item 1, before traffic (0 passes)
A42	Lane 1, Item 1, after 326 passes
A43	Lane 1, Item 1, after 2,600 passes
A44	Lane 1, Item 2, before traffic (0 passes)
A45	Lane 1, Item 2, after 326 passes
A46	Lane 1, Item 2, after 2,600 passes
A47	Lane 1, Item 3, before traffic (0 passes)
A48	Lane 1, Item 3, after 326 passes
A49	Lane 1, Item 3, after 2,600 passes
A50	Lane 1, Item 4, before traffic (0 passes)
A51	Lane 1, Item 4, after 326 passes
A52	Lane 1, Item 4, after 2,600 passes
A53	Lane 1, Item 5, before traffic (0 passes)
A54	Lane 1, Item 5, after 326 passes
A55	Lane 1, Item 5, after 2,600 passes
A56	Lane 2, Item 1, before traffic (0 passes)
A57	Lane 2, Item 1, after 326 passes
A58	Lane 2, Item 1, after 2,600 passes
A59	Close-up of surface, lane 2, Item 1, after 2,600 passes
A60	Lane 2, Item 1, after 2,600 passes (loose material removed from the surface)
A61	Vertical cut through 29 in. of cement stabilized Blend I (lane 2, Item 1)
A62	Lane 2, Item 2, before traffic (0 passes)
A63	Close-up of surface, lane 2, Item 2, after 1,300 passes
A64	Lane 2, Item 2, after 2,600 passes
A65	Close-up of surface, lane 2, Item 2, after 2,600 passes
A66	Lane 2, Item 2, after 2,600 passes (loose material removed from the surface)
A67	Lane 2, Item 3, before traffic (0 passes)
A68	Lane 2, Item 3, after 326 passes
A69	Lane 2, Item 3, after 2,600 passes
A70	Close-up of surface, lane 2, Item 3, after 2,600 passes
A71	Lane 2, Item 3, after 2,600 passes (loose material removed from the surface)
A72	Lane 2, Item 4, before traffic (0 passes)
A73	Lane 2, Item 4, after 326 passes
A74	Lane 2, Item 4, after 2,600 passes
A75	Close-up of surface, lane 2, Item 4, after 2,600 passes

Photo No.	
A76	Lane 2, Item 4, after 2,600 passes (loose material removed from the surface)
A77	Lane 2, Item 5, before traffic (0 passes)
A78	Lane 2, Item 5, after 326 passes
A79	Lane 2, Item 5, after 2,600 passes
A80	Close-up of surface, lane 2, Item 5, after 2,600 passes
A81	Lane 2, Item 5, after 2,600 passes (loose material removed from the surface)
A82	Lane 3, Item 1, before traffic (0 passes)
A83	Lane 3, Item 1, after 326 passes
A84	Lane 3, Item 1, after 2,600 passes
A85	Lane 3, Item 2, before traffic (0 passes)
A86	Lane 3, Item 2, after 326 passes
A87	Lane 3, Item 2, after 2,600 passes
A88	Lane 3, Item 3, before traffic (0 passes)
A89	Lane 3, Item 3, after 326 passes
A90	Lane 3, Item 3, after 2,600 passes
A91	Lane 3, Item 4, before traffic (0 passes)
A92	Lane 3, Item 4, after 326 passes
A93	Lane 3, Item 4, after 2,600 passes
A94	Portion of single-bituminous surface treatment removed after 2,600 passes
A95	Lane 3, Item 5, before traffic (0 passes)
A96	Lane 3, Item 5, after 326 passes
A97	Lane 3, Item 5, after 2,600 passes

CONVERSION FACTORS, NON-SI TO SI (METRIC)
UNITS OF MEASUREMENT

Non-SI units of measurement used in this report can be converted to SI (metric) units as follows:

Multiply	By	To Obtain
feet	0.3048	metres
feet per second	0.3048	metres per second
gallons (US liquid)	3.785412	cubic decimetres
gallons per square yard	4.5273	cubic decimeter per square metres
inches	2.54	centimetres
kips (mass)	4,448.222	newtons
kips (force) per inch	175.1268	kilonewtons per metres
miles (international) per hour	1.609344	kilometres per hour
miles (US statute)	1.609347	kilometres
pounds (force)	4.448222	newtons
pounds (mass)	0.4535924	kilograms
pounds (mass) per cubic foot	16.01846	kilograms per cubic metre
pounds (mass) per cubic inch	27,679.9	kilograms per cubic metre
pounds per cubic yard	0.5932764	kilograms per cubic metre
pounds (force) per foot	14.59390	newtons per metre
pounds per square foot	4.882428	kilograms per square metre
pounds (force) per square inch	6,894.757	pascals
square inches	6.4516	square centimetres
ton (2,000 pounds, mass)	907.1847	kilograms

CORRELATION OF NONDESTRUCTIVE PAVEMENT EVALUATION TEST RESULTS WITH RESULTS OF CONVENTIONAL QUALITY CONTROL AND IN-SITU STRENGTH TESTS ON AN MX ROAD TEST SECTION

VOLUME I: MAIN TEXT

PART I: INTRODUCTION

Background

1. Nondestructive testing (NDT) devices and evaluation systems are presently being used extensively throughout the United States and abroad to analyze the load-carrying capability of existing airfield and roadway pavements. The use of NDT is a great advancement over costly and time-consuming destructive evaluation techniques. However, these same principles have not been effectively applied to other areas of pavement technology. The use of NDT may be expanded to include the evaluation of in-situ soil conditions with respect to construction quality control and pavement design verification. A pilot study (Hall 1978) performed at the US Army Engineer Waterways Experiment Station (WES) indicated that it might be possible to relate NDT results to such soil characteristics as density and strength.

2. In pavement construction, conventional tests for strength generally consist of the California Bearing Ratio (CBR) or plate bearing (subgrade k modulus). These tests are time-consuming, particularly the plate bearing test which requires from 4 to 8 hr per test. Because of the time required to determine the CBR or k of a pavement layer, the quality of pavement layers is generally judged based on in-place moisture and density determinations made during construction. Guide specification for military construction specifies the sand-displacement method for density determinations and the oven-dry method for moisture determinations. These tests are also time-consuming and result in delays in construction because of interference at the work site during the conduct of tests and waiting time for oven drying. Nuclear devices, which are much faster and give immediate moisture and density test results, have become more acceptable but are still commonly used only in support of tests with the conventional methods. Uniformity of compaction (location of weak spots) is often done with heavily loaded proof rollers. A need exists

for a rapid nondestructive technique that has the capability of assessing the in-place parameters of strength, density, and uniformity with a reasonably high level of confidence. It was known from the beginning that the vertical deflection under cyclic or impact load of a 12- to 18-in.*-diam plate on a layered elastic system was a function of the shear moduli, Poisson's ratios, and densities of layers down to several plate diameters with the shear moduli having the strongest influence. It was hoped that in real materials the surface layer would have a dominant influence; although it was recognized that in stiff materials this might not be the case. It was further recognized that at least weak correlation existed between shear modulus and shear strength. Hence, there was a chance, although not a large one, of finding useful correlations between NDT stiffnesses and parameters of direct interest in pavement system layer quality.

Purpose

3. The purposes of this study were to (a) preserve the data collected during the construction and trafficking of a major test section built in support of the MX program at WES and (b) develop and study relationships between extensive NDT test results obtained in this program and various parameters such as thickness, density, and strength in an effort to determine if nondestructive techniques are feasible for pavement design verification and/or quality control of pavement base and subgrade construction.

Scope

4. Data used in this study were collected in conjunction with a study performed by WES for the Air Force concerning the MX Road System. The original scope of work for the MX Road program included the construction of two large test beds at WES. The first of these test beds was designed to investigate the effects of prototype traffic on various thicknesses of high quality crushed limestone and on various soils considered to be representative of those found over much of the proposed deployment area. Performance of various

---

* A table of factors for converting non-SI units of measurement to SI (metric) units is presented on page 13.

surfacings and cover requirements for buried pipes were also to be examined. The second test bed was to be specifically designed for fine-tuning thickness requirements and determining relationships between NDT results and material properties to be used for the development of rapid quality control techniques. The deployment concept was cancelled in October 1981 as a result of a Presidential decision to consider other basing modes. As a result, the MX Road study was terminated before construction of the second test bed, and a large amount of data that would have been extremely beneficial to this study was never collected. Only data from the first test bed are presented in this report. Appendix A includes the construction and traffic data for this test section.

5. Testing and data collection during construction and trafficking of the test bed included NDT (using the WES 16-kip vibrator, a Dynatest Model 8000 Falling Weight Deflectometer, and a Model 2008 Road Rater) and in-place moisture content, density, and CBR measurements on each lift. After completion of the test bed, plate bearing tests were performed on selected items to determine the modulus of soil reaction, k. Test pits were excavated (full depth) both before and after the application of traffic to verify the moisture content, density, and CBR measurements. The NDT, density, thickness, and CBR data will be examined in this report to determine whether useful correlations exist between (a) one NDT test and another and (b) NDT and conventional tests.

PART II: ANALYSIS OF NONDESTRUCTIVE TEST DATA

General

6. The test section described in Appendix A* provided a source of NDT, density, and strength data for a variety of soil types and conditions. Design requirements of low densities, water contents, and strengths resulted in most of the materials being placed dry of optimum moisture content. This and the fact that each material was essentially tested under only one set of conditions (one point on a curve) tend to complicate as well as limit the evaluation of the use of NDT data as a means of quality control. Even though the test section was not specifically designed to yield the complete spectrum of desired information, much useful data were obtained, and relationships between NDT and such parameters as thickness, strength, and density are quite promising.

7. Reallizing inherent limitations of the data set, the intent of this analysis is to focus on basic relationships between NDT and material characteristics, evaluate the reliability of NDT results versus conventional test parameters, and make recommendations for further research. The following elements are discussed with respect to their applicability to pavement construction quality control and field design verification:

a. Development of basic strength-thickness relationships.

b. Direct correlation of NDT results to conventional test parameters (CBR, k , and density).

c. Linear regression using NDT to predict CBR and density.

d. Variation/reliability of NDT results compared to conventional test parameters.

e. Computation of modulus of elasticity (E) using deflection basin data and layered elastic theory.

f. Comparison of predicted deflections to measured deflections at depth.

g. NDT test results during traffic.

h. Correlation between NDT test devices.

Strength-Thickness Relationships

8. The primary NDT parameter to be discussed in this report is the

* Published separately in Volume II.

dynamic stiffness modulus (DSM). DSM is defined for the WES 16-kip vibrator as the slope of the load-deflection curve with units of kips/inch. Road Rater DSM's were obtained by computing the slope of the load-deflection curve defined by deflections at the center of the load plate corresponding to force levels of 5,000 and 7,000 lb. Falling weight deflectometer stiffness values were determined by dividing the force obtained using the maximum drop height (approximately 14,000 lb) by the corresponding deflection measured at the center of the load plate. This information and detailed descriptions of each test device are included in Appendix A. DSM (stiffness) values recorded on each lift (layer) of material during construction of the test section are shown in Figures 1 through 15 for each of the 15 test items. Lift thicknesses were generally 6 to 8 in., and DSM's shown on the plots are an average of two measurements obtained in each item. The plots clearly show how adding thickness to materials of various qualities affects the stiffness of the soil system. With thickness being the only variable, observed rate of change in DSM is, as expected, much greater for higher quality materials such as crushed limestone and cement-stabilized soils. A change in DSM of the poorer materials is much more subtle, but still pronounced, and the tendency is to reach a maximum or minimum value after which little, if any, contribution to the stiffness of the system is realized by adding thickness of the same quality material.

9. DSM data obtained during construction with the WES 16-kip vibrator were chosen for some additional analyses. DSM's plotted in Figure 16 versus actual thicknesses show relative stiffnesses for each of the materials tested. The plot also indicates strong trends for the buckshot, silt, and Blend II materials for which the largest number of data points are available and the widest range of thicknesses evaluated. Best-fit curves are shown plotted with the data in Figure 17. The third-order polynomials determined for each are summarized below along with their standard error and correlation coefficients.

Material	Equation	Standard Error of Estimate	R	R^2
Buckshot Clay	DSM = 220.98745 + 0.10403253(t) - 0.43802507E - 01(t^2) - 0.76039883E - 05(t^3)	14.2	0.90	0.81

(Continued)

Material	Equation	Standard Error of Estimate	R	R^2
Blend II (Sandy Gravel)	DSM = 249.71710 + 7.8048367(t) + 0.10277720E - 01(t^2) - 0.50704821E - 03(t^3)	20.5	0.99	0.98
Silt	DSM = 236.75370 + 4.0658459(t) + 0.20410270E - 01(t^2) - 0.50349427E - 03(t^3)	24.2	0.95	0.90

Best-fit relationships are included with the corresponding data in Figure 18 for the crushed stone and cement-stabilized materials realizing that the thinner layers and small number of data points can only indicate relative trends. Based on a strong correlation for heavy clay (CH), Blend II, and silt (ML) soils, the concept of a limiting DSM can be introduced. The capability of defining a maximum or limiting DSM for a particular material would be significant in the areas of quality control and design verification. For instance, the best-fit DSM versus thickness curves for Blend II and silt can be continuously shifted as shown in Figures 19 and 20 such that for any given initial DSM the thickness required to reach a maximum value of stiffness can be readily obtained. Conversely, from a quality control standpoint, required DSM values for each lift of a particular material to be placed can be determined for a known initial stiffness (assuming that a curve such as those shown in Figures 19 and 20 is available). NDT on a finished lift would rapidly yield DSM's that could be compared with required DSM's from the curve to evaluate the structural adequacy of the layer. Thus, even though defining DSM as a function of thickness may not seem very relevant to quality control since thickness is normally easily and quickly obtainable, knowledge of this relationship for a particular material can have other useful applications toward field construction monitoring.

10. The maximum or minimum DSM that can be expected for a certain material can be determined by constructing test sections; however, this may or may not (depending on the particular job) be feasible. A simpler less time-consuming method would be more advantageous. If the physical properties of a material are known, it may be possible to estimate (within a reasonable degree of accuracy) the limiting DSM based on its dry density. Maximum DSM's of 760 and 450 are well defined for Blend II and silt, respectively, in Figures 19

and 20. A minimum DSM for the buckshot clay material of about 80 kips/in. can be considered a reasonable estimate based on close examination of the curve in Figure 17. These limiting DSM's have been plotted in Figure 21 with the corresponding logarithm of average in-place dry densiy for each soil. The resulting relationship (based on small quanity of data) is approximately linear. By extrapolation, a limiting DSM of approximately 976 kips/in. is projected for the crushed limestone material having a density of 140 pcf. The crushed stone test data in Figure 18 show only one point with a stiffness greater than the estimated maximum, and the 976 kips/in. appears to be a reasonable value for the crushed stone over CH curve. It seems likely that increasing the thickness of crushed stone over Blend II (Figure 18) beyond 12 in. would have yielded higher DSM's, but there are no data to substantiate this.

11. Conventional means of evaluating field quality make use of density and moisture content determinations. Adequacy is evaluated on the basis of laboratory relationships between density, moisture content, and CBR. Laboratory CBR provides a means of obtaining the optimum or most desirable conditions for a particular material. Field CBR's on cohesive soils are generally accepted as being good indicators of performance. Field CBR's on granular or noncohesive soils can, however, give a misleading performance assessment if density is not taken into consideration. This can be illustrated by comparing the buckshot, Blend II, and silt materials. DSM versus thickness plots for these soils are also shown in Figure 22 including the in-place densities and CBR's. The plots suggest a strong relationship between DSM and density (however three points are not enough to be certain that this is more than coincidental). This is significant since density is an important factor in predicting performance. CBR's show a different ranking of materials. In this case, the low CBR for Blend II (sandy gravel) is probably not a very meaningful number mainly because the area of influence of the CBR test is small and to a large extent reflects the surface conditions. The overall stiffness of this material is much higher than indicated by this type of test. Blend II would be expected to perform like a much higher CBR and would actually increase somewhat in density with the application of traffic. From this, it appears that the DSM on the surface of a thick relatively homogeneous layer is a good indicator of overall strength of that layer, could be used to

predict average in-place densities of thick layers, and could provide estimates of performance.

Direct Correlation of NDT Results to Conventional Test Parameters

12. Direct comparison of DSM to conventional test parameters of CBR, density, and k are shown in Figures 23 through 25 for each of the NDT test devices. The substantial amount of scatter in the CBR and density plots was expected since it was determined in the previous section that DSM varies significantly as a function of thickness while the more localized CBR and density measurements are generally independent of thickness. To be meaningful, these plots would have to be separated by material type and layer thickness, but this would have resulted in a number of plots (many of which contained only one data point). However, better correlation was anticipated for the plate test results. Notes by Hadala (1983) revealed some interesting wave propagation theory which suggests that vibratory and possibly impulse responses obtained with various NDT devices should approximate the static load-displacement response. The works of Lysmer (1965) and Carroll (1963) are referenced in Hadala's notes. An attempt will be made to relate the works of Lysmer and Carroll to vibratory loading of a rigid plate on an elastic foundation as pertaining to nondestructive vibratory test equipment illustrated in the sketch below.

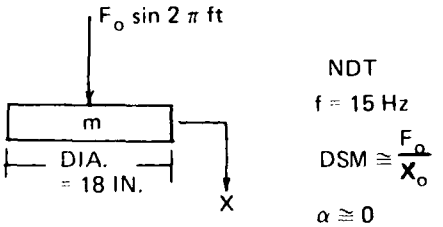

EQUATION FOR MOTION:

$$X_T = X_o \sin (2\pi ft - \alpha)$$

It should be noted that the theory to be presented is developed for a homogeneous, isotropic, linear elastic half-space.

13. Lysmer considered a simple damped oscillator which could, as far as displacement, δ, is concerned, be used as an analog for the massless system represented by

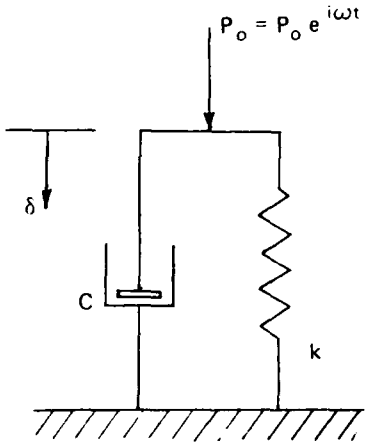

The equation of motion for this system is

$$i\omega CF + KF = k$$

where

i = an imaginary unit

ω = angular frequency of steady state motion

C = frequency dependent coefficient of viscous damping

F = time-independent, complex function $F = F_1 + iF_2$ of the frequency ω and the properties of the system (displacement function)

K = frequency dependent spring constant

k = spring constant

for which the solutions are

$$K = \frac{F_1}{\left(F_1^2 + F_1^2\right)} k$$

$$C = \frac{\frac{-F_2}{\omega}}{F_1^2 + F_2^2} k$$

where

F_1 = real part of F

F_2 = imaginary part of F

From this solution he showed that the parameters C and k could be determined as a function of the frequency of the exciting force.

14. Lysmer next considered a dynamic system formed by adding a rigid mass m to obtain

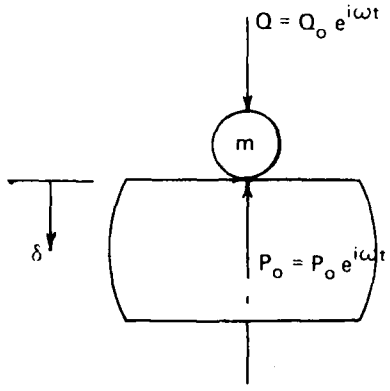

This system is excited by a vertical harmonic force $Q = Q_o e^{i\omega t}$ acting on the added mass. The displacement of the mass is

$$\delta = \frac{Q_o}{k} \bar{F} e^{i\omega t}$$

where

δ = vertical displacement

Q_o = amplitude of force

$\bar{F}$ = complex displacement function

e = base of natural logarithms

t = time

The use of this theory was then illustrated for the displacement function for the simple damped case as

$$F = \frac{1}{1 + i \frac{c}{k} \omega} = \frac{1}{1 + i a_o}$$

where

c = coefficient of viscous damping

$\bar{a}_o$ = frequency ratio

At this point two dimensionless ratios, $\bar{a}_o$ and $\bar{B}$, were introduced such that

$$\bar{a}_o = \text{frequency ratio for damped oscillator} = \frac{c}{k} \omega$$

$\bar{B}$ = mass ratio, scaled measure of mass = $\frac{km}{c^2}$

These ratios were used instead of the more commonly seen $\omega\sqrt{m/k}$ and $c/2$ km because they allow the effects of mass and frequency to be studied separately. The displacement for a more general oscillator (shown below) was then determined to be $\delta = (Q_o/k)M \cos(\omega t + o)$.

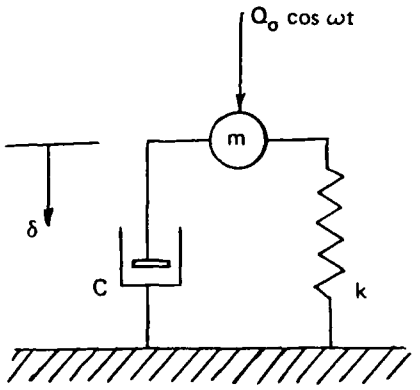

The magnification factor (M) is given by the expression

$$M = \sqrt{\frac{1}{\left(1 - \bar{B}\,\bar{a}_o^2\right)^2 + \bar{a}_o^2}}$$

Using this equation, the response curves in Figure 26 were developed for a single-degree-of-freedom system with the effect of mass and frequency separated. It is shown in the figure that for $\bar{B} > 1/2$, the response spectra will exhibit resonance peaks $\max M = \bar{B}/\sqrt{\bar{B} - 1/4}$ at frequencies $\bar{a}_o = \sqrt{\bar{B} - 1/2}/\bar{B}$. For $\bar{B} < 1/2$, no peaks exist, and the largest displacement occurs during static loading (i.e., frequency ratio = 0).

15. Close examination of the vibratory NDT equipment reveals essentially the same system with a sinusoidal excitation as shown below.

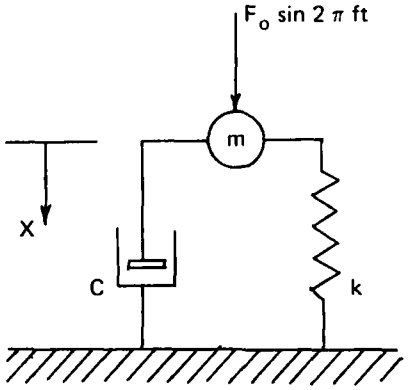

For this system, the differential equation of motion is $m\ddot{x} + c\dot{x} + kx = F_o \sin 2\pi ft$. The damping terms represent the fact that there is no bottom boundary, i.e., energy radiated out will not return. For evaluating the case of a rigid circular footing on a linear elastic half-space, the static spring constant is known to be

$$k = \frac{4Gr_o}{1 - \mu}$$

where

G = shear modulus

r_o = radius

μ = Poisson's ratio

Parmeters for the spring-dashpot analog are

$$K = k_1 k$$

$$C = c_1 \frac{kr_o}{V_s}$$

where

k_1 = dimensionless spring constant

c_1 = dimensionless damping coefficient

r_o = radius of footing

V_s = velocity of J-waves in elastic half space

Lysmer showed that his analog should be valid for small values of $\bar{a}_o$ (≤ 0.8)

and in the range K_1 and C_1 can be estimated as 1.0 and 0.85, respectively, so that

$$k = K$$

$$C = \frac{3.4}{1 - \mu} r_o^2 \sqrt{G\rho}$$

where ρ = mass density. Ratios $\bar{a}_o$ and $\bar{B}$ can now be determined for conditions representative of those encountered in NDT testing. Determination of the magnification factor, M , will indicate how close the dynamic response should be to the static value. Several examples are presented for which the following initial conditions are assumed:

mass of steel vibrator plate, $m = \frac{150 \text{ lb}}{32.16 \text{ ft/sec}^2} = 4.66 \frac{\text{lb-sec}^2}{\text{ft}}$

diameter of the plate, D = 1.5 ft

Poisson's ratio of the soil medium, $\mu = 0.3$

density of the soil medium, γ_m = 120 pcf

Shear wave velocities of 500 and 1,500 ft/sec considered in the examples should provide a range within which many commonly occurring soils will fall. Frequencies of 15 and 50 Hz are evaluated in the following cases:

Case	Cs ft/sec	Hz	$\frac{2\pi fr}{C_s}$	$G = \frac{\gamma_m}{32.16}(C_s)^2$ lb/sq ft	$k = \frac{4Gr_o}{1-\mu}$ lb/ft	$C = \frac{3.4}{1-\mu} r_o^2 G\rho$ lb-sec/ft	$\bar{B}$ $\frac{km}{c^2}$	$\bar{a}_o$ $\frac{2\pi fc}{k}$
1	500	15	0.14	9.33×10^5	4×10^6	5.1×10^3	0.72	0.12
2	500	50	0.47	9.33×10^5	4×10^6	5.1×10^3	0.72	0.40
3	1,500	15	0.05	8.39×10^6	3.6×10^7	1.53×10^4	0.72	0.04

For each example case, the magnification factor from Figure 26 is very close to 1.0 indicating that for the range of typical frequencies and wave velocities normally encountered with NDT, the dynamic response should approximate the static response for an equivalent force level.

16. An earlier work by (1963) Carroll revealed similar findings. Carroll studied the relation of three-dimensional dynamic footing problems to

plane wave phenomena and three-dimensional static footing behavior. He investigated the response of the linear Pauw-Selig pyramid model to step, linear, parabolic, and sinusoidal transient pressure pulses and to static loading. The sinusoidal pulse was characterized by $p = p_o \sin(\pi t/2t_o)$ Relations were derived for the various pulse types in terms of a factor

$$N = \frac{C_o t_o}{B} (2 \tan \psi)$$

where

C_o = initial wave velocity

t_o = time to peak applied transient bearing load

B = width of footing

ψ = angle which the sloping sides of the pyramid make with the vertical. Its purpose in the model is to bring about a spatial attenuation of vertical stress with depth

From this, a tentative criterion for ignoring the inertial stress effects on the dynamic pressure-displacement ($p_o - \delta_o$) relation was suggested to be

$$\frac{C_R t_o}{B} \geq 3.5$$

where

C_R = rod wave velocity

t_o = rise time

B = width of footing

Carroll was then able to estimate when the vibratory load-displacement behavior is at serious variance from static load-displacement behavior by making use of Sung's vibratory solutions approach (Sung 1953) and evaluating the relationship

$$\delta_o \left(\frac{E}{p_o}\right) = \pi (1 + \mu) F_1$$

Results confirmed the tentative criterion by indicating that for large values of $C_R t_o/B$, the vibratory $p_o - \delta_o$ relation approximates the static load-displacement behavior but deviates significantly as $C_R t_o/B$ decreases to a small number. Carroll's conclusion was that the discrepancy between vibratory $p_o - \delta_o$ and static load-displacement behavior is not important for

$$\frac{c_R t_o}{B} \geq 3.5$$

and that this statement is also tentatively true for impulsive sinusoidal transient pressure pulses on circular footings.

17. Carroll's criterion will now be applied to the three NDT devices described in this report in the form

$$\frac{ct_R}{D}$$

where

c = wave velocity of soil medium (ft/sec)

t_R = rise time for peak force (sec)

D = diameter of load plate (ft)

A value of 500 ft/sec will be assumed for the wave velocity of the soil medium. For the 16-kip vibrator operating at a frequency of 15 Hz with an 18-in.-diam load plate the following is obtained:

$$\frac{(500 \text{ ft/sec})(0.017 \text{ sec})}{1.5 \text{ ft}} = 5.7 \ (>3.5)$$

For the Road Rater 2008 operating at a frequency of 20 Hz with an 18-in.-diam plate the result is

$$\frac{(500 \text{ ft/sec})(0.0125 \text{ sec})}{1.5 \text{ ft}} = 4.2 \ (>3.5)$$

For the falling weight deflectometer having a rise time of 0.0125 sec and a 12-in.-diam load plate the following is obtained:

$$\frac{(500 \text{ ft/sec})(0.0125 \text{ sec})}{1.0 \text{ ft}} = 6.25 \ (>3.5)$$

18. The theory and discussion presented strongly implies that stiffness (maximum load ÷ maximum dislacement) results from vibratory, and impulse NDT devices should correlate well with static bearing tests. Soil modulus, k (psi/in) , values measured on the test section were converted to kips and inches and plotted versus DSM in Figure 27. Although the linear relationships are not clearly defined for either of the three devices, the theory is not discounted since the plate sizes for static bearing, vibratory, and impulse

tests were each different, and some of the testing was done on granular soils where plate size effects are definitely not the same as on cohesive soils. DSM is very much a function of plate size. It has also been determined that the effect of plate size on the DSM is highly dependent on the stiffness of the material being considered, and there is presently no accurate way of adjusting the DSM to reflect a different plate size. Another consideration is the effect of creep or long-term deflection on stiffness values from the static plate bearing test. Sufficient time is allowed after application of each load increment during the performance of this test for the system to essentially reach an equilibrium condition. Effects of the additional deflection due to the time rate of loading would be more pronounced for weaker materials.

19. It is concluded that there is a lack of data to either substantiate or disprove the theory that dynamic load-displacement relations are equivalent to static load-displacement behavior. The relative magnitudes of the stiffness values for each type of test are generally within the same range, and it is very possible that better results would have been obtained if the tests reported had been performed with a common plate size. Correlation of NDT results to soil modulus, k , would be significant in the areas of design and evaluation and would be extremely attractive from the standpoint of time and convenience.

Linear Regression Using NDT to Predict CBR and Density

20. Even though previous sections of this report have indicated that strong relationships appear to exist between NDT and conventional test parameters, DSM is not directly correlatable to either density or CBR. A multiple linear regression analysis was performed on the 16-kip vibratory test data obtained during construction in an attempt to develop correlations by accounting for the influence of such parameters as thickness on DSM values. The computer program SPSS (Statistical Package for the Social Sciences) (Nie et al. 1975) was employed to aid in this task. Variables introduced into the regression equations included DSM, subgrade DSM, deflection at the center of the load plate due to the application of a 2,500-lb dynamic force, deflection ratio (deflection at 60 in. divided by the deflection at 18 in. for a dynamic force of 2,500 lb), thickness, density, and CBR. Three data sets were considered in

the analysis. The first of these (Data Set 1) consisted of all data obtained during construction of the test bed. A total of 95 cases was available for the CH, Blends I and II, ML, crushed limestone, and cement-stabilized soils. The cement-stabilized materials were omitted from the second data set (Data Set 2) since CBR and density measurements could be somewhat altered in meaning due to the chemical stiffening effects. Eighty-seven cases were included in the second data set for CH, Blends I and II, ML, and crushed stone materials. The third data set (Data Set 3) contained 76 cases, and only CH, Blend II, and ML soils were considered. More data were available for these three soils, and DSM-thickness relationships were better defined.

21. Results of the regression analysis with density being the independent variable were very good. Variables having the most significant influence in the prediction of density were DSM, thickness, and subgrade DSM. Plate deflections (ranging from 1.3 to 10.6) and deflection ratios (ranging from 0.19 to 0.65) contributed very little to the correlations. Relationships having the highest correlation coefficients are summarized below.

Data Set	No. of Cases	Equation	R	R^2	STD. Error of Estimate
1	95	DEN = 0.05292 (DSM) - 0.01645 (Subgrade DSM) - 0.31755 (THK) + 105.36875	0.71	0.50	11.0
2	87	DEN = 0.07589 (DSM) - 0.46378 (THK) - 0.02074 (Subgrade DSM) + 101.76169	0.76	0.57	10.1
2	87	DEN = 0.07725 (DSM) - 32.46489 LOG_{10} (THK) - 0.03468 (Subgrade DSM) + 135.69287	0.79	0.62	9.5
2	87	DEN = 31.14306 $LOG_{10}\left(\frac{DSM - Subgrade\ DSM}{THK}\right)$ + 93.51330	0.75	0.56	10.2
3	76	DEN = 0.09528 (DSM) - 0.49112 (THK) + 88.16125	0.83	0.69	7.4
3	76	DEN = 0.09177 (DSM) - 32.09943 LOG_{10} (THK) + 119.41290	0.85	0.72	6.9
3	76	DEN = 3.32136 $\left(\frac{DSM - Subgrade\ DSM}{THK}\right)$ + 93.02259	0.90	0.81	5.6

22. As expected, the best correlations were obtained for equations developed from Data Set 3. These equations were used to generate the families of density curves shown in Figures 28 through 30 on the DSM-thickness plots for CH, Blend II, and ML soils. In Figure 28, density is shown as a function of the ratio of change in DSM to thickness. The average subgrade DSM for the points shown (238 kips/in.) was used to develop the density plots. Dry densities measured on the compacted surface of the lean clay subgrade with a nuclear gage during construction and in pretraffic test pits ranged from 98 to 104 pcf with the average being 103 pcf. At a depth of 2 ft the density of the subgrade ranged from 85 to 98 pcf, and the average was 92 pcf. This relationship provides the most accurate model for the three soils considered. Predicted densities fit the data very well up to the breakover point, or limiting DSM, after which there is significant deviation from computed density lines.

23. Density is shown as a linear function of DSM and thickness in Figure 29. General agreement with actual densities is observed for the Blend II and silt soils where measured DSM's are greater than the subgrade DSM. Deviation between observed and predicted values for the silt is again observed for thicknesses beyond the point at which a limiting DSM value is reached. Poor agreement is shown for the buckshot clay, and it is apparent that this relationship is not valid for materials having densities or strengths less than those measured on the subgrade.

24. Density is shown as a function of DSM and the common logarithm of thickness in Figure 30. The logarithmic curves provide somewhat better agreement between actual and predicted densities over a wider range of thicknesses than the linear plots in Figure 29. This relationship also appears to be valid for thicknesses beyond the point where a limiting DSM is reached. Poor agreement is again observed for the relatively low-strength, low-density buckshot clay.

25. Correlations obtained from the regression analysis with CBR being the independent variable were much poorer than those obtained for density. Correlation coefficients were low when only CH, Blend II, and ML soils were considered, and the standard errors were excessively high when all materials were considered. Some of the results are shown below.

Data Set	No. of Cases	Equation	R	R^2	STD. Error of Estimate
1	95	CBR = 0.15642 (DSM) - 1.17472 (THK) - 7.30371	0.83	0.69	25.0
1	95	CBR = 0.20977 (DSM) + 8.17690 (Plate Deflection) - 106.00490]	0.69	0.48	32.4
1	95	CBR = 0.10335 (DSM) + 0.72962 (DEN) - 103.94167	0.69	0.47	32.5
1	95	CBR = 0.22321 (DSM) - 154.40178 (Deflection Ratio) + 4.72501 (Plate Deflection) - 43.26524	0.72	0.52	31.1
2	87	CBR = 0.12930 (DSM) - 0.89925 (THK) - 6.94421	0.71	0.51	21.5
3	76	CBR = $8.58074 \log_{10}\left(\frac{\text{DSM - Subgrade DSM}}{\text{THK}}\right) + 6.63156$	0.52	0.23	4.84
3	76	CBR = -3.05276 (Plate Deflection) - 0.02753 (DSM) - 6.60083 (Deflection Ratio) + 41.1907	0.49	0.24	4.98

26. CBR curves shown in Figure 31 were developed as a function of DSM and thickness. Also included on the plot are the test results from Data Set 3 from which this particular relationship was derived. Some of the difficulties in correlating NDT results to CBR were discussed earlier and illustrated in Figure 22. The scatter observed in Figure 31 and the low correlation coefficients presented in this section are not encouraging, and it appears that successfully relating directly obtainable NDT parameters to CBR is improbable. However, it is possible that better relationships could be obtained for a particular soil or soil type (e.g., cohesive soils only as opposed to the variety of materials considered here).

Variation and Reliability of NDT and Conventional Test Results

27. Reliability of test equipment and variability of test results are major factors to be considered in the evaluation of NDT for quality control and design verification. Feasibility of a particular test is highly dependent

on sampling requirements for a satisfactorily high level of confidence, time requirements for each test, and the complexity of the actual test. Statistical evaluations and comparisons of DSM with CBR and density measurements on various materials are presented in this section. Since it is statistically desirable to have a large number of samples such that the mean and standard deviation of the population are well defined, much of the analysis will be centered around data collected on Blend II which was the most commonly occurring material in the test section.

28. Some assessment must be made as to the actual variability built into the test bed. Low density and moisture content requirements for Blend II are a cause for concern even though material conditions and placement procedures were carefully monitored during construction. Nuclear density and moisture determinations for Blend II are presented in Table 1 along with the mean, standard deviation, and coefficient of variation for each construction lift. Density and moisture content on the first lift were purposely high to provide a suitably firm working surface. The average moisture content for lifts 2 through 8 (42 points) was 4 percent with a standard deviation of 0.4 percent and a coefficient of variation of 10.8 percent. An average density of 119 pcf and a standard deviation of 2.56 pcf were determined for lifts 2 through 8 (42 points) of Blend II. The coefficient of variation of 2.1 percent is approximately the normal expectation for the variability of the nuclear test device. This is a good indication that material variability is low. Having established the relative homogenuity of the in-place material, it can be assumed that the majority of any test variability can be attributed to a particular test device or procedure.

29. DSM and CBR data including the mean, standard deviation, and coefficient of variation are summarized in Table 2 for the eight construction lifts of Blend II. Significant influence of either depth or thickness on the magnitude of DSM values is clearly evidenced. Since there is a substantially large difference in magnitude of the means of these data sets, variability will be compared using the coefficient of variation. The coefficient of variation gives the standard deviation as a percentage of the mean and is independent of the scale of measurement. Average coefficients of variation of 5.6, 14.7, and 21.7 percent were obtained for the WES 16-kip DSM, road rater DSM, and CBR, respectively.

30. NDT results on the Blend II are shown to be substantially less

variable than CBR's. Also, the DSM from the WES 16-kip vibrator is much less variable than the DSM obtained with the road rater which is essentially a scaled-down version of the larger machine. These low values of test variability for the NDT devices are encouraging; however, there is some concern as to whether this is a true measure of in-place material variability. It is possible that in-situ conditions are being altered as the vibratory test is performed. If some compaction occurs, the DSM could be reflecting the stiffness which exists after the system has essentially reached an equilibrium. The extent of this alteration (if in fact there is any significant change) has not been evaluated, but it seems that this may be an important factor influencing the sensitivity of NDT to small fluctations in density.

31. The higher variability obtained for the CBR test was somewhat expected. It is recognized that the CBR test is much more localized than the NDT, and the nature of the test itself (small diameter piston, etc.) suggests that it would be extremely susceptible to even minor surface variations. Even though nuclear densities in Table 1 indicated uniformity, it is reasonable to assume that at least some of the variability can be attributed to the loose condition of the surface of Blend II resulting from minimal compaction at a low moisture content. Also, Blend II is not a soil type on which CBR tests would typically be performed. Validity of the test on granular materials is often questioned, and field CBR's are usually performed on subgrade soils possessing some degree of cohesion.

32. To evaluate the effect of material type on the magnitude of observed test variability, WES 16-kip DSM and CBR test results shown in Table 3 for the silt and buckshot clay materials were compared with the average results obtained on Blend II. Since there are only two CBR's per lift, the mean, standard deviation, and coefficient of variation shown in Table 3 were determined using the combined CBR data from all construction lifts. Statistical analysis should provide fairly representative values for the silt and buckshot materials even though these data sets are much smaller than Blend II. Results summarized in Table 4 show coefficients of variation ranging from 15.6 to 21.7 percent (average = 19.4 percent) for the CBR test and from 5.6 to 14.3 percent (average = 8.8 percent) for the WES 16-kip DSM. These narrow ranges defined by the test variabilities on three different materials suggest that the magnitude of test variability (for these particular tests) is relatively independent of soil type. Again, the validity of these

numbers is somewhat questionable due to the small sample size and should be interpreted accordingly.

33. The falling weight device was not available during the majority of construction and was not included in Table 2. Variability of the falling weight deflectometer as compared to the vibratory devices was evaluated using test results obtained during traffic on three items that were selected because they exhibited very little change in stiffness as the 2,600 passes were applied. Test data and statistics (mean, standard deviation, and coefficient of variation) for the WES 16-kip, road rater, and falling weight deflectometer DSM's are presented in Table 5. A minimum of 10 cases were available in each of the data sets. An average coefficient of variation of 10.3 percent was obtained for the falling weight as compared to 4.7 and 23.8 percent for the WES 16-kip vibrator and road rater, respectively. There was little difference between the 16-kip variability during traffic and the variability obtained during construction. An increase in variability of about 70 percent was observed for the road rater tests performed during traffic. This large increase, which was experienced on all three items, seems to indicate that the variability of the smaller vibrator may be a function of the stiffness of the material being tested. In any event, the 10 percent variability for the falling weight ranks between the 16 kip (5 percent) and the road rater (14.7 percent during construction).

34. Having compared the variability of various nondestructive devices to that of conventionally determined densities and CBR's, the number of samples required by each procedure to ensure a particular level of confidence can be calculated from the statistical data previously computed. This is important since the speed at which a test can be performed will sometimes compensate for a somewhat larger test variability. For comparison, a confidence level of 95 percent will be assumed as a requirement with certain specified limits (plus or minus a percentage of the mean). These limits must be chosen on test by test basis since a given percent deviation in density will have a different meaning than will the same percent deviation in DSM. Since these test parameters are not directly correlatable, limits of uncertainty for density and CBR were arbitrarily selected as plus-or-minus 2 percent and 10 percent, respectively. These values are considered reasonable based on past experience. A definite procedure has not been established for the use of NDT results for evaluation of in-place soils; therefore, desired tolerances are

unknown. However, moderately good relationships were observed between DSM and dry density. From Figure 21, it was determined that a deviation of 2 percent in dry density corresponds to a 5 percent deviation in the limiting value of the WES 16-kip DSM. A limit of a plus-or-minus 5 percent for the NDT devices appears reasonable and was selected for use in the calculations below.

35. For comparison purposes, the required number of samples for a two-sided confidence interval with the standard deviation known can be determined as follows:

$$(\bar{X} - \mu) = K_{\frac{\alpha}{2}} \left(\frac{\sigma}{\sqrt{n}}\right)$$

where

$(\bar{X} - \mu)$ = deviation from the population mean

$K_{\frac{\alpha}{2}}$ = standard normal variate with cumulative probability levels $\frac{\alpha}{2}$ and $1 - \frac{\alpha}{2}$

σ = standard deviation

n = required number of tests

For 95 percent confidence

$\alpha = 0.05$

$\frac{\alpha}{2} = 0.025$

$K_{\frac{\alpha}{2}} = 1.960$ (from a table of normal probability)

Thus,

$$n = \frac{1.960\ \sigma}{L\ (\bar{X})}^{2}$$

where

n = required number of tests

σ = standard deviation (approximated as s, the sample standard deviation)

L = specified limits ($\pm$)

$\bar{X}$ = sample mean

36. Sampling requirements for density, CBR, 16-kip DSM, and road rater DSM on Blend II are shown in Table 6. It is important to note that reported

DSM's are single test values while reported densities are an average of two tests per location, and reported CBR's are an average of at least three tests per location. Therefore, the actual number of individual tests required would be as follows:

Test Parameter	Required No. of Samples		No. of Tests Per Sample	Actual No. of Tests Required
Density	4.5	x	2	9.0
CBR	20.9	x	3	62.7
16-kip DSM	4.5	x	1	4.5
Road rater DSM	32.6	x	1	32.6

Assuming that specified tolerance limits are within reason and also that sample means and standard deviations for the small data sets are relatively good approximations of the true values, NDT results compare favorably with conventional test results in terms of variability and reliability.

37. Sampling requirements for the three NDT devices are compared in Table 7 for test data collected during traffic on Item 3, lane 1 and Items 3 and 4, lane 3. The average number of tests required by each device is as follows:

	16-kip DSM	Road Rater DSM	Falling Weight DSM
No. of tests required	3.4	87.6	16.1

The high sampling requirement for the road rater DSM is the result of an increase in test variability observed for the during traffic tests with this device.

38. The statistical evaluation shows that high levels of confidence can be achieved with NDT devices on a wide variety of soil types by performing a reasonable number of tests. Since NDT can be performed very rapidly, the sampling requirement could be met (and possibly exceeded) within the same approximate time frame as the nuclear density requirement and much more quickly than required CBR's could be obtained. An additional benefit of NDT is that the larger number of tests which could be performed would essentially be proofing an area and increasing the chance of locating trouble spots or localized weak areas.

Computation of Modulus of Elasticity (E) Using Deflection Basin Data and Layered Elastic Theory

39. The use of layered elastic theory is becoming much more widespread, and the concept is being increasingly accepted as a viable approach to pavement design and evaluation. Over the past several years WES has experienced a great deal of success in applying elastic layered theory to both flexible and rigid airfield pavement evaluation. Almost all of the efforts to this point have been directed toward conventional, in-service pavements with little attention being given to unsurfaced pavements or quality control applications. An evaluation of modulus values computed on a lift-by-lift basis during construction of the test section using layered elastic theory with NDT deflection data is presented in this section for a variety of soil types. The following procedure (Bush 1980) provided the means by which the modulus values were determined.

40. The deflection basin produced by applying a load to the pavement with either of the three NDT devices described in this report gives a minimum of three or four input parameters to the system analysis that can be used to derive the strength parameters of the pavement layers. A program called BISDEF was developed to determine a set of modulus values that provide the best fit between a measured deflection basin and a computed deflection basin when given an initial estimate of the modulus values, a range of modulus values, and a set of measured deflections. Consider the pavement system where

a. The modulus is unknown for a number of layers (NL).

b. The deflection due to plate load is measured at a number of deflection (ND) locations.

c. ND is greater than NL.

The objective is to determine the set of E's that will minimize the error between the computed deflection Δ and the measured deflection RRD . To accomplish the objective, a relationship was developed for the deflection at a point j as a function of the unknown E's , i.e.,

$$\Delta j = f(E_1 , E_2 \ldots E_{NL})$$

then the error at a position where the deflection was measured is

$$RRD_j - \Delta_j = RRD_j - f(E_1 , E_2 \ldots E_{NL})$$

This expression is then squared and summed with respect to each measured deflection

$$\sum_{j=1}^{ND} ERROR^2 = \sum_{j=1}^{ND} RRD_j - f_j(E_1 \ldots E_{NL})^2$$

To minimize the error with respect to an unknown E, the partial derivation of the error function is taken with respect to the E. By taking a derivation with respect to each unknown E, then a set of NL equations is obtained that can be solved giving the set of E's for the minimum error between the measured basin and the computed basin.

41. First, a set of E-values is assumed and the deflection Δ_j^o is computed corresponding to the measured deflection RRD_j. Each unknown E is varied individually, and a new set of deflections is computed for each variation. Using the two computed deflections and the two values of each E, a function is determined for each deflection. For example,

$$E\ell = \log_{10} E$$

Then the deflection at location 1 is given as a function of E_1, i.e.,

$$\Delta_1 = A_{11} + S_{11} E\ell_1$$

where

$$S_{11} = \frac{\Delta_1^o - \Delta_1^1}{E\ell_1^o - E\ell_1^1}$$

$$A_{11} = \Delta_1^o - S_{11} E_1^o$$

$E\ell_1^o$ = $\log_{10}$ of first assumed value of E_1

$E\ell_1^1$ = $\log_{10}$ of E_1 after the variation

Δ_1^o = computed deflection at position 1 for E_1^o

Δ_1^1 = computed deflection at position 1 for E_1^1

Likewise, functions are determined for each deflection and each unknown E, resulting in $j = 1$ to ND and $i = 1$ to NL. Then

$$\Delta_j = A_{ji} + S_{ji} E\ell_i$$

To write an expression for Δ_j as a function of all E's, the following is used:

$$\Delta_j = \Delta_j^o + (\text{changes in } \Delta_j^o \text{ due to changes in the } E\text{'s})$$

Consider when the modulus of layer changes from E_1^o to E_1^1, the change in Δ_j would be $S_{ji}\left(E\ell_1^1 - E\ell_1^o\right)$.
Thus

$$\Delta_j = \Delta_j^o + \sum_{i=1}^{NL} S_{ji}\ E\ell_i - E\ell_i^o$$

The value of Δ_j^o can be expressed in terms of any of the unknown E's, i.e., E_{NL}, as

$$\Delta_j^o = A_{jNL} + S_{jNL} E\ell_{NL}^o$$

The expression for Δ_j now becomes

$$\Delta_j = A_{jNL} + S_{jNL} E\ell_{NL}^o + \sum_{i=1}^{NL} S_{ji}\ E\ell_i - E\ell_i^o$$

The error squared for the j^{th} position is $RRD_j - \Delta_j{}^2$ or

$$ERROR_j^2 = RRD_j - A_{jNL} + S_{jNL} E\ell_{NL}^o + \sum_{i=1}^{NL} S_{ji}\ E\ell_i - E\ell_i^o \Big)^2$$

The summation of the error for all readings is

$$\sum_{j=1}^{NL} ERROR_j^2 = \sum_{j=1}^{NL} RRD_j - A_{jNL} + S_{jNL} E\ell_{NL}^o + \sum_{i=1}^{NL} S_{ji}\ E\ell_i - E\ell_i^o \Big)^2$$

If a weight term W_j for each reading is to be applied, then the expression becomes

$$\sum_{j=1}^{ND} W_j - (ERROR)^2 = \sum_{j=1}^{ND} W_j \, RRD_j - A_{jNL} + S_{jNL} E\ell^o_{NL} + \sum_{i=1}^{NL} S_{ji} \, E\ell_i - E\ell^o_i \Big]^2$$

Taking the partial derivation with respect to each E and setting the partial derivation equal to zero, the following is obtained:

$$0 = \sum_{j=1}^{ND} S_{jk} W_j \, RRD_j - A_{jNL} + S_{jNL} E\ell^o_{NL} + \sum_{i=1}^{NL} S_{ji} \, E\ell_i - E\ell^o_i$$

If the equations derived are put in the form

$$[B] \{E\} = \{C\}$$

the $\{C\}$ terms are the constant part of the equation. For $k = 1$ to NL

$$C_k = \sum_{j=1}^{ND} S_{jk} W_j \, RRD_j - A_{jNL} + S_{jNL} E\ell^o_{NL} - \sum_{i=1}^{NL} S_{ji} E\ell^o_i$$

and the $[B]$ for $k = 1$ to NL and $i = 1$ to NL is

$$B_{ki} = \sum_{j=1}^{ND} S_{jk} W_j S_{ji}$$

If the weight term is chosen to be $W_j = 1/RRD_j$, the result is the same as developing the equation from

$$ERROR_j = \frac{RRD_j - \Delta_j}{RRD_j}$$

which is a percent type error. The solution of the equation is the set of E's that minimizes the percent error. The efficiency of the procedure will depend on how well the functions represent the actual relationship between the computed deflection and the E's.

42. It appears that as long as the final E-values are within the initial input limits, the $\Delta = f(\log_{10} E)$ is a good representation of the relationship.

43. The computer program BISDEF consisting of the procedure described above was used for the actual computation of E values. BISDEF uses the BISAR (Koninklijke/Shell Laboratorium 1972) layered elastic program as a subroutine to compute surface deflections. The summation of strains in the bottom layer to infinity by the layered elastic model tends to give larger deflections than the measured values. Bush (1980) showed that better agreement is observed between measured and predicted deflection basins if a rigid boundary is placed in the system model to compensate for this effect. Therefore, a rigid layer was assumed at a depth of 20 ft below the surface for each of the cases considered.

44. Deflection basin data collected with the WES 16-kip vibrator during construction were input into BISDEF to compute modulus values for buckshot clay (Item 1, lane 1), silt (Item 5, lane 1), and Blend II and lean concrete (Item 3, lane 2). Modulus values were computed on a lift-by-lift basis for each of these materials using two different approaches. A description of each and a comparison of results are provided in the following paragraphs.

45. In the first approach, each case is considered a two-layer system for which neither of the E-values is known initially. This would represent an evaluation case where the thickness of the upper layer is known, and no NDT test results are available for the underlying material. This is similar to what is done in conventional pavement evaluation where nondestructive deflection basin data obtained on the surface layer (asphalt or concrete) are used to compute modulus values for the surface layer, base course, and subgrade for which only thicknesses are known. Modulus values computed using this approach are shown in Figures 32 through 34. The thickness of the upper layer used in the computations was the cumulative thickness for the particular material under consideration (either buckshot clay, silt, Blend II, or lean concrete). This thickness appears along the left side of the figures. In each instance, the lower layer (subgrade) was assumed to extend to a rigid boundary placed at a depth of 20 ft below the surface. For example, looking at the top portion of Figure 32, modulus values of 86,205 and 7,289 psi were computed for the first lift (8.6 in.) of crushed stone and the subgrade (material beneath the crushed stone), respectively. Sixteen-kip deflection data obtained on the

surface of the 8.6-in. layer of crushed stone were input into BISDEF for computation of these modulus values. Likewise, it is shown that modulus values of 128,505 and 13,246 psi were obtained for the 36-in. layer of crushed stone and subgrade, respectively. Deflection data obtained on the surface of the 36 in. of crushed stone were used to compute the modulus values.

46. In the second approach, each case is considered a multilayer system for which E-values for all layers except the uppermost are known. This would represent a design verification or possibly a quality control situation where NDT's have been performed and modulus values computed for each of the underlying layers during construction. Modulus values from BISDEF for the crushed stone, buckshot clay, silt, Blend II, and lean concrete are shown in Figures 35 throgh 37. Again, the thickness of the upper layer (the only layer for which E's are being computed in this approach) is the cumulative thickness of the layer under consideration which appears on the left side of each figure. Modulus values for the material below the test bed were determined from BISDEF using 16-kip deflections measured at the bottom of the completed excavation prior to the placement of any backfill. The subgrade was considered as a two-layer system with the upper 48 in. representing the material above the water table and the lower layer extending to the rigid boundary assumed at a depth of 20 ft below the surface. Results shown in Figure 35 for the crushed stone can be presented to further illustrate this approach. Modulus values of 20,389 and 4,400 psi for the upper and lower subgrade layers, respectively, were determined using BISDEF and 16-kip deflection basin data collected on the surface of the completed excavation in lane 1, Item 1 before the placement of the first lift of buckshot clay. The modulus of 10,676 psi was then determined for the 36-in. layer of buckshot clay by inputting the known subgrade moduli and 16-kip deflection data obtained on the surface of the clay layer into BISDEF. Finally, with the modulus values for all the underlying layers known, 16-kip deflection data obtained on the surface of each lift of crushed stone were input into BISDEF for calculation of modulus values for the various layer thicknesses shown in Figure 35.

47. Comparison of E-values from the one- and two-variable layer systems shows very good agreement for Blend II, silt, and lean mix concrete with some relatively small discrepancies appearing for the buckshot clay and crushed limestone materials. Modulus values computed for the first layer in every case were much higher than and did not fit the trends established by the

thicker layers. Plots of E versus thickness for the two approaches are presented in Figures 38 and 39 with best-fit curves included. The apparently erroneous E-values for the thin layers were not considered in the determination of best-fit polynomial equations. These data points are shown on the plots only to provide an indication of the relative magnitudes of inconsistency with respect to results obtained for thicker layers. This discrepancy cannot be fully explained, but there are several factors that might possibly contribute to some error in the modulus value computed for a thin, weak, surface layer.

48. First, one of the limitations of this approach is that layered elastic theory assumes a uniform pressure applied to the surface. With the 16-kip vibrator, the load is applied through a rigid circular plate with the center deflection measured on top of that plate. Therefore, a difference does exist in the measured center deflection and a deflection computed from elastic layer procedures at the center of the load area. For the analysis presented in Figures 32 through 37, the center deflection was applied at an offset of one-half the radius (4.5 in.) as is commonly used when evaluating deflections measured on pavement surfaces. The effect of increasing the offset distance on the layered elastic solution is illustrated in Figure 40. The higher deflection predicted at the center of the uniformly loaded area (indicated by the dashed line) for the larger offset would yield a considerably lower modulus. For example, the modulus value of the surface layer (14.0 in. of silt) obtained using the deflection basin in Figure 40 and a 9.0-in. offset would be reduced from the 53,519 psi shown in Figure 33 (for a 4.5-in. offset) to only 30,735 psi. If computations were made to determine exactly where the elastic layer solution and field data coincide, it would likely be somewhere between the one-half and one-radius offsets depending primarily on the modulus of the surface layer. The problem defined here would have a more pronounced effect on a thin surface layer because the modulus value would be strongly influenced by the deflection measured nearest the load area.

49. Secondly, when testing on relatively soft materials, the ocurrence of permanent deformation may affect the measured displacement of the load plate. The extent of this deviation has not been previously evaluated. For the 16-kip vibrator, deflections are obtained by direct integration of signals from velocity transducers. For the steady-state vibratory loading case, velocity will be in the form of a sine wave. This signal can be somewhat

altered if excessive permanent deformation is experienced beneath the plate during the performance of a test. Essentially, if the surface moves downward and is not able to completely recover, the lower half of the sine wave may have a smaller peak value than the upper half. Integration of the altered sine wave would yield a low deflection value. This error will be especially critical for a thin surface layer where the E-value is primarily dependent on the plate deflection. If the thickness were increased, offset deflections would have a more significant influence on the E-value computed for the upper layer, and any error in the plate deflection would be less detrimental.

50. It appears that about 15 in. is the minimum surface layer thickness for which E's can be accurately computed on a weak layer without somehow accounting for the limitations discussed in the preceding paragraphs. For surface layers greater than 15 in. thick, computed modulus values appeared reasonable and compared relatively well with laboratory resilient modulus test results shown in Table A2. Results are summarized in the following:

	E from BISDEF, psi		Resilient Modulus Test		
Material	2-Variable Layers psi	1-Variable Layer psi	σ_{3_C} psi	Range of Resilient Modulus for Pulse (σ/σ_3) Varying from 2 to 5 psi	Average Resilient Modulus psi
Crushed limestone	94,954 (65,157-128,505)	97,309 (37,860-194,371)	5	133,878-169,671	159,862
			10	191,254-269,919	224,303
			20	175,195-534,332	407,946
			40	345,063-892,082	510,348
Buckshot	19,837 (15,546-26,513)	13,941 (10,201-18,074)	5	2,989- 10,642	6,287
			10	3,087- 7,320	5,203
			+	--	--
			+	--	--
Silt	37,651 (33,775-41,290)	13,941 (32,658-40,851)	5	19,046- 23,227	20,678
			10	21,251- 22,441	21,685
			20	28,821- 32,006	30,259
			40	26,752- 46,887	41,131
Blend II	67,939 (51,619-82,644)	64,179 (46,476-83,988)	5	30,149- 32,695	31,486
			10	40,904- 43,393	42,264
			20	56,799- 60,981	59,371
			40	88,721- 98,569	93,487

+ Test terminated at 8 pulses due to excessive axial deformation.

E-values computed from field data for both Blend II and silt were approximately the same magnitude as laboratory values obtained at the higher confining pressures (σ_3 = 20--0 psi). Both field and laboratory determinations

indicated the modulus of Blend II to be about twice the magnitude of the silt modulus. The same would have probably been true for the buckshot if the laboratory test had not been discontinued during the 10-psi iteration due to excessive axial deformation. Modulus values for the crushed limestone more nearly approximated the laboratory resilient modulus at a lower confining pressure (σ_3 = 5 psi).

51. Plots of DSM versus thickness for the three test items under consideration are shown in Figure 41. A great deal of similarity exists between the DSM-thickness and E-thickness relationships (see also Figures 38 and 39). E-values computed from BISDEF for both the one- and two-variable layer cases are plotted in Figures 42 and 43 with the corresponding 16-kip DSM's. Relationships between E and DSM developed for the data in Figures 37, 38, and 41 appear to be approximately linear and largely dependent on soil type with the materials representing three separate groups. Buckshot clay, silt, and lean clay can apparently be grouped together as one soil type while Blend II and crushed limestone represent two additional groups. Linear best-fit equations and correlation coefficients determined for each soil type are included in the figures. Average r-square values of 0.96 and 0.78 were obtained for the one- and two-variable layer cases, respectively. Further study will be required to determine whether these relationships are affected by varying the modulus of the underlying materials. Direct correlation of DSM to E would provide a relatively easy, quick method of determining input parameters for design and evaluation based on layered elastic theory.

Comparison of Predicted Deflections to Measured Deflections at Depth

52. A series of falling weight deflectometer tests was performed over each of the six linear variable differential transformer (LVDT) gages in lane 1 immediately after traffic testing was completed and just before all instrumentation was to be removed from the test bed. Falling weight deflections measured at the center of the load plate at force levels of approximately 4, 6, 9, and 14 kips and the corresponding LVDT deflections at depth are presented in Table 8. Vertical displacements at the surface and each LVDT gage location are plotted versus dynamic force applied at the surface in Figures 44 through 46. Deflection response of material beneath the surface is shown to be linear up to the 14-kip load level. Surface deflections for

Items 1 and 3 are approximately linear only up to the 9-kip load level.

53. Falling weight deflection basins measured at the 14-kip load level were input into the computer program BISDEF to determine modulus values for the materials in each of the three items. A two-variable layer system was assumed for each item with a rigid boundary placed at a depth of 20 ft below the surface. With these modulus values, the BISAR program was then used to compute deflections for the surface and depths corresponding to each LVDT gage location for a load equivalent to that obtained with the falling weight device. Falling weight basin data, modulus values from BISDEF, and comparisons between measured and computed deflections are shown in Table 9. Measured and computed deflections are plotted with depth for each item in Figure 47. Computed surface deflections differed from the falling weight deflections measured at the center of the load plate by less than 3 percent. The average deviation between deflections computed below the surface using BISAR and corresponding displacements measured with the LVDT's was 29.7 percent with the largest difference (77 percent) occurring at the interface between the crushed limestone and buckshot clay in Item 1. Results of the limited analysis provide a good indication that material properties and also their behavior under loading can be accurately estimated using NDT and layered elastic theory.

NDT Test Results During Traffic

54. NDT tests were performed periodically during traffic testing as an overall monitor of the structural integrity of each item and to possibly provide indications of structural deterioration due to the repeated load applications. Test results plotted in Figures 48 through 68 for each of the NDT devices at 0, 326, and 2,600 passes reveal a general tendency of the stiffness to decrease as the number of passes is increased; however, this is not true for all cases. It should be noted that various diameter culvert pipes were installed in Item 2 (lanes 1 and 2), and their presence is reflected in the falling weight stiffness profiles (Figures 55 and 60). Closer examination of the relationship between the 16-kip DSM and number of load applications is provided in Figures 69 through 71. In all cases, the most substantial change in DSM was realized early (between 0 and 326 passes) after which a subtle decrease in stiffness occurred during application of the remainder of the

2,600 passes. Best-fit linear equations determined for the latter portions of each of the DSM versus passes plots show that the DSM's actually decrease on slopes of -0.0025 to -0.07. The marked decrease in stiffness observed for lane 2 during the first 130 passes is the result of cracking of the cement-stabilized and lean concrete materials. Relatively small changes in DSM measured between 300 and 2,600 passes for all three lanes can be substantiated by the fact that little apparent structural damage was evidenced in the form of rutting. It was also observed that the cement-stabilized materials in lane 2 remained solidly intact even though numerous cracks were present.

55. The assumption that performance can be directly correlated to deflection data has recently been the subject of a great deal of controversy. The data collected during this study does show a definite, although small, decrease in stiffness occurring during the application of 2,600 passes of the MX load cart. Unfortunately, traffic was stopped before failures occured, and all indications were that most of the items would have been capable of withstanding a large number of additional passes. Therefore, it was not determined how or to what extent the deflection response would be affected by the approach of failure. Even though the implications are good, attempts to make performance predictions based on the limited data presented would not be feasible.

Correlation of NDT Test Devices

56. Most of the analysis shown in this report has been focused on data obtained with the 16-kip vibrator (the 16-kip DSM). Comparisons of output from the three NDT test devices and correlation between DSM's for each device are evaluated in this section. Deflection basins measured on the completed test bed just prior to traffic testing are shown in Figures 72 through 74. Deflections have been normalized to a 5,000-lb force level so that direct comparisons can be made. With the exception of those deflections measured at the center of the load plate, much similarity is observed between the basins for each device. As a result of the large difference in pre-load between the two vibratory devices (4,000 lb for the road rater as compared to 16,000 for the 16-kip vibrator), plate deflections measured for the smaller road rater are slightly higher than those measured with the 16-kip vibrator at the equivalent force levels. Plate deflections for the falling weight were

generally much larger than for either of the vibratory devices. This can be attributed to the fact that significantly higher pressures would be realized beneath the smaller load plate used on the falling weight (12-in. diam as compared to 18-in. diam for the vibratory devices). Even though these comparisons are valid for this particular force level, it should be noted that 5,000 lb is near the upper limit of output capability for the road rater but would be considered a low force output for both the 16-kip vibrator and the falling weight deflectometer.

57. Similarity between the output for each of the NDT test devices suggests that correlation of DSM's might be possible. However, since DSM is a function of plate deflection, a one-to-one relationship will not exist. Falling weight- and road rater-DSM's were correlated to the 16-kip DSM, and results are shown in Figures 75 and 76. An r-square value of 0.74 and a standard error of 117.3 were obtained for the falling weight DSM correlation (based on 328 tests). Scatter in the data appears relatively constant throughout the range of DSM's evaluated. A lower r-square value of 0.61 was obtained for the road rater correlation (based on 398 tests), and the standard error was 178.2. A large increase in scatter is observed at the higher DSM levels. The significance of such correlations is the abiliy to use a particular NDT device to obtain input parameters for a design or evaluation procedure developed around a different NDT device or, in effect, equipment destandardization. Good indications are shown for correlation between the 16-kip vibrator and the falling weight deflectometer while the large amount of scatter observed for the road rater implies that a reliable correlation for this device is unlikely.

PART III: SUMMARY AND CONCLUSIONS

58. An evaluation and comparison of NDT and conventional test parameters measured during the construction and trafficking of a test bed built in support of the MX Road Criteria Study are presented in this report. DSM was the primary NDT parameter considered in the study. The fact that DSM provides a measure of a layered soil system's resistance to deformation and has been correlated to allowable load for pavement evaluation procedures leads to the idea of substituting NDT data as a measure of soil strength and using it for compaction control and as a primary design parameter. The development of such an idea into usable procedures would provide vast improvements over existing methodologies. Findings of this investigation are, however, inconclusive with regard to the feasiability of NDT for pavement construction quality control and design verification during construction. This is due in part to limitations of the data set. Even though a large volume of data was available (Appendix A), it was not the result of a well designed experiment aimed at evaluating the use of NDT, but rather a collection of supplemental data that would have been more useful if the planned follow-on test section had not been cancelled. The MX data did provide some good information in terms of direct comparisons between NDT results and conventional test parameters, but, since the individual materials were essentially tested under only one set of conditions (density, moisture content, and CBR), their relative sensitivities with respect to variation in placement conditions (quality control) could not be evaluated. Thus, the results presented in this report, although inconclusive, may prove to be a valuable stepping stone toward further research and developmental programs based on NDT techniques.

59. Significant findings of this report along with some general conclusions are presented as follows:

a. It appears that DSM versus thickness relationships can be determined for any soil type and that there will exist a limiting stiffness for each material. Based on those materials tested, indications are that a linear relationship exists between the limiting DSM and the common logarithm of field dry density. Once sufficient thickness has been added to achieve the limiting value, no change in DSM can be realized by further addition of the same quality material. Additional research is needed to further study the DSM-thickness relationship as it pertains to the evaluation of in-place material properties. It appears feasible that through further research normalized relationships could be developed for various quality materials. Laboratory

parameters such as resilient modulus might prove to be useful in establishing these relationships by providing a means of accounting for the effects of widely varying material properties.

b. Based on a relative structural ranking of the materials evaluated in this study, it can be suggested that perhaps DSM is a better indicator of in-place strength with respect to performance than CBR. This is especially true when testing granular materials where surface effects and the nature of the material itself can greatly influence the measured CBR value, and results may not reflect the actual performance potential of the material. DSM is a potentially good indicator of strength for all soil types; however, it was also shown to be a function of thickness as well as strength.

c. DSM-thickness relationships were observed to be largely influenced by material densitites. Results from a linear regression analysis of the data indicate a good correlation between density and surface DSM, thickness of material above the subgrade, and subgrade DSM. Further investigation could result in some improvement of this correlation and possibly allow for direct determination of density from deflection data. This will depend mostly on the sensitivity of NDT results to relatively small changes in the density of a particular material.

d. Efforts to directly correlate NDT test results to the conventional strength parameters of CBR and k were relatively unsuccessful. A linear regression analysis performed with CBR as the dependent variable failed to yield any significantly high correlation coefficients. Some of the independent variables entered into the regression with CBR included the surface DSM, subgrade DSM, deflection measured at the center of the load plate, deflection ratio, and layer thickness. Apparently, because of the vast differences in the nature of CBR and NDT tests, the two are essentially noncorrelatable. Theory presented in this report strongly indicates that for the NDT devices the dynamic deflection response for a given load level should be approximately equivalent to the deflection response from a static load of the same magnitude. This theory could not be fully substantiated due to the limited number of plate tests performed during the study and because the NDT and plate bearing tests were each performed with different size load plates.

e. A comparison between the test variabilities obtained for the nuclear moisture-density gage, field CBR, 16-kip DSM, and road rater DSM yielded the following results:

Material Type	Test Parameter	Coefficient of Variation Percent
Blend II	Density (pcf)	2.1

(Continued)

Material Type	Test Parameter	Coefficient of Variation Percent
Blend II	CBR (percent)	21.7
Blend II	16-kip DSM (kips/in.)	5.6
Blend II	Road rater DSM (kips/in.)	14.7

A comparison of these results with 16-kip- and CBR-coefficients of variation on silt and buckshot clay materials shows that the magnitude of variability for these test parameters is relatively independent of soil type. Average coefficients of variation of 4.7, 10.3, and 23.8 percent were obtained for the 16-kip, falling weight deflectometer, and road rater DSM's, respectively, based on test data collected during traffic testing on three separate items. The coefficient of variation for the road rater increased from 14.7 percent during construction to 23.8 percent during traffic testing. It appears that variability of the road rater DSM increases as the magnitude of the DSM increases. Statistical data were then used to compute the number of tests required by each procedure to achieve a hypothetical 95 percent confidence level within specified limits. It was shown that high levels of confidence can be obtained for the 16-kip and falling weight devices by performing a reasonable number of tests. Based on these results, reliability of the road rater is somewhat questionable but the variability of this device should be reevaluated before any final conclusions are drawn.

f. The use of NDT deflection data with layered elastic theory is a viable alternative for design verification and structural evaluation. The computer program BISDEF was developed to compute modulus values for each layer in a multi-layer pavement system using the deflection basin from an NDT device and the procedures described in this report. Modulus values were computed for several of the materials in the test section using BISDEF and deflection basins measured with the 16-kip vibrator. In all cases, the moduli for thin surface layers were erroneously high. For subsurface layers and surface layers greater than about 15 in. thick, computed modulus values appeared reasonable and compared relatively well with laboratory resilient modulus values. With this procedure, the modulus of a thin layer at the surface will be greatly influenced by the center deflection reading from an NDT device even though weighting factors are applied to more evenly distribute the effects of each deflection. The fact that the load is being applied through a rigid circular plate rather than as a uniform pressure on the surface and the occurrence of excessive permanent deformation during a test are two possible sources of error in the center deflection reading. Further study is

required to determine to what extent these factors will affect the measured deflection response and devise ways of eliminating or correcting errors.

g. Vertical deflections at depth predicted from BISAR using E-values determined from BISDEF and falling weight deflectometer deflection basins compared favorably with vertical displacements measured at depth with LVDT gages.

h. NDT results obtained periodically throughout the traffic testing phase reveal a general tendency of the stiffness to decrease slightly as the number of passes is increased. This subtle decrease in DSM was not, however, observed for all test items. Very little useful performance data were gained because traffic on the test section was stopped after 2,600 passes (before structural failures occurred). Therefore, it was not determined how or to what extent the NDT results might have been affected by the approach of failure. In order to successfully use a design or evaluation procedure such as the one described in this report (based on layered elastic theory) to verify the design of pavement sublayers or evaluate unsurfaced pavement structures, development of an adequate performance criteria is essential.

i. Deflection basins from each of the NDT devices appear very similar (except for the deflection measured at the center of the load plate) when normalized to a common force level. Differences in magnitude of the observed center deflection are attributed to the effects of static preloads applied by the vibratory devices and the difference in load plate diameter between the vibrators and the falling weight deflectometer. Relatively good correlation was found between 16-kip and falling weight deflectometer DSM's (r-square = 0.74). The correlation between 16-kip and road rater DSM's was, however, weaker (r-square = 0.61) due to a large amount of scatter in the higher DSM values obtained with the road rater.

PART IV: RECOMMENDATIONS

60. The following recommendations are offered toward further research, development, and validation of NDT procedures and methodologies for pavement construction quality control, design/design verification, and evaluation.

a. Additional data from highly controlled test sections should be collected on several different soil types and analyzed to refine DSM versus thickness relationships. Efforts should be directed toward normalization of these DSM-thickness relationships and improvement of density correlations through regression analysis. Each soil should be tested over a range of densities to evaluate the sensitivity of NDT devices to relatively small variations of in-place material properties. The total thickness of each material considered should be great enough to allow for determination of the limiting DSM. Special consideration should be given to the smaller more mobile test devices such as the falling weight deflectometer and road rater. Further study of their variability and reliability should be performed. If both appear feasible, correlation between the two should be attempted.

b. Work involving tests on various soil types on actual construction projects should be done to provide needed input for development and validation of NDT construction quality control and design verification techniques.

c. To further enhance the idea of using some type of NDT result as a primary design parameter, the possibility of developing laboratory procedures to yield relationships between DSM or E and such parameters as density, moisture content, and resilient modulus should be investigated. This would provide a means of evaluating the performance of a material in the laboratory in a manner that would be directly translatable to field test results. The effects of saturation on nondestructive test parameters should also be studied.

d. For field in-place design verification or evaluation, a study is needed to develop correlations between NDT results (DSM) and k (from static plate-bearing tests). Theory has been presented which indicates that upon an elastic half-space the deflection response from the NDT devices should be approximately equivalent to a static load-deflection response. A series of tests should be performed on a variety of soil types (layered and unlayered) to determine whether direct correlations exist. All tests should be performed with a common load-plate diameter. Factors which could affect the correlation such as the creep or long-term deflection that is a characteristic of the plate-bearing test should also be investigated.

e. A study should be conducted to evaluate possible sources of error in the modulus values computed for thin surface layers using 16-kip vibrator deflection data and layered elastic theory. Modulus values should be computed for thin surface

layers using data obtained with the falling weight deflectometer to determine how these results would compare to those obtained with the vibratory device.

f. The problem of directly relating information obtained with an NDT device to performance should be given a high priority. Both structural and functional modes of failure must be considered. This study would require the construction of a test section (preferably instrumented with deflection gages) to be trafficked to failure with prototype loads. Performance should be monitored throughout traffic testing and the findings used to develop failure criteria for subgrade and base course materials. Design and evaluation procedures could then be developed based on the DSM and/or layered elastic theory using limiting strain criteria.

REFERENCES

American Society for Testing and Materials. 1982a. "Standard Test Method for Compressive Strength of Cylindrical Concrete Specimens," Designation: C 39-80, 1982 Book of ASTM Standards, Philadelphia, Pa.

_____. 1982b. "Standard Test Method for Compressive Strength of Molded Soil-Cement Cylinders," Designation: D 1633-63 (Reapproved 1979), 1982 Book of ASTM Standards, Philadelphia, Pa.

_____. 1982c. "Standard Test Method for Density of Soil and Soil-Aggregate In Place by Nuclear Methods (Shallow Depth)," Designation: D 2922-81, 1982 Book of ASTM Standards, Philadelphia, Pa.

_____. 1982d. "Standard Test Method for Density of Soil In Place by the Rubber-Balloon Method," Designation: D 2167-66 (Reapproved 1977), 1982 Book of ASTM Standards, Philadelphia, Pa.

_____. 1982e. "Standard Test Method for Flexural Strength of Concrete Using Simple Beam with Third-Point Loading," Designation: C 78-75, 1982 Book of ASTM Standards, Philadelphia, Pa.

_____. 1982f. "Standard Test Method for Moisture Content of Soil and Soil-Aggregate In Place by Nuclear Method (Shallow Depth)" Designation: D 3017-78, 1982 Book of ASTM Standards, Philadelphia, Pa.

_____. 1982g. "Standard Test Method of Making and Curing Concrete Test Secimens in the Field," Designation: C 31-69, 1982 Book of ASTM Standards, Philadelphia, Pa.

_____. 1982h. "Standard Test Method of Making and Curing Soil-Cement Compression and Flexure Test Specimens in the Laboratory," Designation: D 1632-63 (Reapproved 1979), 1982 Book of ASTM Standards, Philadelphia, Pa.

Bush, A. J., III. 1980. "Nondestructive Testing for Light Aircraft Pavements; Phase II, Development of the Nondestructive Evaluation Methodology," Report No. FAA-RD-80-9-II, Department of Transportation, Federal Aviation Administration, Washington, DC.

Carroll, W. F. 1963 (Sep). "Dynamic Bearing Capacity of Soils-Vertical Displacements of Spread Footings on Clay: Static and Impulsive Loads," Technical Report No. 3-599, Report 5, US Army Engineer Waterways Experiment Station, Vicksburg, Miss.

Department of Defense. 1964 (Dec). "Military Standard Test Method for Pavement, Subgrade, Subbase, and Base-Course Materials," MIL-STD-621A, Washington, DC.

Hadala, P. F. 1983 (Nov). "Earth Waves in Pavement Systems," Unpublished Class notes, US Army Engineer Waterways Experiment Station, Vicksburg, Miss.

Hall, J. W., Jr. 1978 (Nov). "Quality Control of Pavement Construction," draft of unpublished report, US Army Engineer Waterways Experiment Station, Vicksburg, Miss.

Koninklijke/Shell Laboratorium. 1972 (Jul). "BISAR Users Manual; Layered System Under Normal and Tangential Loads," Amsterdam, Holland.

Lysmer, J. 1965 (Jun). "Vertical Motion of Rigid Footings," Contract Report No. 3-115, US Army Engineer Waterways Experiment Station, Vicksburg, Miss.

Nie, N. H., Hull, C. H., Jenkins, J. G., Steinbrenner, K., and Bent, D. H. 1975. "SPSS-Statistical Package for the Social Sciences," 2nd ed., McGraw-Hill, New York, N. Y.

Sung, T. Y. 1953. "Vibrations in Semi-Infinite Solids Due to Periodic Surface Loading," Symposium Dynamic Testing of Soils, ASTM Special Technical Publication No. 156, p 44.

Table 1

Variation of Density and Moisture Content of Blend II During Construction

Material	Construction Lift	Lane 1 Item 2		Lane 1 Item 3		Lane 1 Item 4		Lane 2 Item 2		Lane 2 Item 3		Lane 2 Item 4		Mean $\bar{x}$		Standard Deviation σ		Coefficient of Variation %	
		γ_d*	ω**	γ_d	ω	γ_d	ω	γ_d	ω	γ_d	ω	γ_d	ω	γ_d	ω	γ_d	ω	γ_d	ω
Blend II	1	130	7.0	130	7.0	129	8.0	128	7.0	131	7.0	129	6.0	129	7.0	1.0	0.63	0.8	9.0
	2	114	4.1	119	4.0	116	4.3	119	4.5	122	4.0	118	5.1	118	4.3	2.8	0.42	2.3	9.7
	3	122	3.8	123	3.8	121	4.1	120	3.9	123	3.8	118	4.0	121	3.9	1.9	0.13	1.6	3.3
	4	118	3.9	119	4.0	120	3.5	120	3.8	124	3.4	124	3.5	121	3.7	2.6	0.25	2.1	6.8
	5	117	4.8	117	3.5	117	3.1	120	4.2	118	4.1	116	4.1	117	4.0	1.4	0.59	1.2	14.9
	6	118	4.6	115	4.2	122	4.9	123	4.6	119	4.3	122	4.2	120	4.5	3.1	0.28	2.5	6.3
	7	120	3.3	116	3.6	115	4.5	119	3.5	121	3.6	119	3.6	118	3.7	2.3	0.42	2.0	11.4
	8	120	4.3	117	4.0	123	4.0	120	3.7	120	4.0	121	4.0	120	4.0	1.9	0.19	1.6	4.7

* Dry density from nuclear gage (pcf) - two tests per location.

** Moisture content from nuclear gage (%) - two tests per location.

Table 2

Comparison of Variability of WES 16-Kip Vibrator, Road Rater 2008, and CBR on Blend II During Construction

Material	Lift	Lane 1, Item 2			Lane 1, Item 3			Lane 1, Item 4			Lanes 2,3, Item 2			Lanes 2,3 Item 3			Lanes 2,3 Item 4			Mean			Standard Deviation			Coefficient of Variation		
		16-kip DSM*	RR 2008 DSM*	CBR**	16-kip DSM	RR 2008 DSM	CBR	16-kip DSM	RR 2008 DSM	CBR	16-kip DSM	RR 2008 DSM	CBR	16-kip DSM	RR 2008 DSM	CBR	16-kip DSM	RR 2008 DSM	CBR	16-kip DSM	RR 2008 DSM	CBR	16-kip DSM	RR 2008 DSM	CBR	16-kip DSM	RR 208 DSM	CBR
Blend II	1	330	121	19	300	119	18	340	163	12	325	145	24	350	153	26	380	211	28	324	147	21.2	26.0	27.3	5.9	8.0	18.5	28.1
		310	125		340	170		320	118		285	143		310	134		300	164										
	2	370	230	7	370	225	3.2	360	232	9	380	294	6	400	306	10	390	288	9	369	243	7.4	20.6	34.6	2.5	5.6	14.2	34.2
		380	231		390	260		340	217		340	215		340	213		370	209										
	3	420	278	15	420	323	16	400	289	17	400	347	12	460	428	12	420	320	15	413	308	14.5	20.6	45.3	2.1	5.0	14.7	14.3
		390	284		430	300		400	250		430	304		390	277		400	302										
	4	470	400	8	600	380	13	490	338	9	510	380	14	520	396	14	480	363	18	494	375	12.7	40.1	27.6	3.7	8.1	7.4	29.0
		490	408		500	330		480	416		480	385		430	353		480	355										
	5	540	366	12	530	297	14	520	353	10	550	429	12	580	400	10	570	348	11	550	356	11.5	31.6	51.3	1.5	5.7	14.4	13.2
		530	300		540	353		520	407		560	406		530	354		630	257										
	6	590	422	13	590	389	13	580	578	15	610	468	12	640	411	12	640	505	12	600	411	12.8	25.9	72.9	1.2	4.3	17.7	9.1
		560	396		580	356		590	360		630	342		610	356		580	346										
	7	610	433	9	630	391	10	620	412	13	620	450	16	680	527	11	630	495	10	627	451	11.5	23.8	50.5	2.6	3.8	11.2	22.5
		620	365		590	488		640	427		660	465		620	438		610	523										
	8	630	297	9	650	588	15	640	473	13	640	530	17	700	609	10	620	564	13	646	480	12.8	29.1	93.8	3.0	4.5	19.5	23.3
		660	426		670	391		660	498		670	502		620	369		590	518										
																	Averages:			503	346	11.9†	27.2	50.4	2.8	5.6	14.7	21.7

* 16-kip DSM's and RR2008 DSM's are single-test values from two locations within each item.

** CBR is an average of at least three tests at one location.

† Lift 1 not used in computing the average.

Table 3

Comparison of Variability of WES 16-Kip Vibrator DSM and CBR on Silt and Buckshot Clay During Construction

Lift	Lane 1, Item 5		Lanes 2 & 3, Item 5		Mean		Standard Deviation		Coefficient Variation	
	16-Kip DSM	CBR	16-Kip DSM	CBR	16-Kip DSM	CBR	16-Kip DSM	CBR	16-Kip DSM	CBR
Silt										
1	-- --	16	260 140	15	--	--	--	--	--	--
2	310 330	17	280 160	17	270	--	76.2	--	28.2	--
3	360 390	15	340 250	16	335	--	60.3	--	18.0	--
4	390 400	18	330 320	19	360	--	40.8	--	11.3	--
5	440 430	19	430 400	16	425	--	17.3	--	4.1	--
6	440 440	17	430 430	21	435	--	5.8	--	1.3	--
7	440 430	21	410 450	14	432	--	17.1	--	3.9	--
8	430 400	11	420 450	--	425	--	20.8	--	4.9	--
				Averages:	360	16.8	40.4	2.6	14.3	15.6

Buckshot Clay

Lane 1, Item 1		Lanes 2 & 3, Item 5		Mean		Standard Deviation		Coefficient Variation	
16-Kip DSM	CBR	16-Kip DSM	CBR	16-Kip DSM	CBR	16-Kip DSM	CBR	16-Kip DSM	CBR
230 225	4.6	215 230	4.2	225	--	7.1	--	3.1	--
210 210	4.0	200 200	4.9	205	--	5.8	--	2.8	--

(Continued)

Note: Mean, standard deviation, and coefficient of variation are shown only for cases having more than two data points. Average values shown for CBR were determined using the combined data from all construction lifts.

Table 3 (Concluded)

Lane 1, Item 1		Lanes 2 & 3, Item 5		Mean		Standard Deviation		Coefficient Variation	
16-Kip DSM	CBR	16-Kip DSM	CBR	16-Kip DSM	CBR	16-Kip DSM	CBR	16-Kip DSM	CBR
			Buckshot Clay (Continued)						
200 190	3.5	200 190	3.1	195	--	5.8	--	3.0	--
140 130	2.4	180 190	3.3	160	--	29.4	--	18.4	--
180 170	4.0	160 170	3.0	170	--	8.2	--	4.8	--
			Averages:	191	3.7	11.3	0.78	6.4	21.0

Table 4

Comparison of 16-Kip DSM and CBR Test Variability on Blend II, Silt, and Buckshot Clay During Construction

Material	Test Parameter	No. of Tests	Sample Mean ($\bar{x}$)	Sample Standard Deviation σ	Coefficient of Variation Percent
Blend II	CBR	48*	11.9	2.8	21.7
	DSM	96*	503	27.2	5.6
Silt	CBR	15	16.8	2.6	15.6
	DSM	30*	360	40.4	14.3
Buckshot	CBR	10	3.7	0.78	21.0
	DSM	20*	191	11.3	6.4

* Total number of tests performed (mean, standard deviation, and coefficient of variation are actually an average of the mean values determined for each layer during construction).

Table 5

Variability of Test Results from the WES 16-Kip Vibrator, the Road Rater 2008, and the Falling Weight Deflectometer*

Material	Lane	Item	Number of Tests			Mean DSM			Standard Deviation			Coefficient of Variation		
			16-Kip	RR 2008	FWD	16-Kip	RR 2008	FWD	16-Kip	RR 2008	FWD	16-Kip	RR 2008	FWD
Blend II	1	3	20	10	27	671	337	378	33	88	41	4.9	26.3	10.9
Blend II (optimum) with a DBST	3	3	20	14	21	729	480	592	32	117	61	4.4	24.5	10.3
Blend I (optimum) with a SBST over Blend II	3	4	20	14	21	664	492	473	32	102	45	4.9	20.7	9.6

* Results were tabulated during traffic on three selected items which exhibited little change in stiffness due to traffic.

Table 6

Comparison of Required Number of Tests for Prediction of Density, CBR, and WES 16-Kip DSM for Blend II During Construction

Test Parameter	Sample Mean ($\bar{x}$)	Standard Deviation σ	Coefficient of Variation %	Prediction Within ± L % at a 95% Confidence Level		
				Specified Limit, L %	L($\bar{x}$)	Required Number of Tests
Density (PCF)	119	2.6	2.1	2	2.4	4.5
CBR (%)	11.9	2.8	21.7	10	1.2	20.9
16-kip DSM (kips/in.)	503	27.2	5.6	5	25.1	4.5
Road rater DSM (kips/in.)	346	50.4	14.7	5	17.3	32.6

Table 7

Comparison of Required Number of Tests for Prediction of WES 16-Kip, Road Rater, and Falling Weight Deflectometer DSM's on Selected Items During Traffic Testing

Test Parameter	Lane	Item	Sample Mean $\bar{x}$	Sample Standard Deviation σ	Coefficient of Variation %	Prediction Within ±5% at 95% Confidence Level: Number of Samples	5% of $\bar{x}$	Required Number of Tests
16-kip DSM (kips/in.)	1	3	671	33	4.9	20	33.5	3.7
	3	3	729	32	4.4	20	36.4	3.0
	3	4	664	32	4.9	20	33.2	3.6
Road rater DSM (kips/in.)	1	3	337	88	26.3	10	16.8	105.4
	3	3	480	117	24.5	14	24.0	91.3
	3	4	492	102	20.7	14	24.6	66.0
Falling weight DSM (kips/in.)	1	3	378	41	10.9	27	18.9	18.1
	3	3	592	61	10.3	21	29.6	16.3
	3	4	473	45	9.6	21	23.6	14.0

Table 8

Results from Falling Weight Deflectometer Tests Performed Directly Over LVDT Gages

Item	Upper Layer Material	Upper Layer Thickness in.	Lower Layer Material	Lower Layer Thickness in.	Station ft	Force lb	Surface Deflection in.	Depth of Gage in.	Deflection at Depth in.
1	Crushed limestone	36	Heavy clay	36	0+21	4,290	0.0067	37.68	0.0024
						6,441	0.0109		0.0037
						8,909	0.0143		0.0051
						14,714	0.0210		0.0085
					0+18	4,349	0.0056	59.40	0.0011
						6,451	0.0081		0.0014
						8,935	0.0114		0.0021
						14,592	0.0181		0.0030
3	Blend II	56	--	--	1+33	4,386	0.0125	23.16	0.0031
						6,377	0.0189		0.0046
						9,126	0.0234		0.0067
						14,581	0.0354		0.0107
					1+30	4,370	0.0118	49.32	0.0011
						6,393	0.0202		0.0015
						8,803	0.0232		0.0019
						14,439	0.0340		0.0031
5	Silt	53	--	--	2+33	4,126	0.0275	14.28	0.0051
						6,335	0.0378		0.0079
						9,020	0.0512		0.0122
						14,518	0.0755		0.0196
					2+30	4,115	0.0314	47.04	0.0001
						6,229	0.0422		0.0024
						8,898	0.0562		0.0033
						14,545	0.0815		0.0055

Table 9

Falling Weight Deflectometer Deflection Data Obtained Over LVDT Gages, Modulus Values Determined from BISDEF, and a Comparison of Measured and Predicted Deflections

Item	Station	Falling Weight Deflectometer Force lb	Deflection, mils Distance from Center of Plate, in. 0	18	36	For a Two-Layer System Layer 1 Thickness in.	Material	E from BISDEF psi	Layer 2 Thickness in.	Material	E from BISDEF psi	Depth in.	Measured Vertical Displacement mils	Computed Vertical Displacement mils	Error %
1	0+21	14,714	21.0	6.5	3.4	36.0	Crushed stone	71,538	--	CH/CL	20,881	0	21.0	21.2	1.0
												37.68	8.5	5.9	30.6
	0+18	14,592	18.1	6.6	3.3	36.0	Crushed stone	86,051	--	CH/CL	19,582	0	18.1	18.3	1.1
												59.4	3.0	3.7	23.3
3	1+33	14,581	35.4	7.8	3.9	72.0	Blend II	37,507	--	CL	13,255	0	35.4	35.6	0.3
												23.16	10.7	9.5	11.2
	1+30	14,439	34.0	7.7	4.0	72.0	Blend II	39,012	--	CL	12,127	0	34.0	34.3	0.9
												49.32	3.1	5.5	77.4
5	2+33	14,518	75.5	10.6	4.4	72.0	Silt	16,815	--	CL	30,062	0	75.5	73.5	2.6
												14.28	19.6	24.8	26.5
	2+30	14,545	81.5	10.9	4.6	72.0	Silt	15,543	--	CL	33,041	0	81.5	79.3	2.7
												47.0	5.5	6.0	9.1

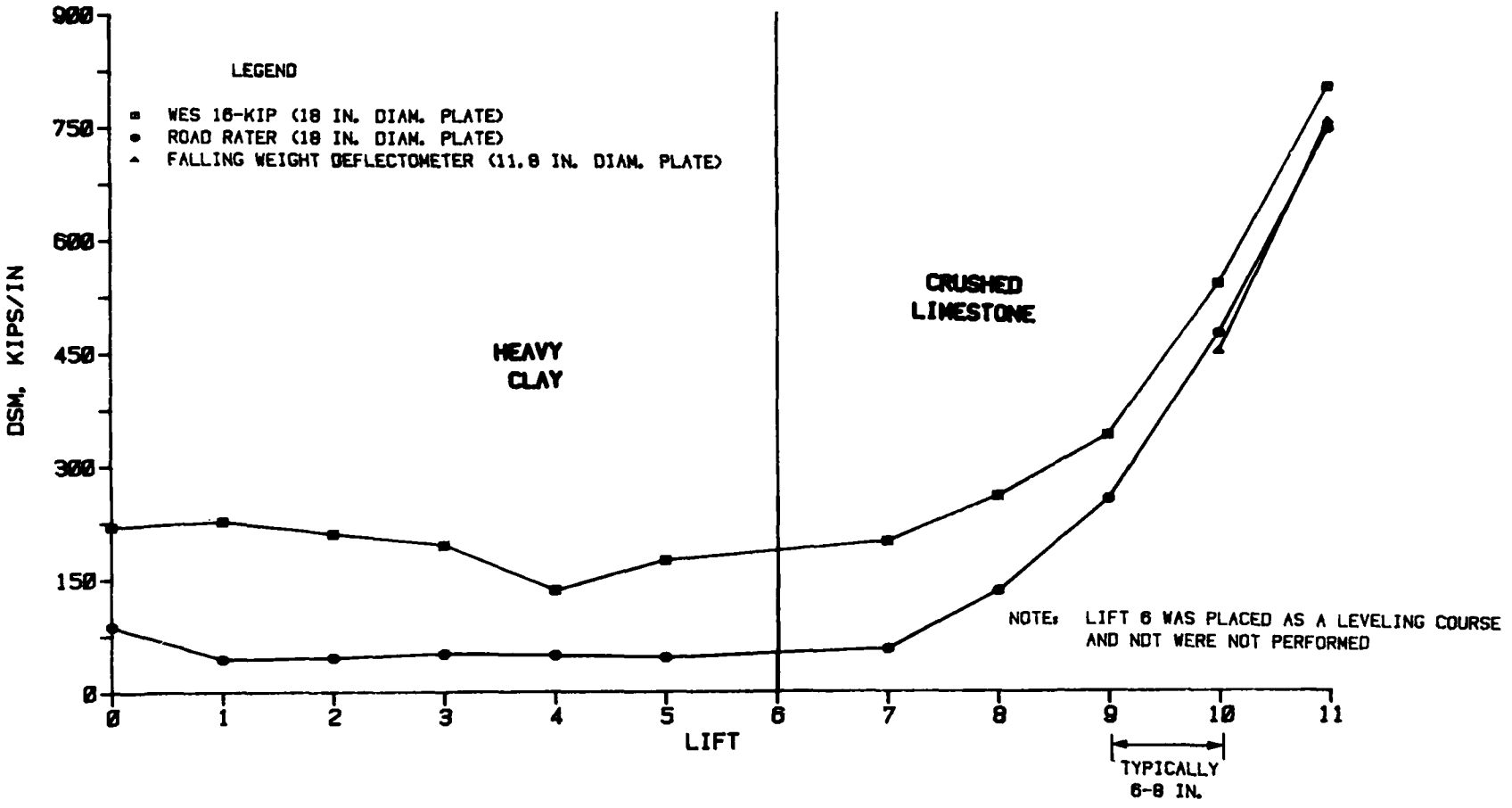

Figure 1. Nondestructive test results during construction; lane 1, Item 1

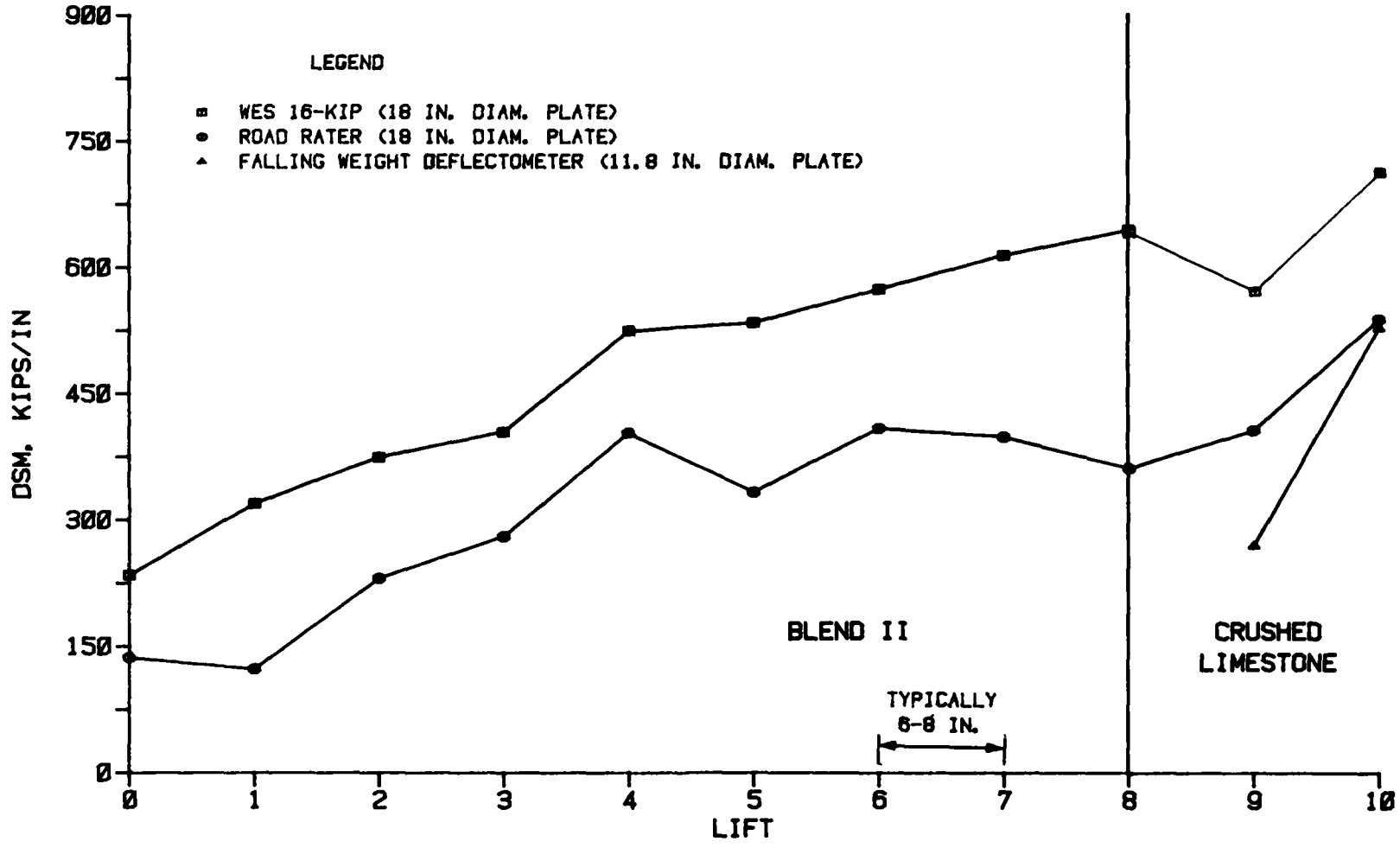

Figure 2. Nondestructive test results during construction; lane 1, Item 2

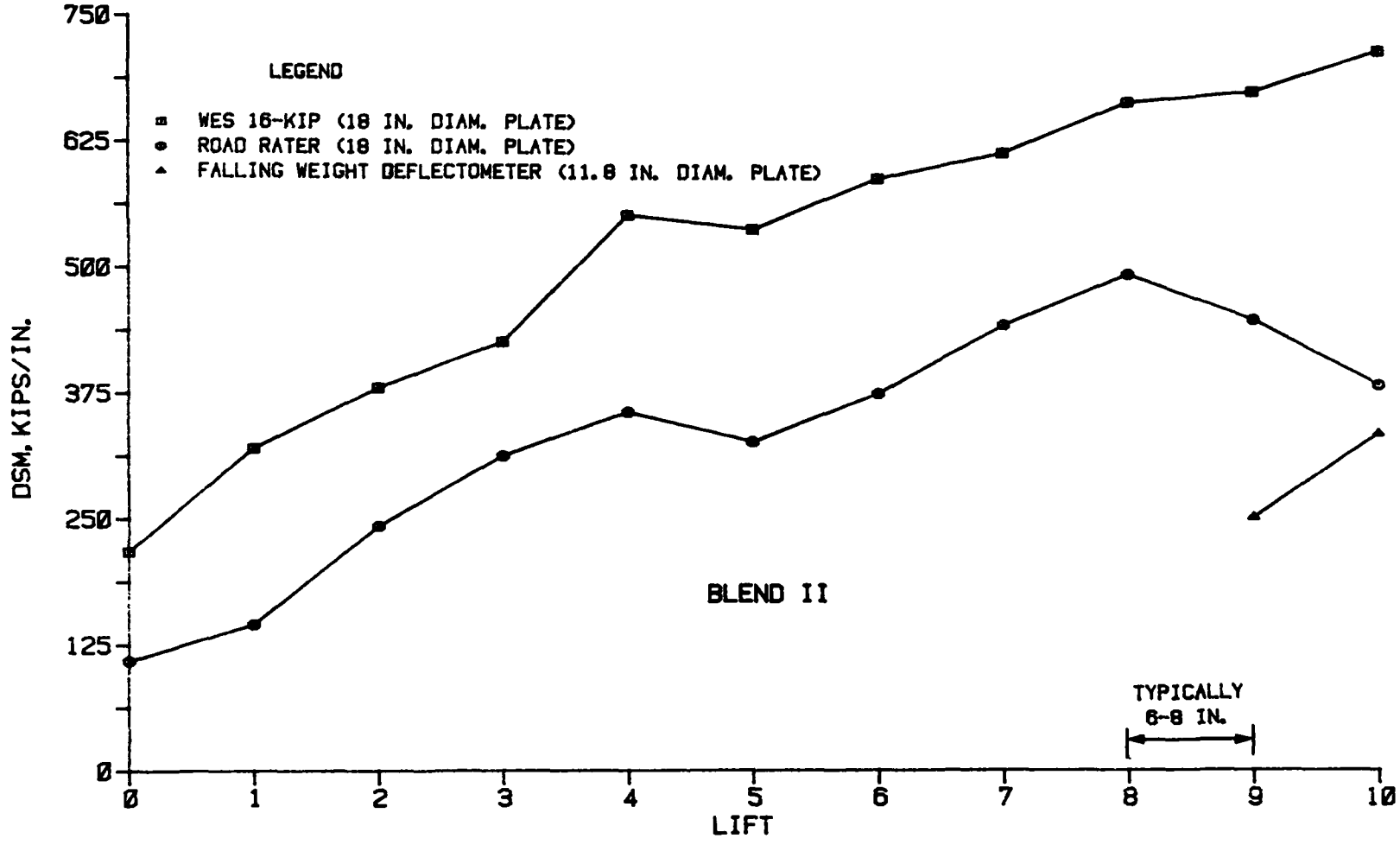

Figure 3. Nondestructive test results during construction; lane 1, Item 3

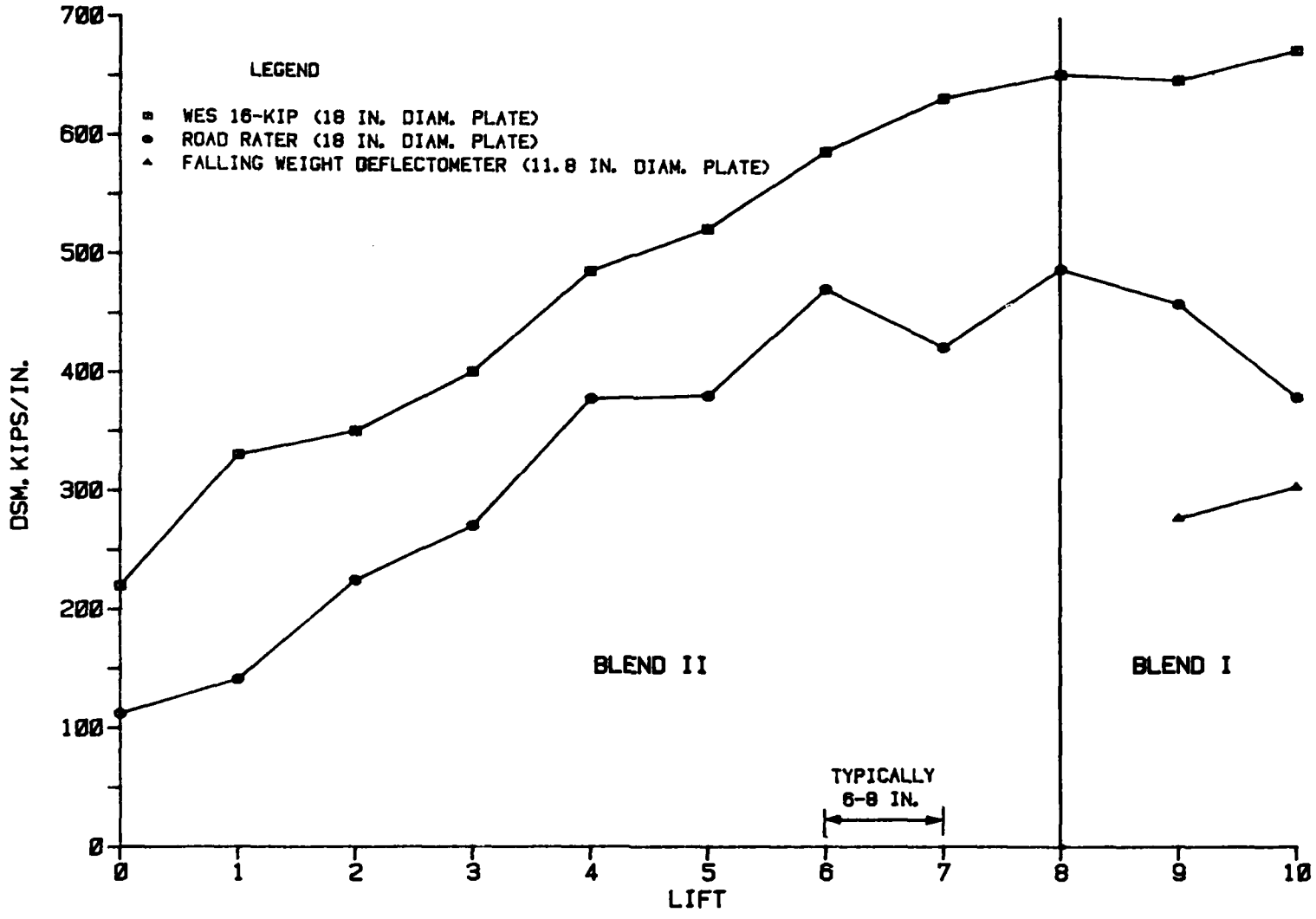

Figure 4. Nondestructive test results during construction; lane 1, Item 4

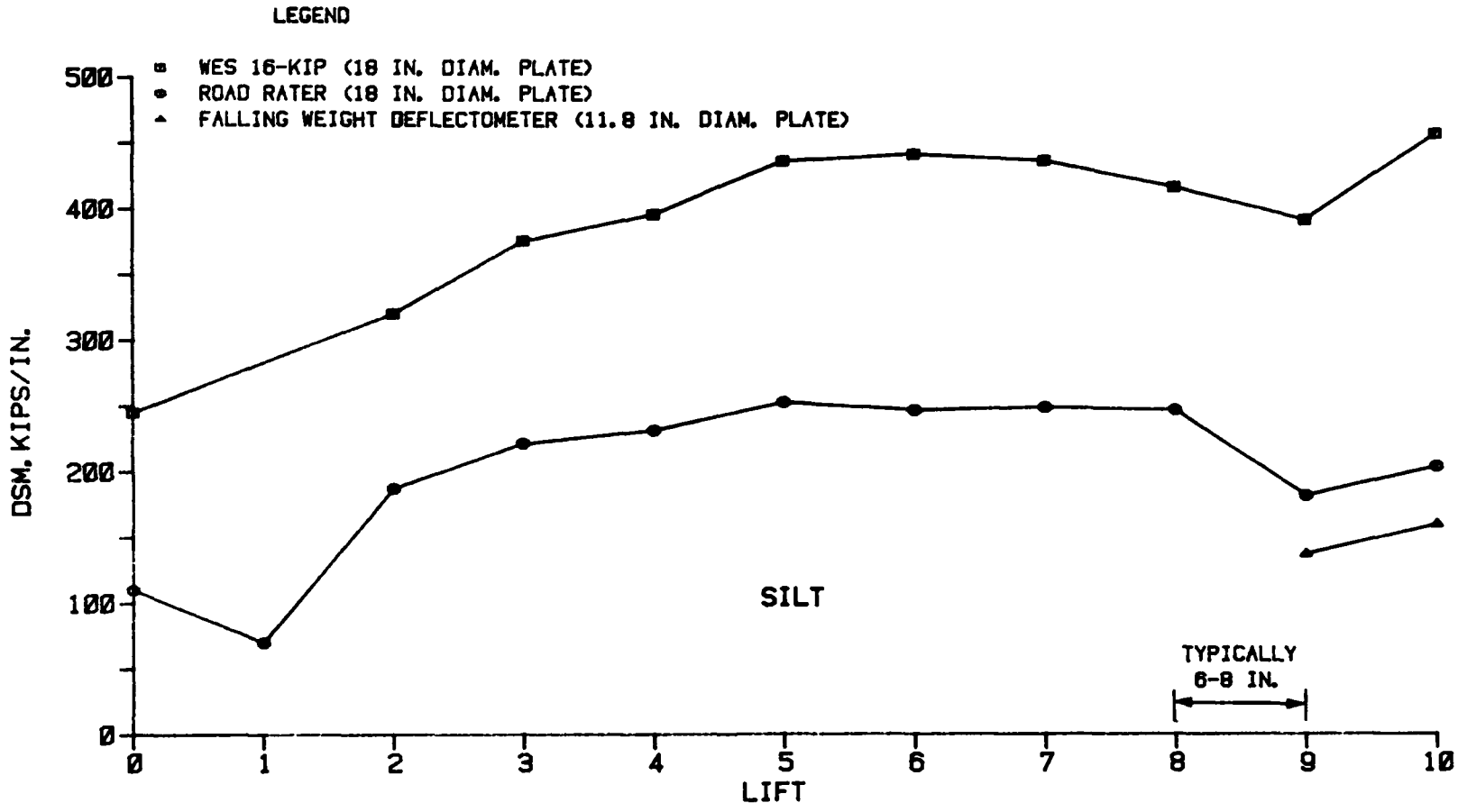

Figure 5. Nondestructive test results during construction; lane 1, Item 5

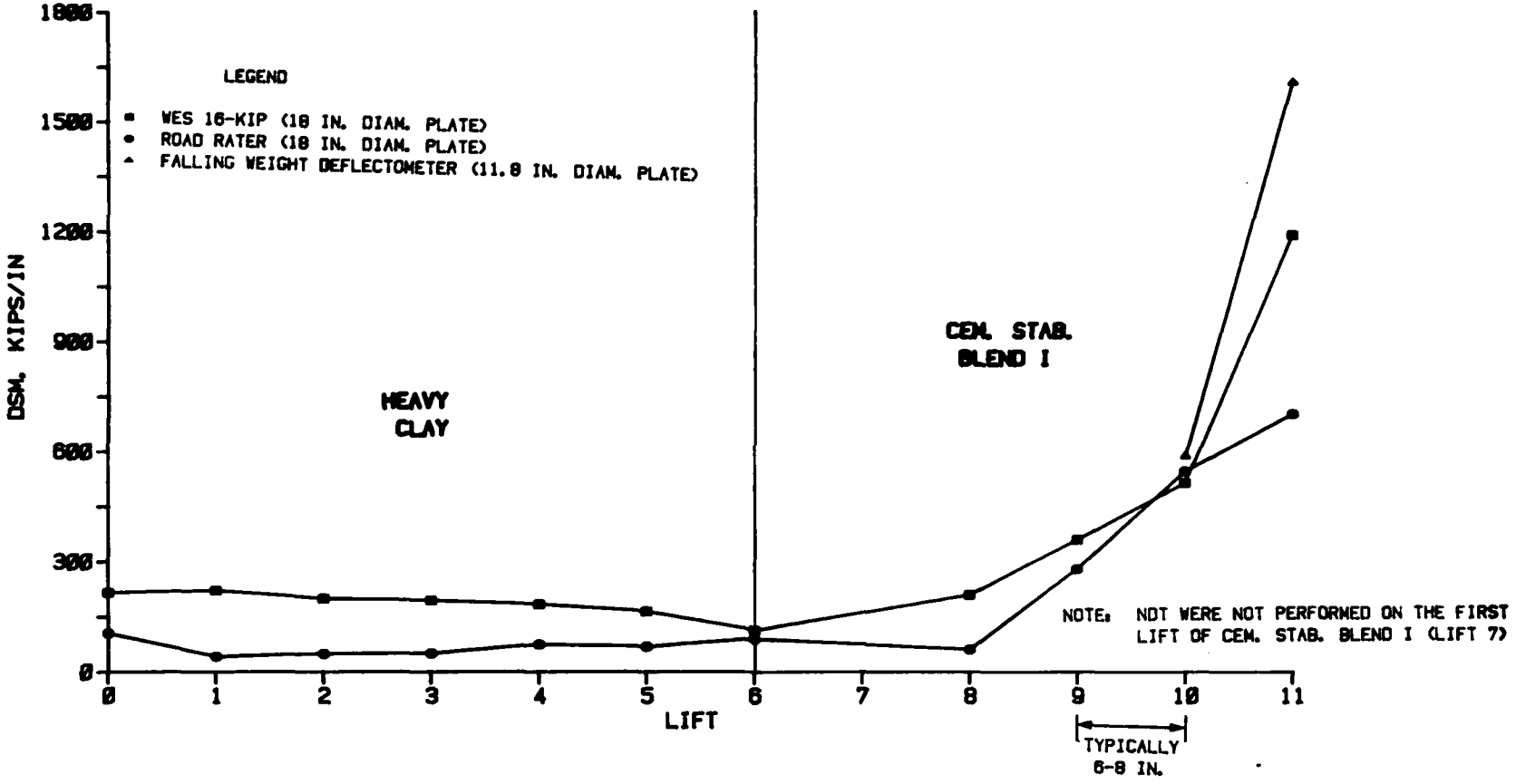

Figure 6. Nondestructive test results during construction; lane 2, Item 1

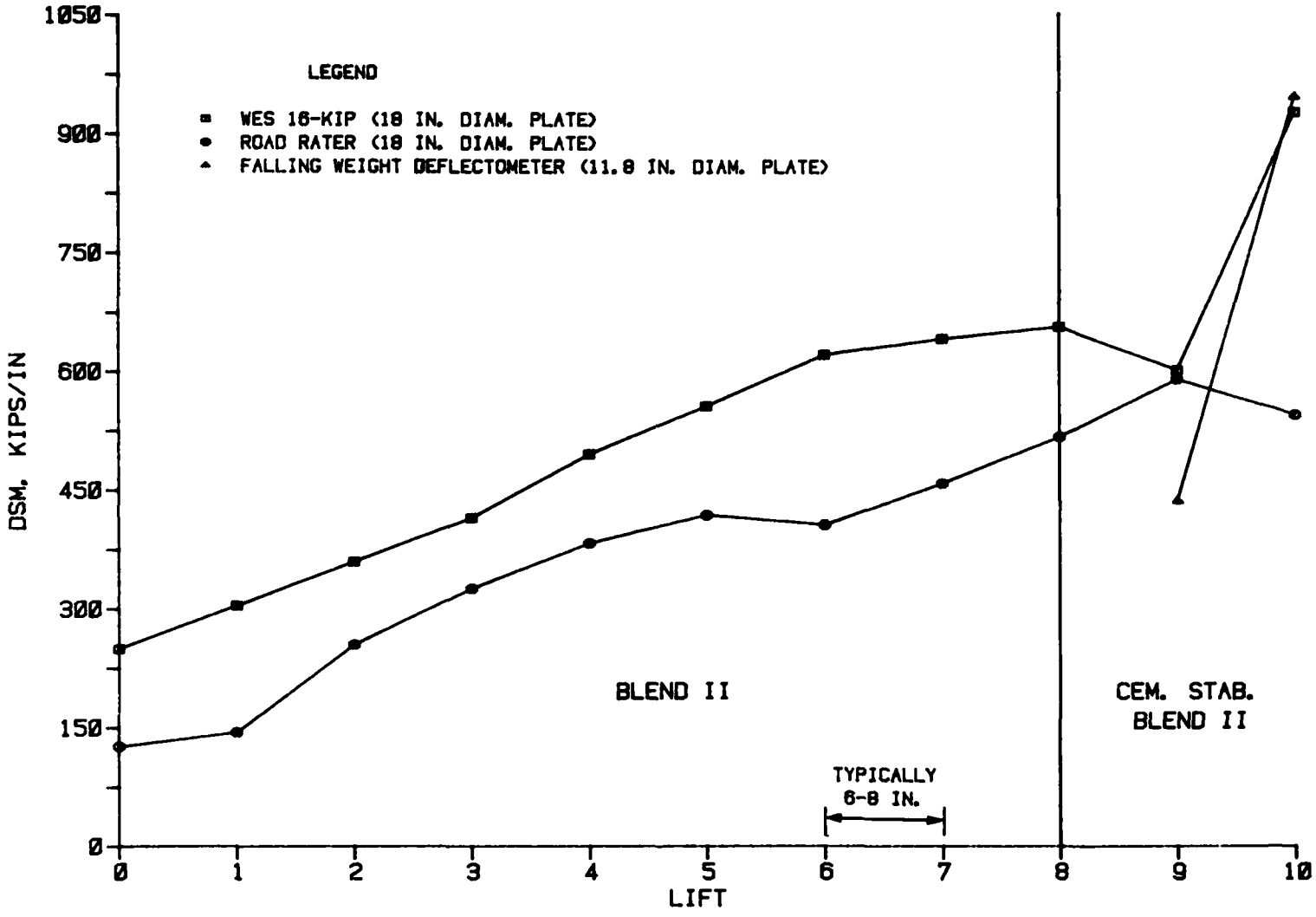

Figure 7. Nondestructive test results during construction; lane 2, Item 2

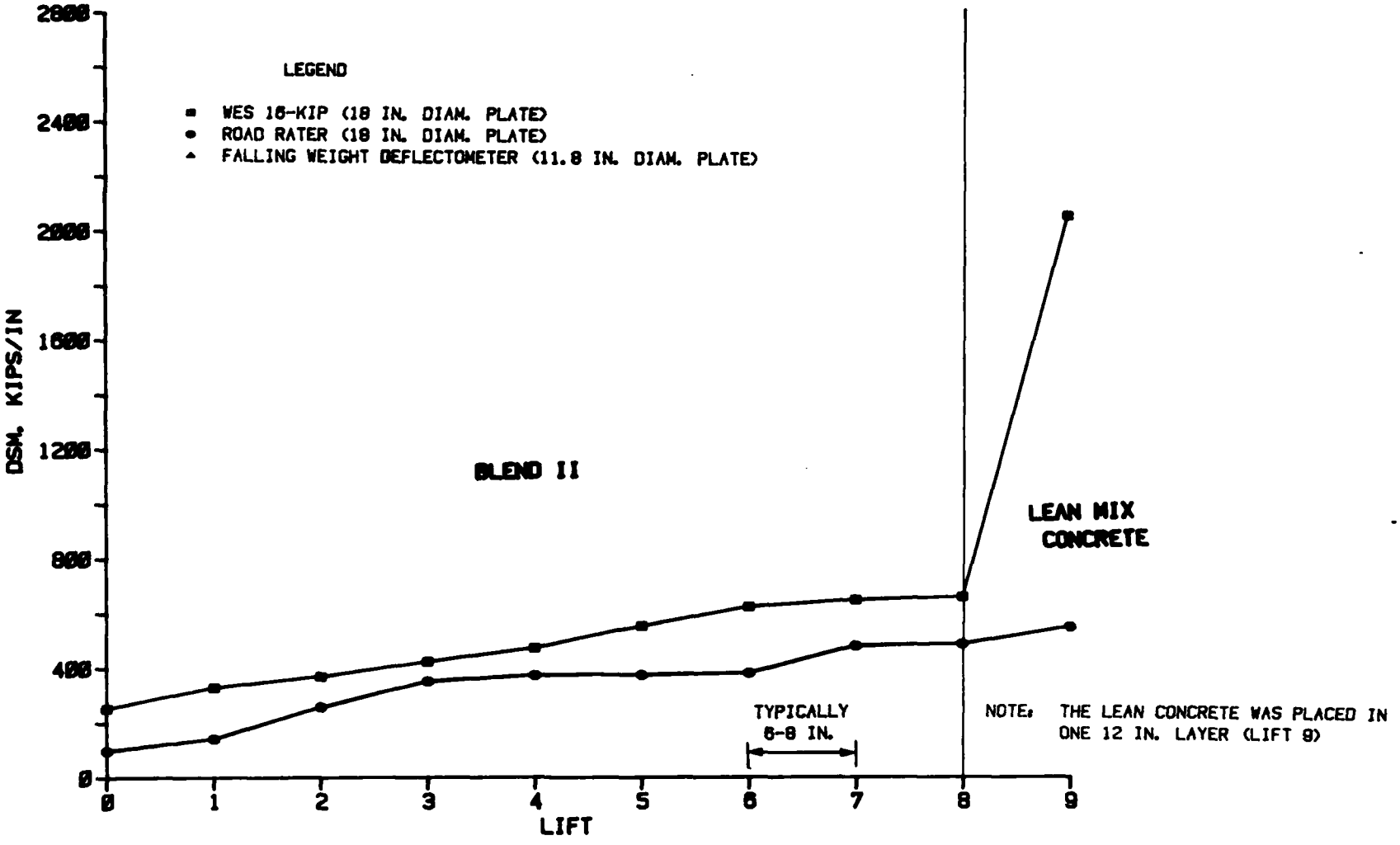

Figure 8. Nondestructive test results during construction; lane 2, Item 3

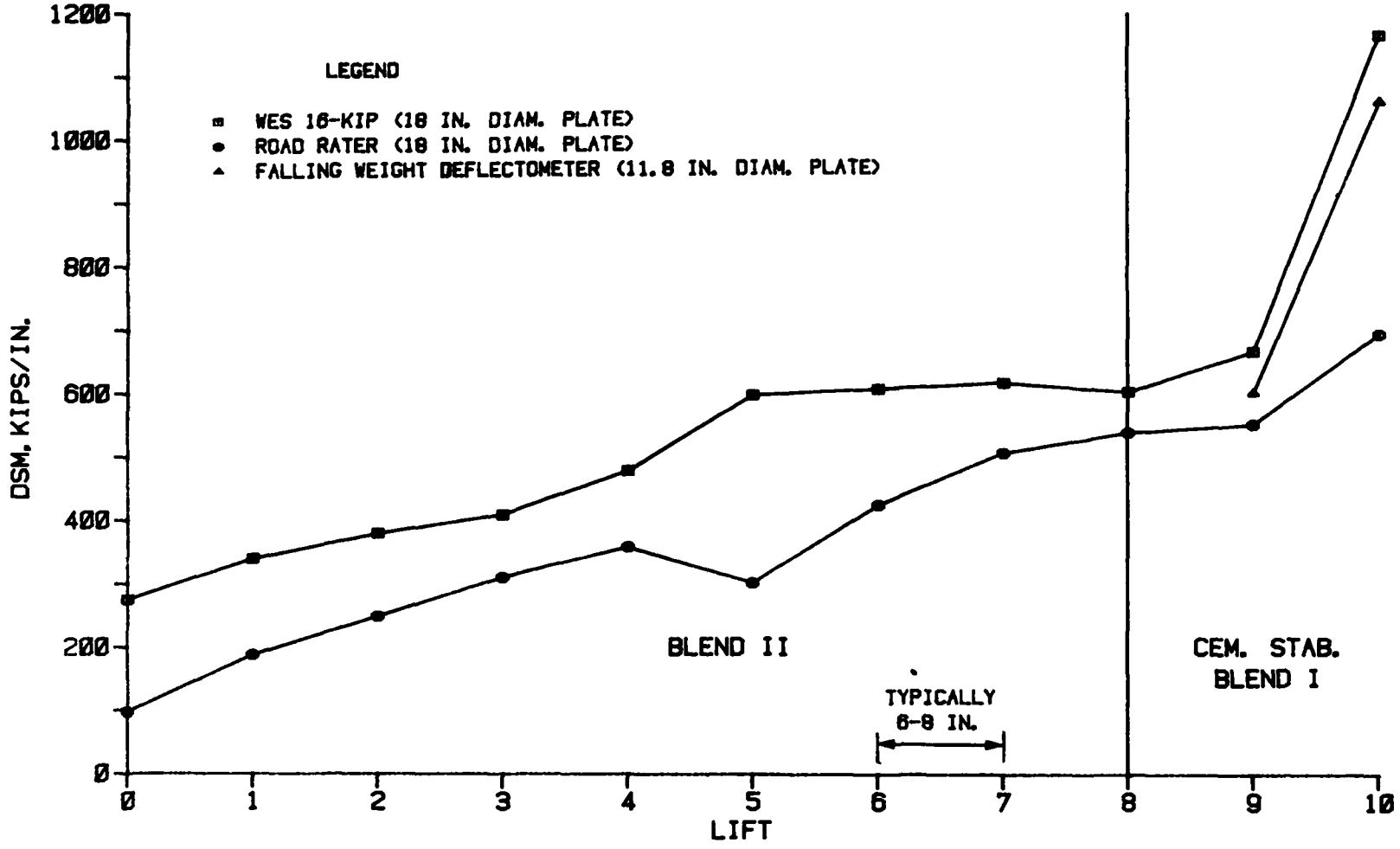

Figure 9. Nondestructive test results during construction; lane 2, Item 4

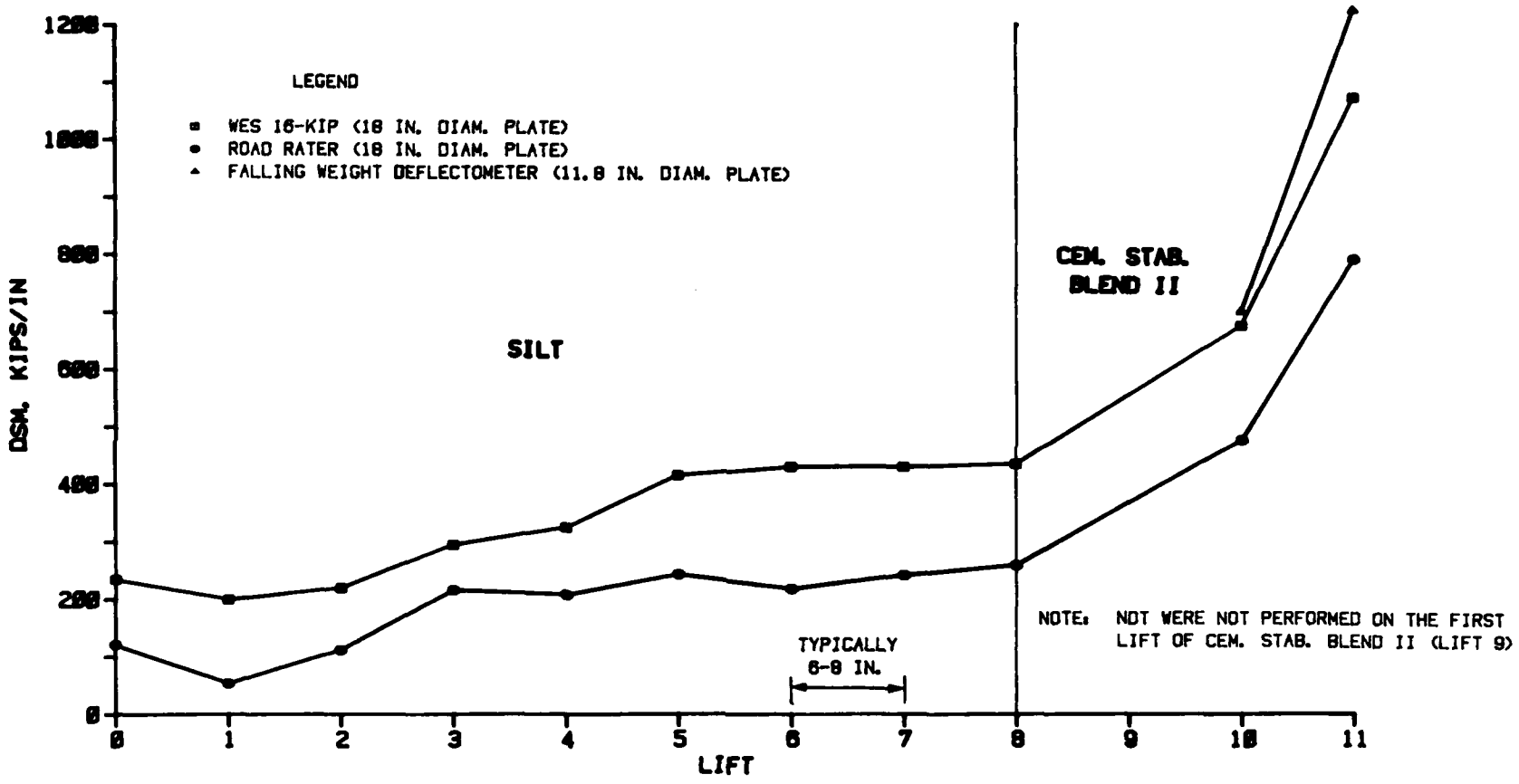

Figure 10. Nondestructive test results during construction; lane 2, Item 5

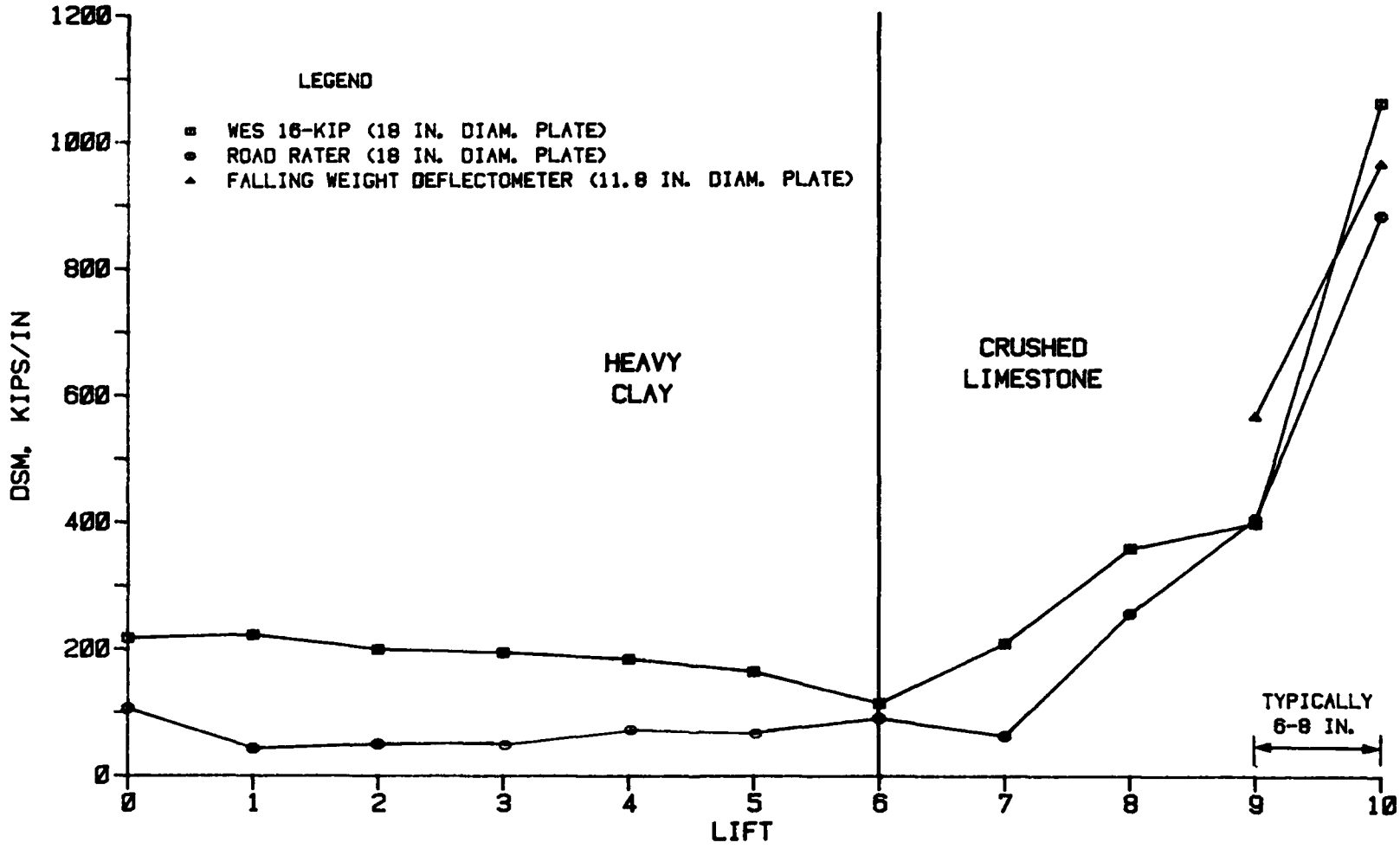

Figure 11. Nondestructive test results during construction; lane 3, Item 1

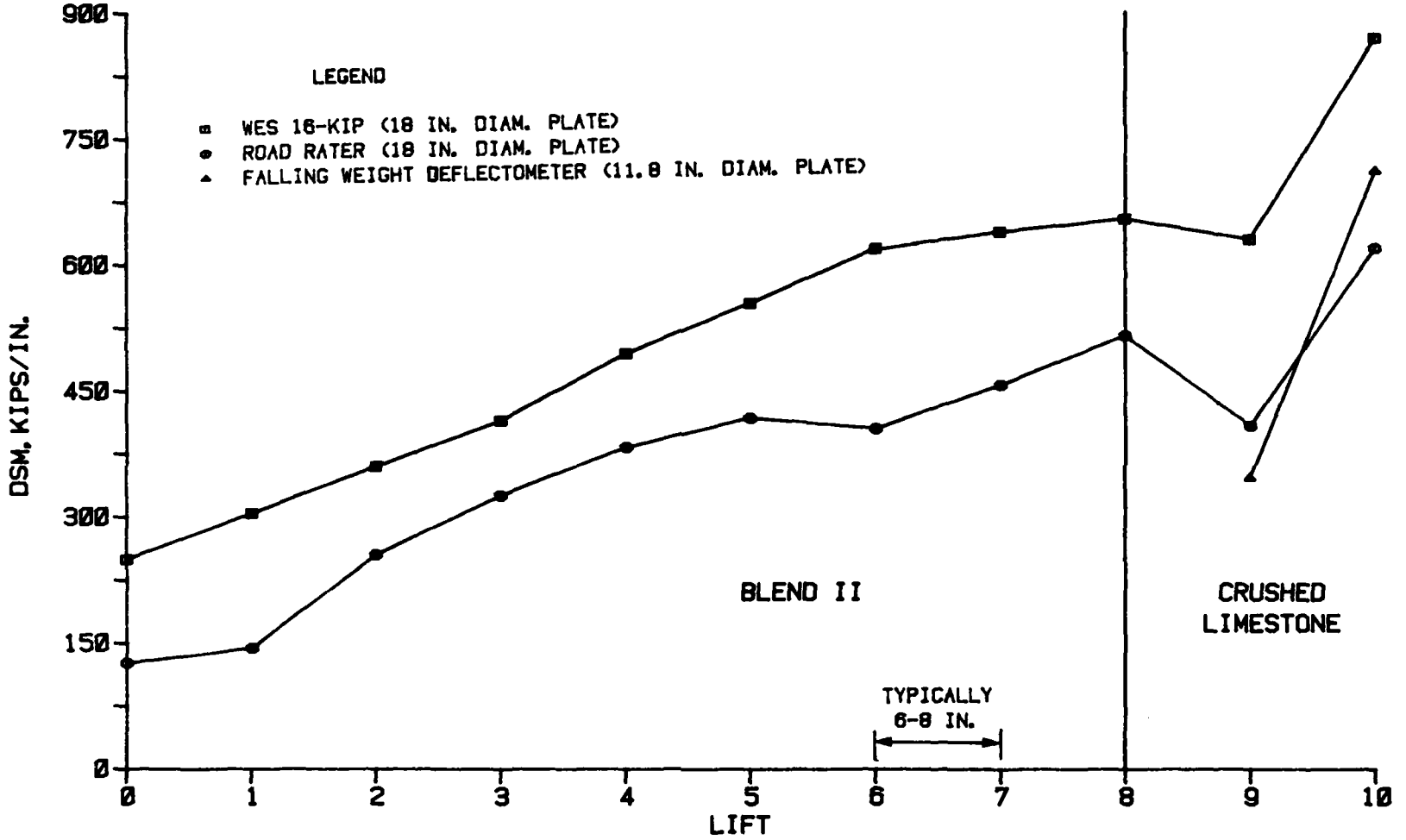

Figure 12. Nondestructive test results during construction; lane 3, Item 2

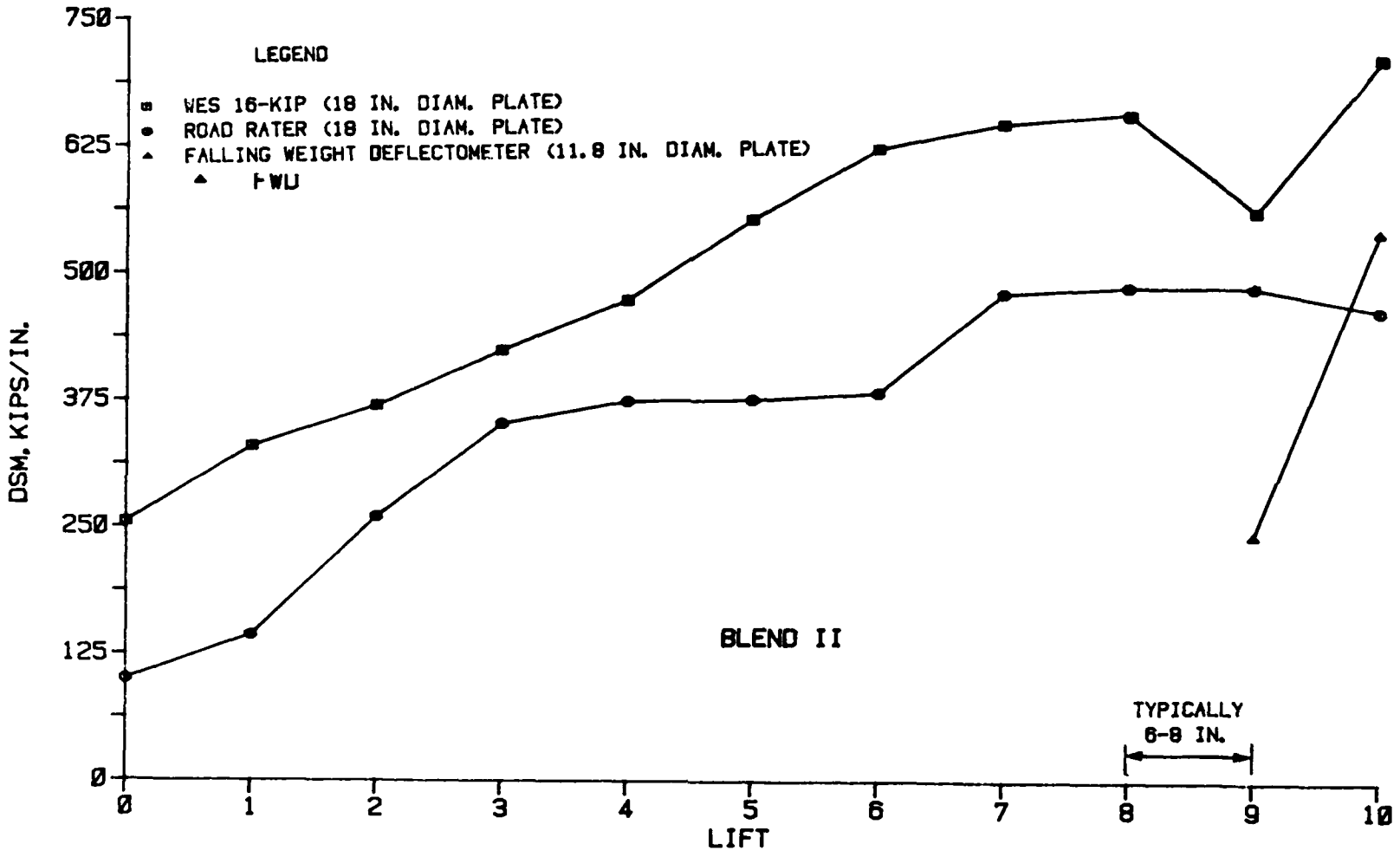

Figure 13. Nondestructive test results during construction; lane 3, Item 3

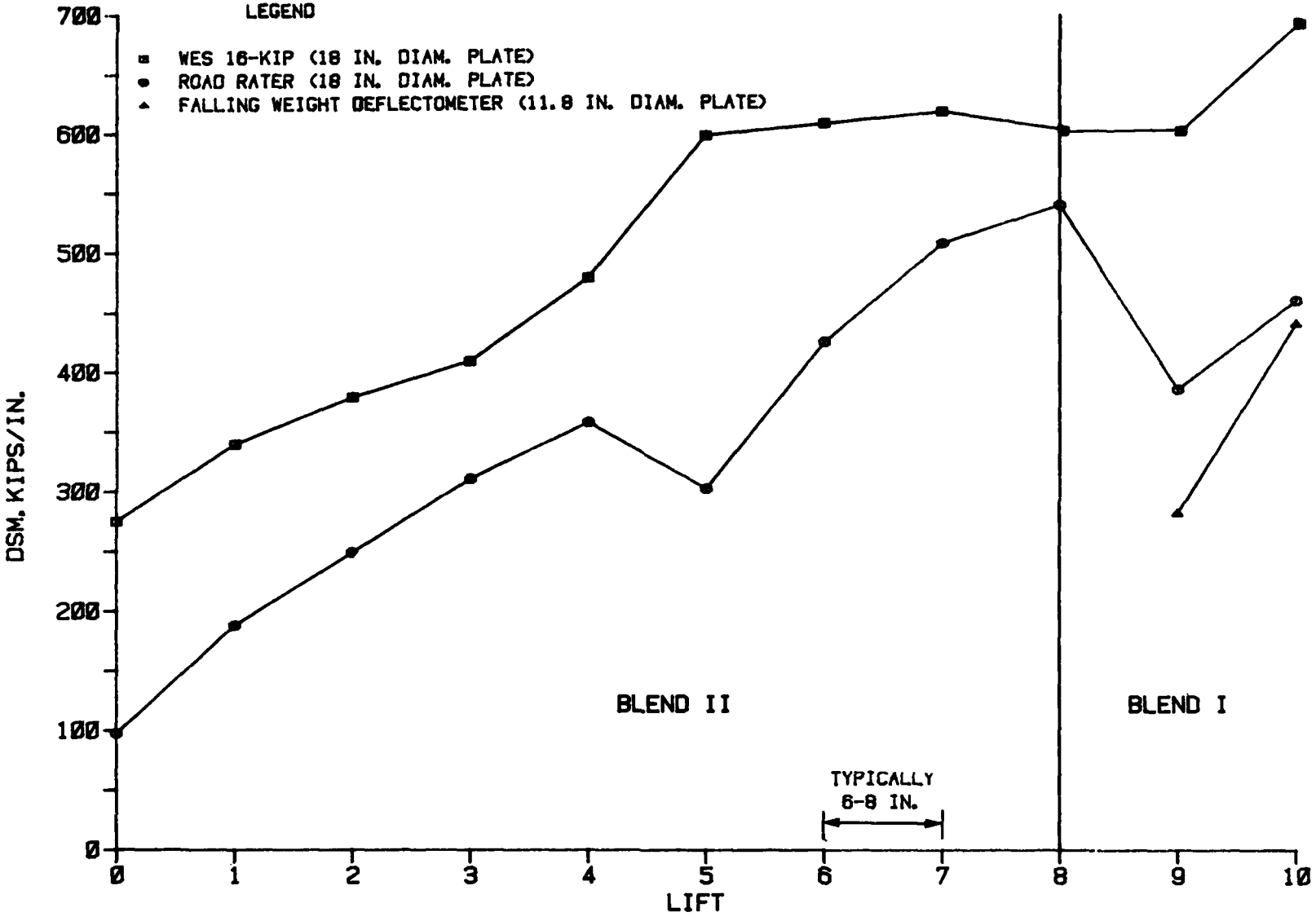

Figure 14. Nondestructive test results during construction; lane 3, Item 4

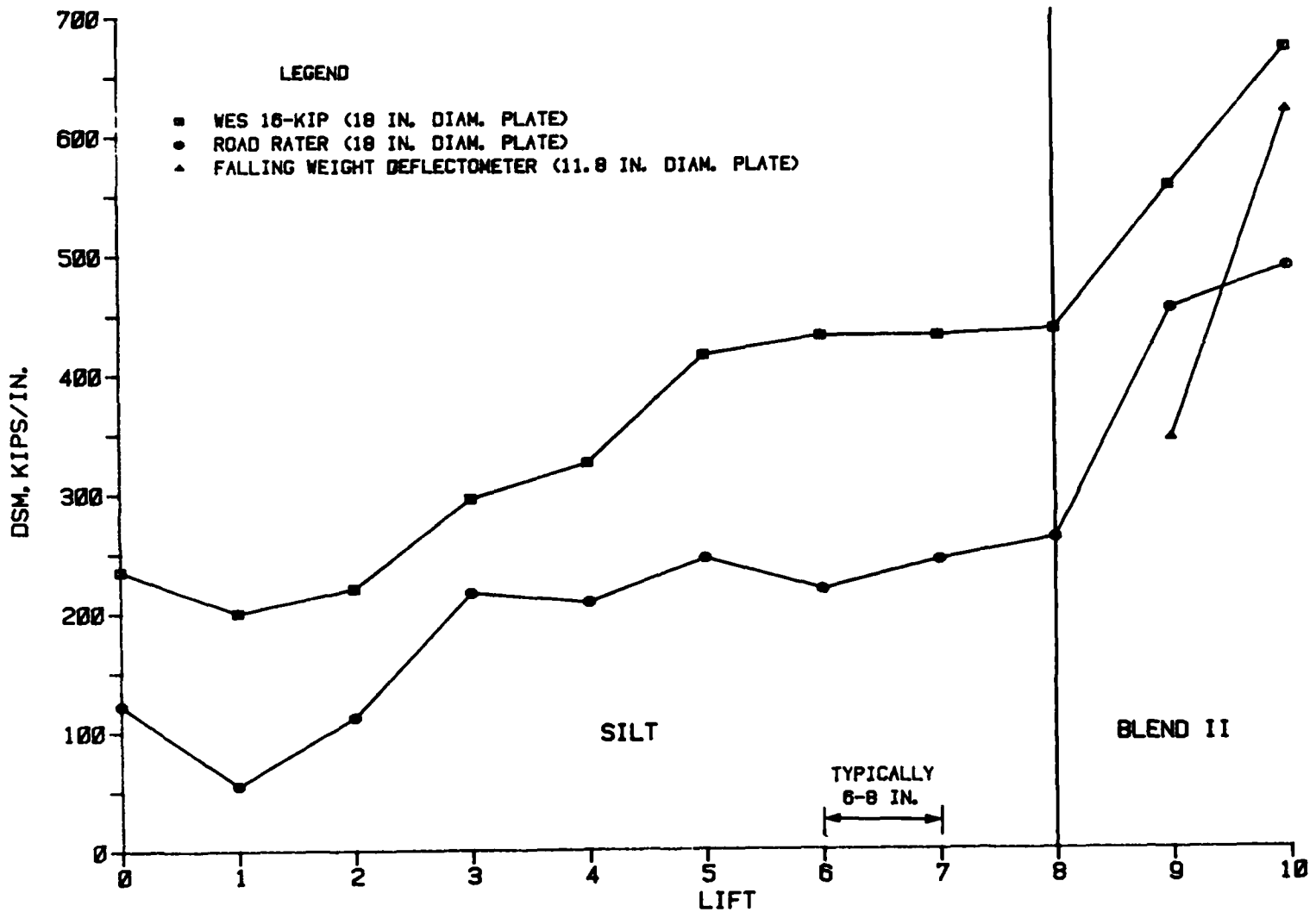

Figure 15. Nondestructive test results during construction; lane 3, Item 5

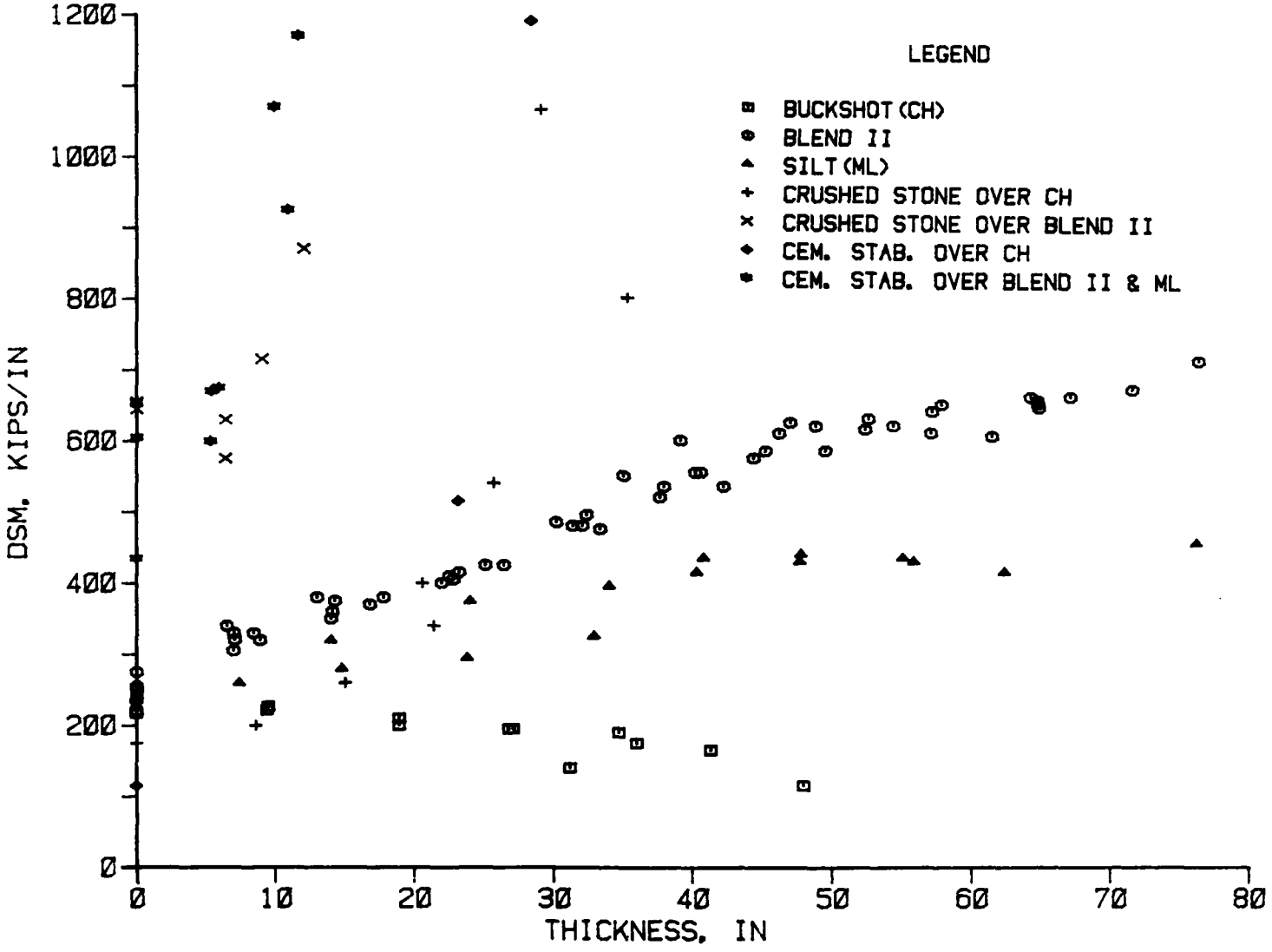

Figure 16. 16-kip DSM versus thickness (during construction)

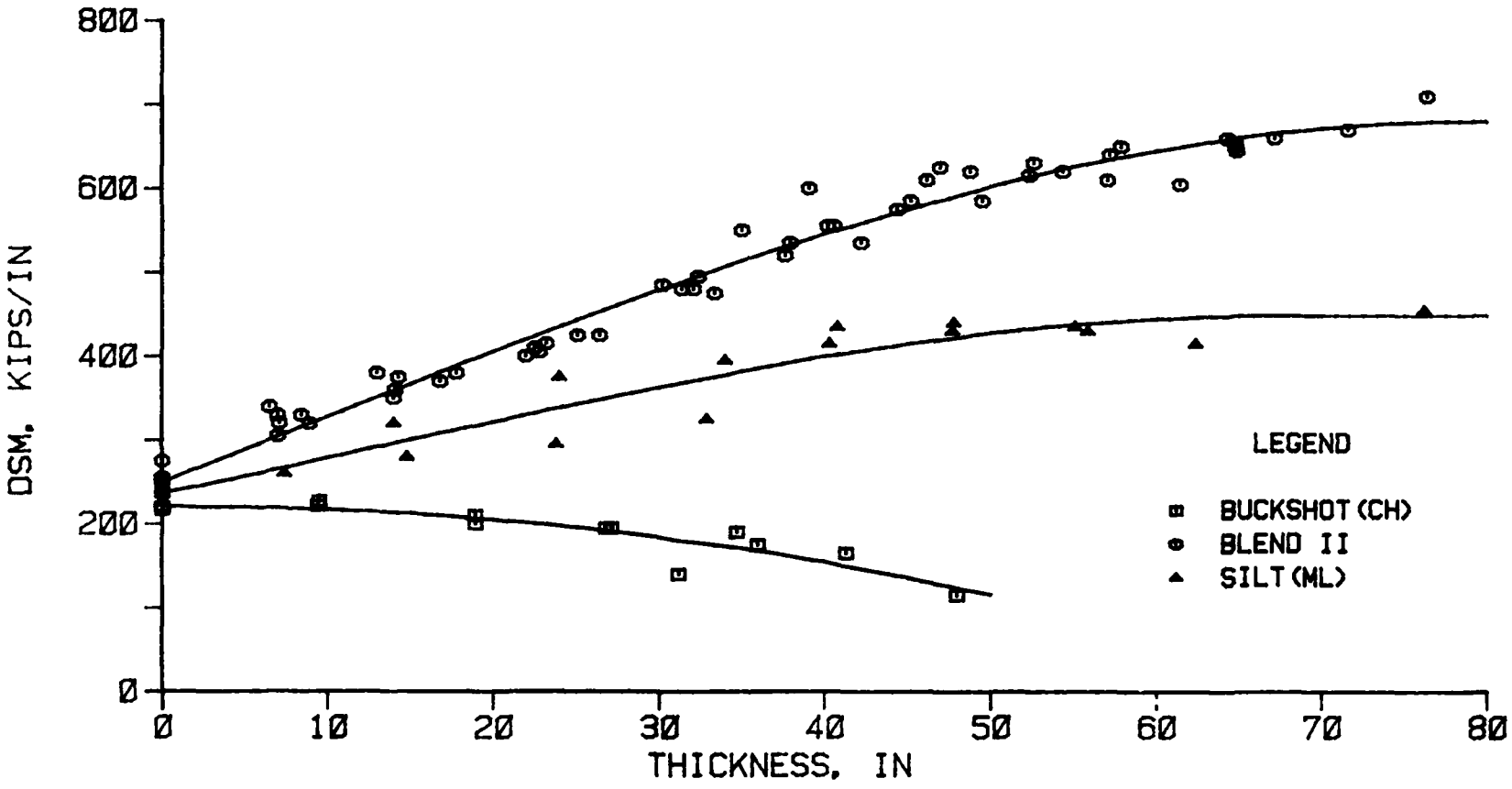

Figure 17. 16-kip DSM versus thickness of buckshot, Blend II, and silt with best-fit curves

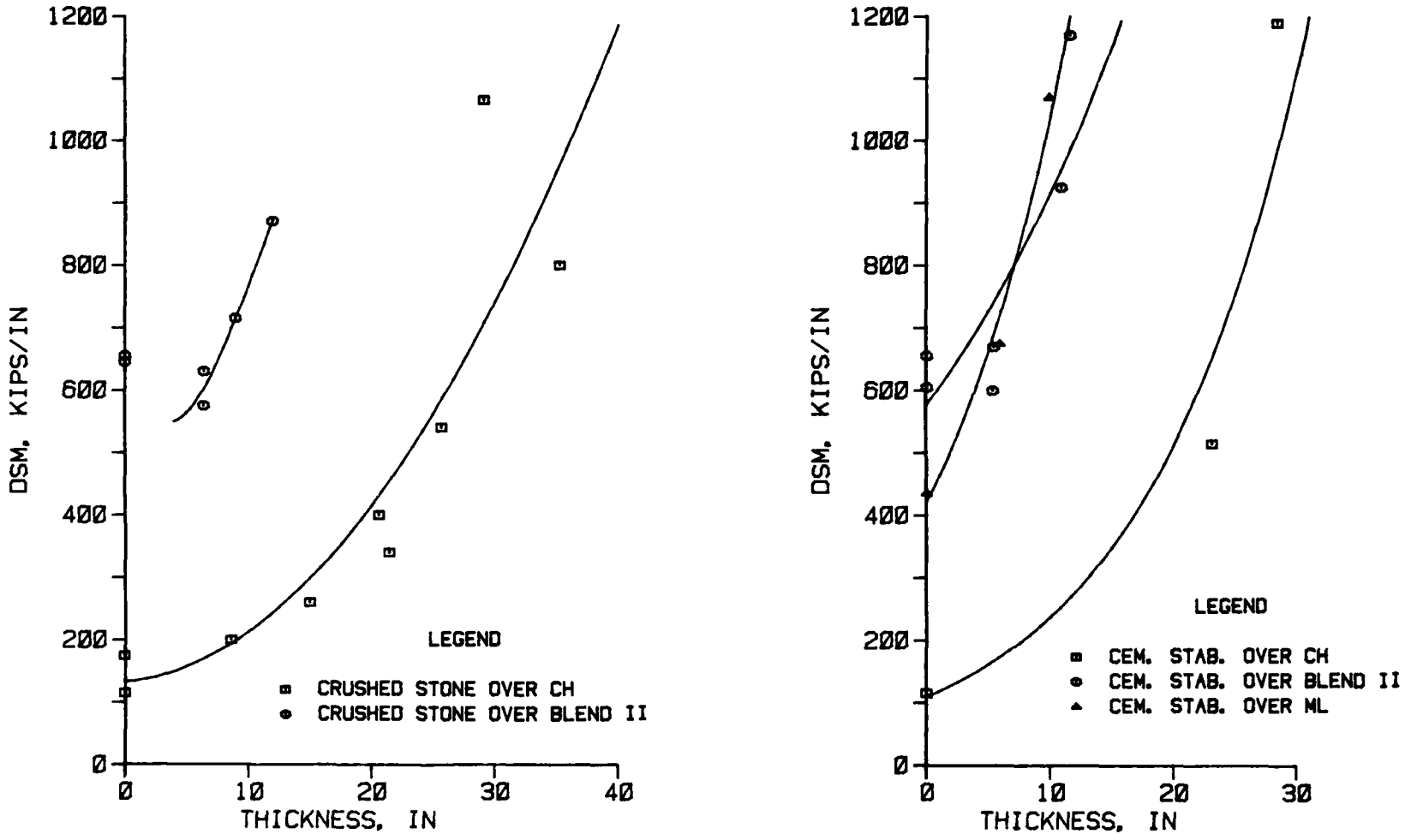

Figure 18. 16-kip DSM versus thickness for crushed stone and cement-stabilized soils with best-fit curves

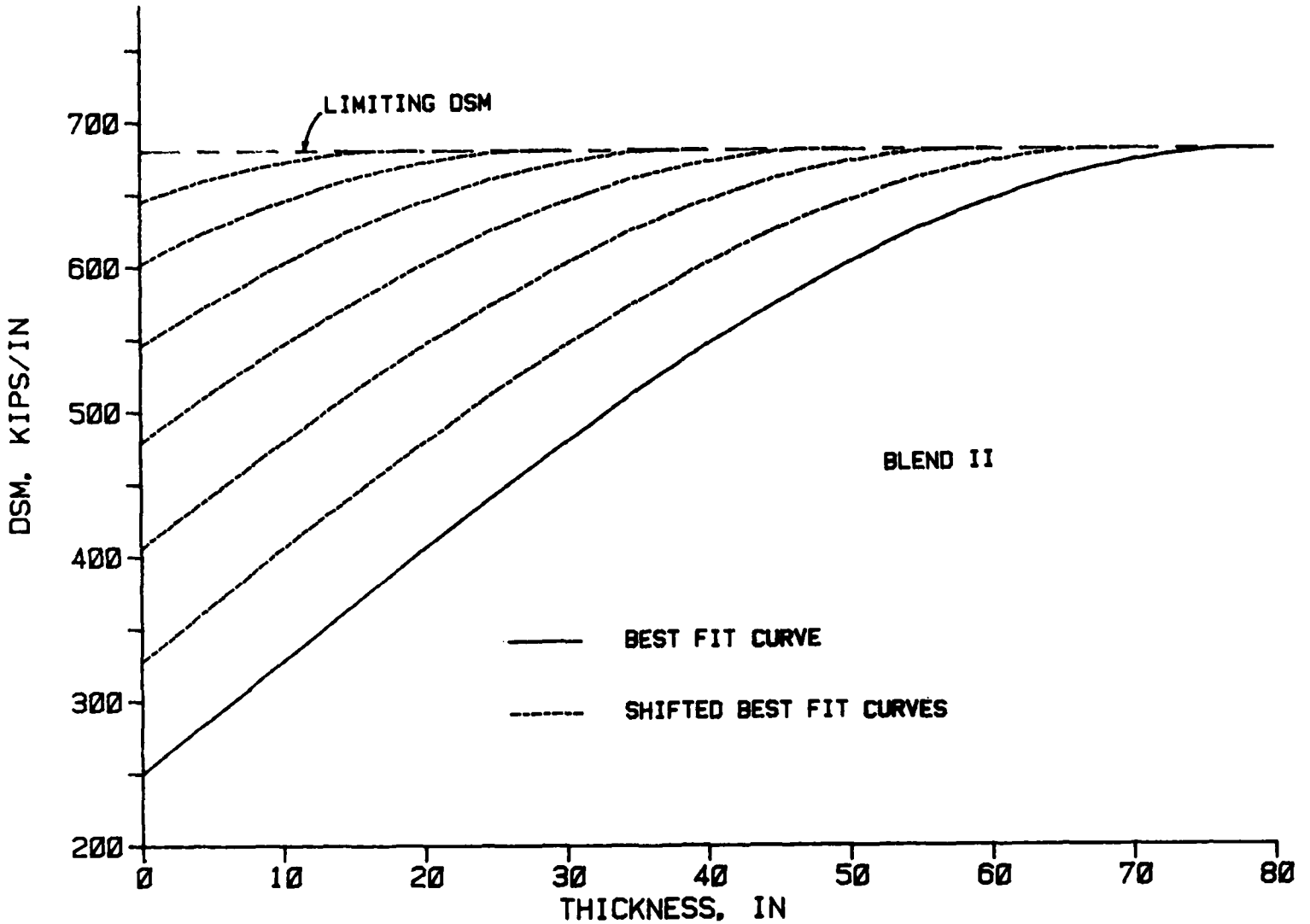

Figure 19. Limiting DSM concept of Blend II based on a best-fit curve from the test data

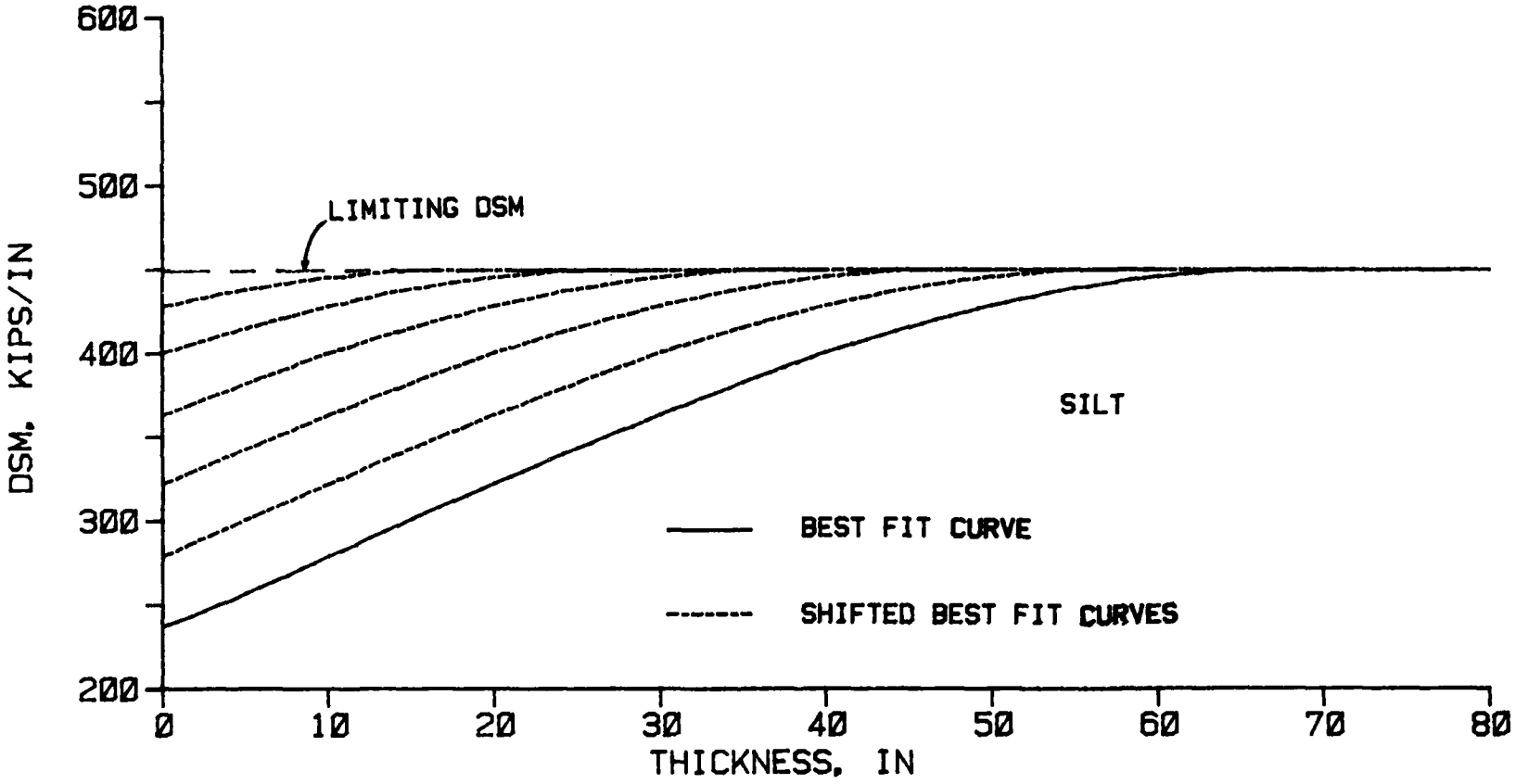

Figure 20. Limiting DSM concept for silt based on a best-fit curve from the test data

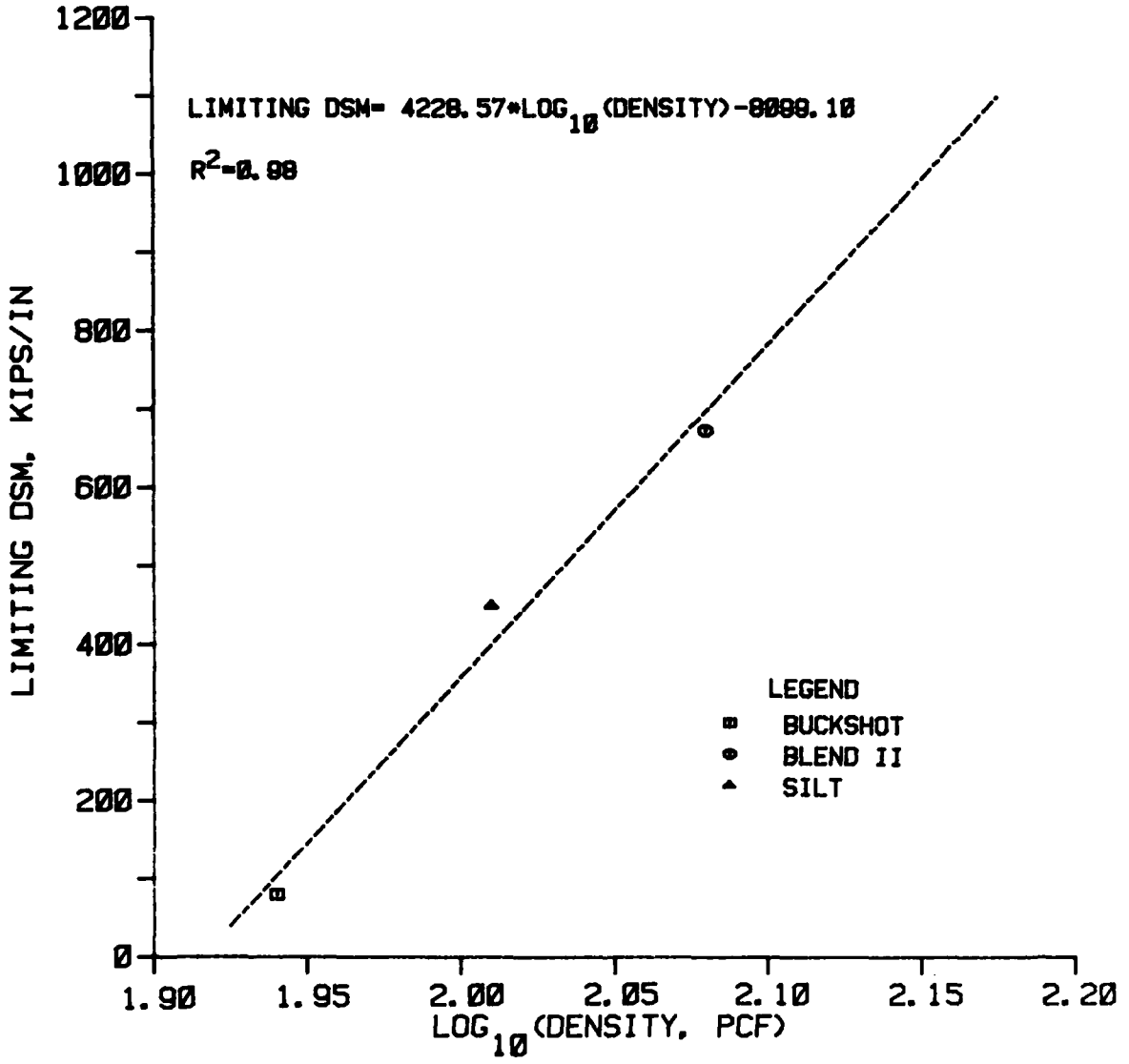

Figure 21. Limiting DSM versus in-place dry density

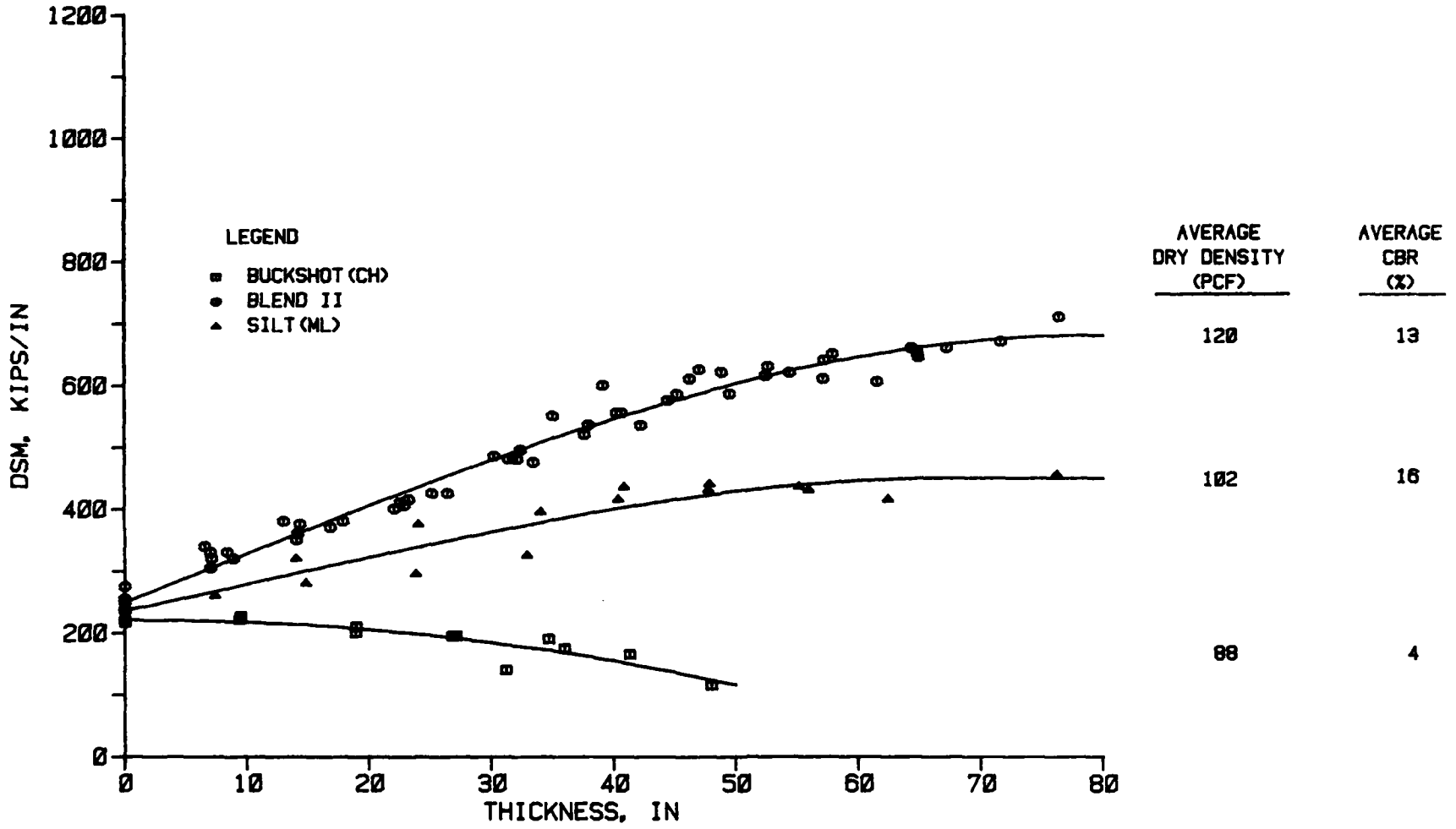

Figure 22. DSM versus thickness for CH, Blend II, and ML soils with in-place densities and CBR's

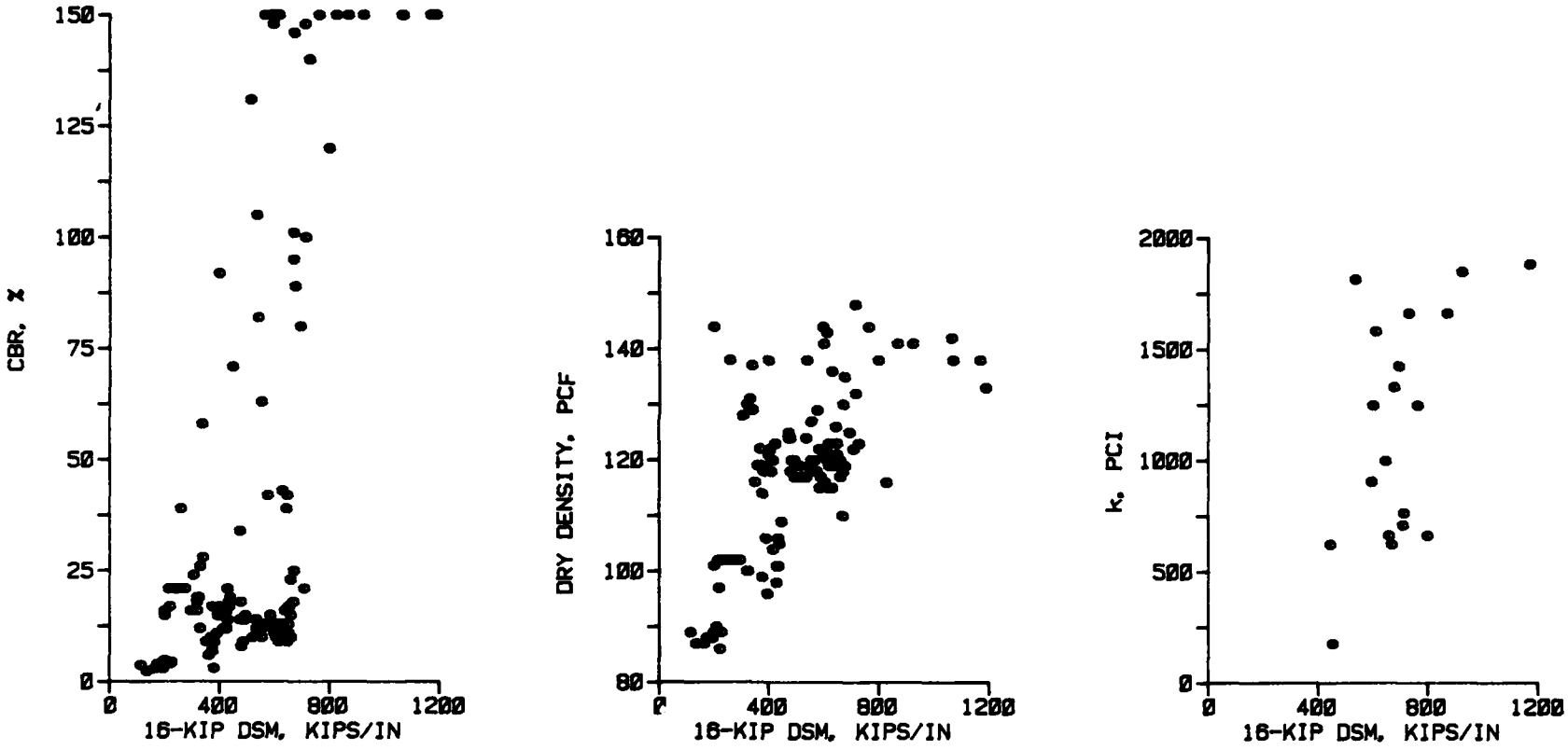

Figure 23. Comparison of 16-kip DSM to CBR, density, and k

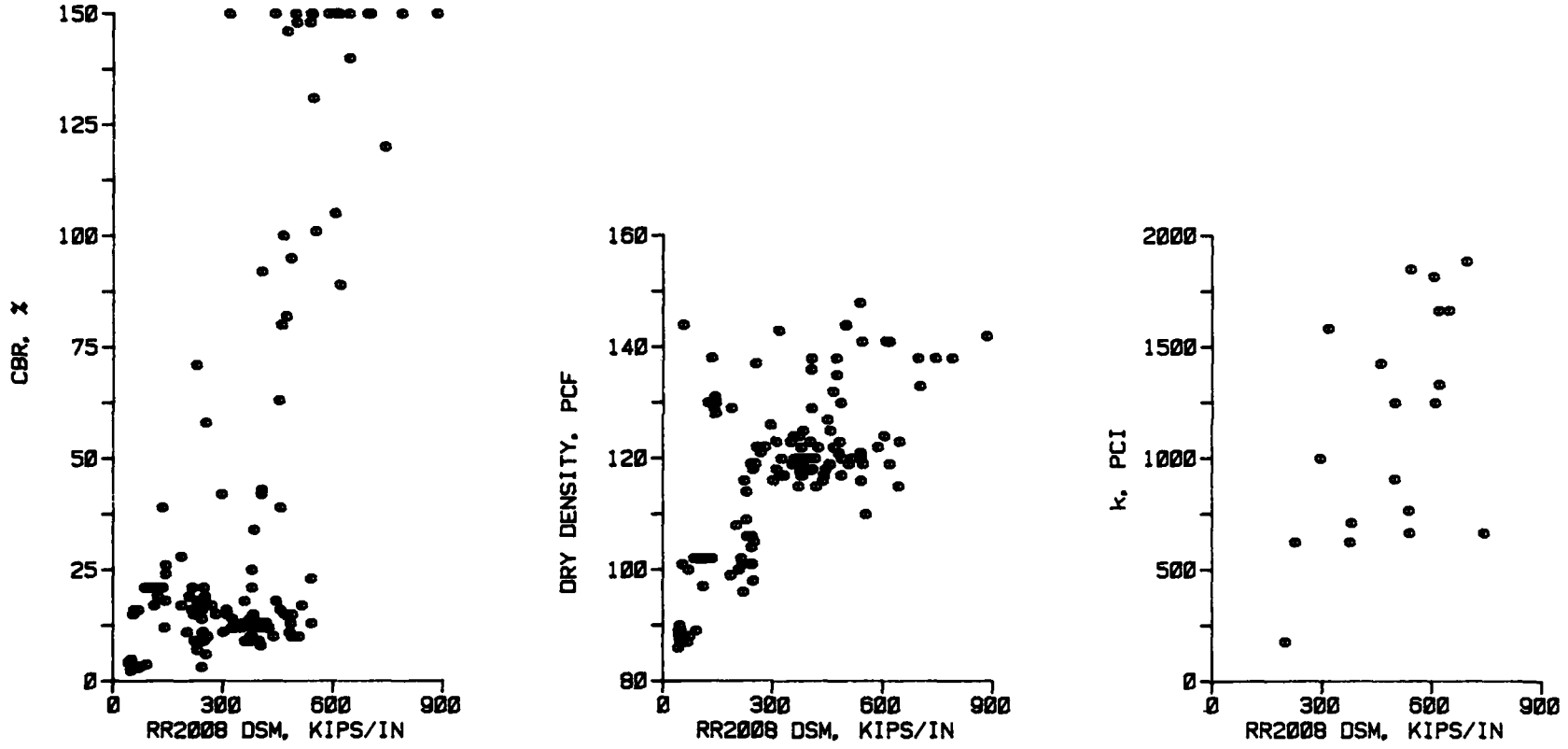

Figure 24. Comparison of Road Rater 2008 DSM to CBR, density, and k

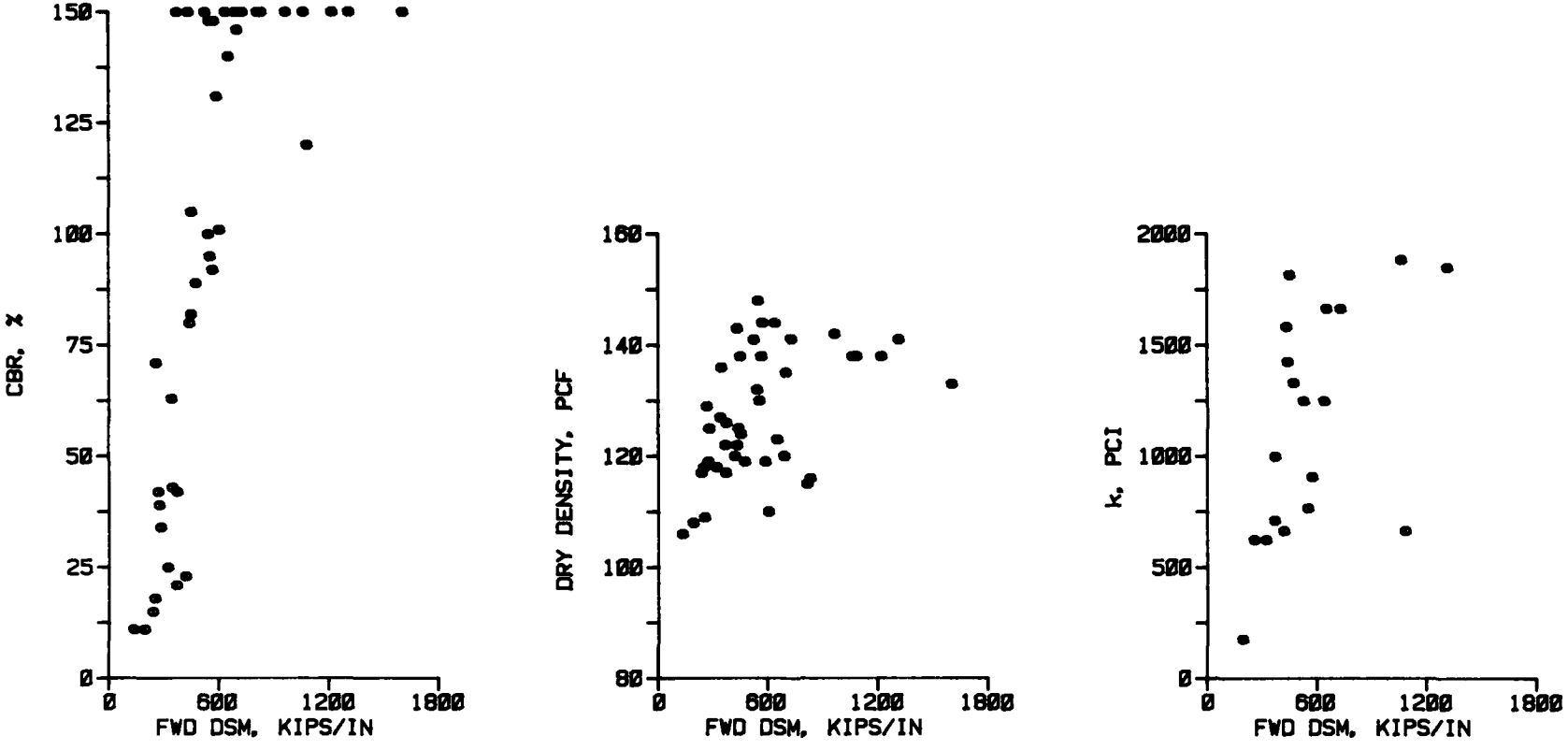

Figure 25. Comparison of Falling Weight Deflectometer DSM to CBR, density, and k

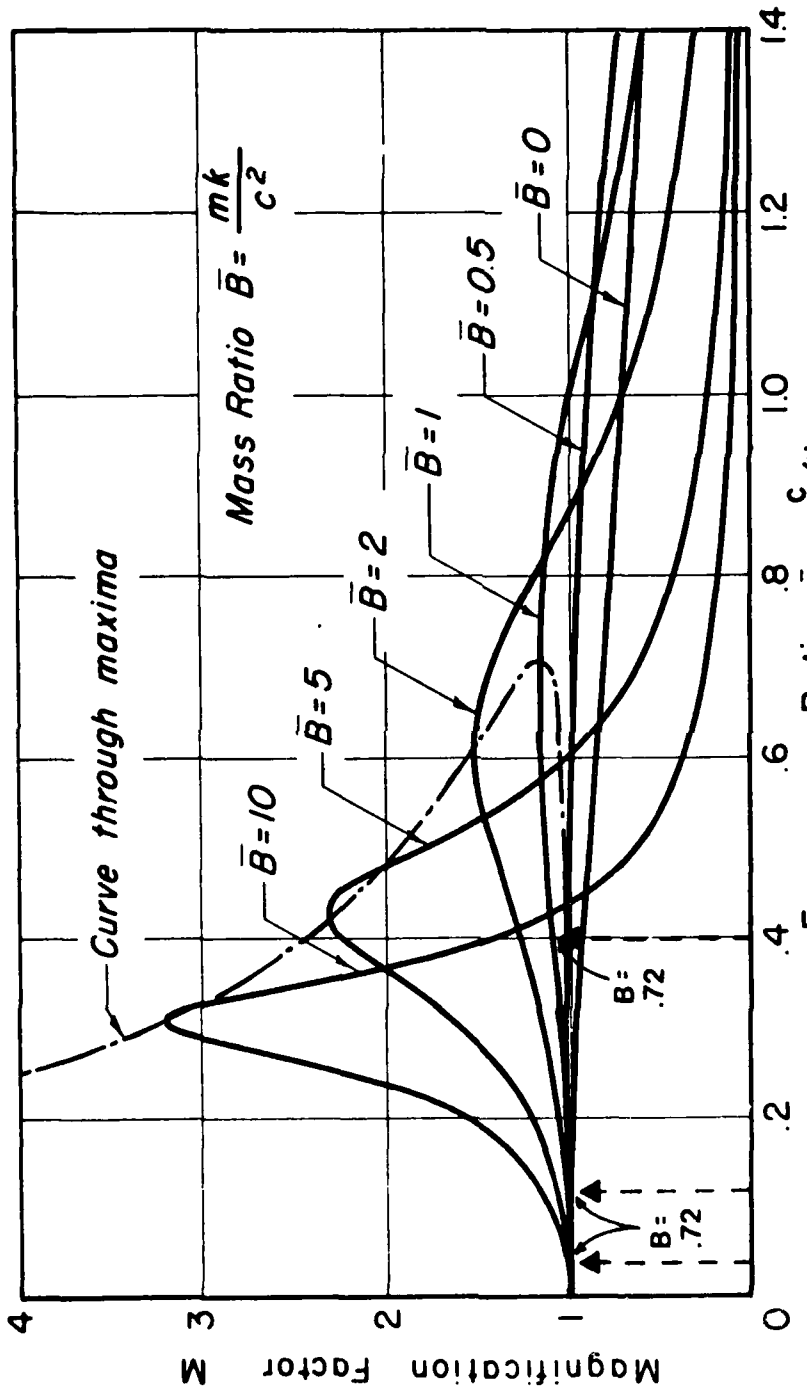

Figure 26. Steady-state spectra for simple damped oscillator

AD-A167 672 CORRELATION OF NONDESTRUCTIVE PAVEMENT EVALUATION TEST RESULTS WITH RESUL..(U) ARMY ENGINEER WATERWAYS EXPERIMENT STATION VICKSBURG MS GEOTE.. D R ALEXANDER 2/2

UNCLASSIFIED FEB 86 WES/TR/GL-86-1-VOL-1 F/G 14/2 NL

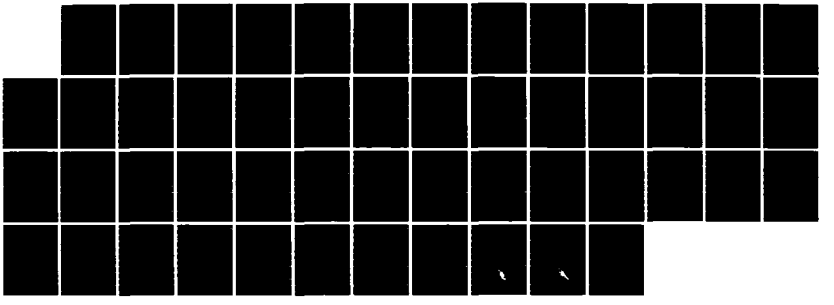

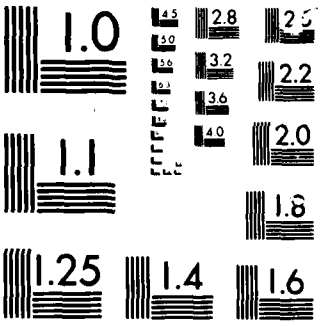

MICROCOPY CHART

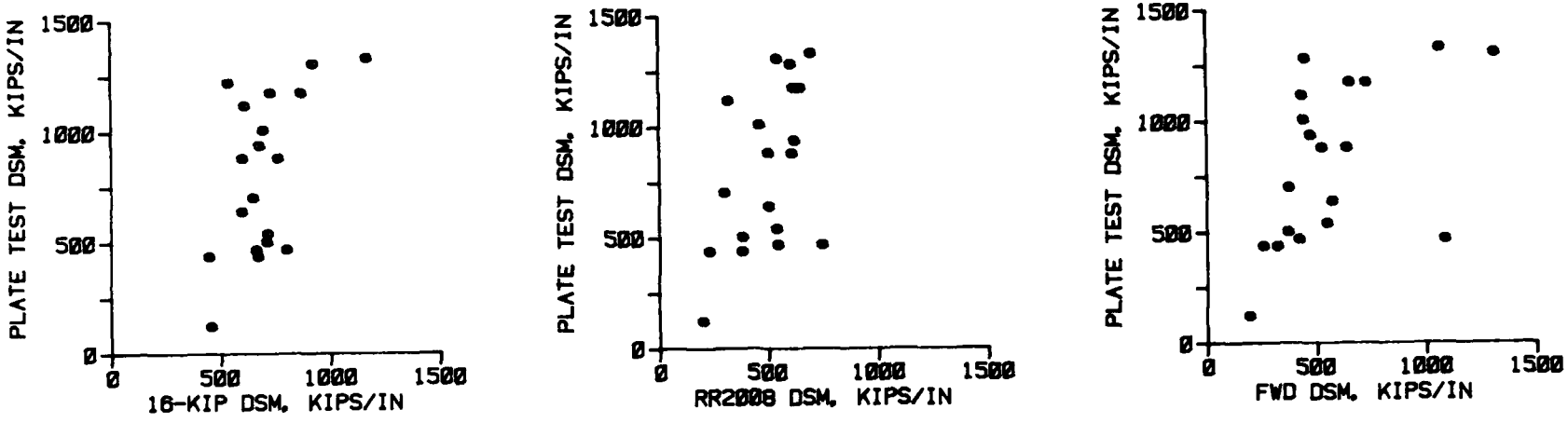

Figure 27. Plate test DSM (from the static plate bearing test) versus 16-kip, road rater, and Falling Weight Deflectometer DSM's

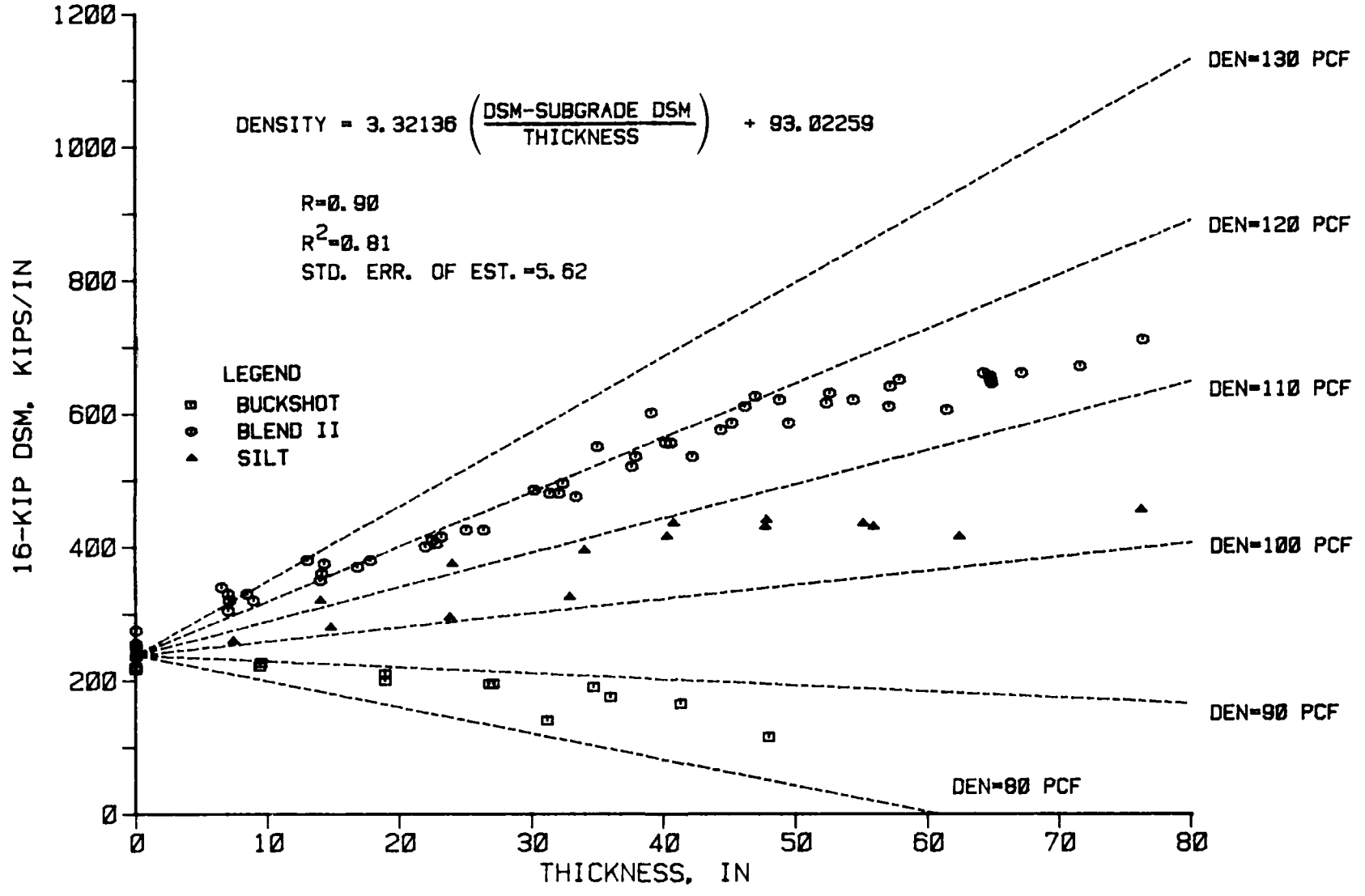

Figure 28. Predicted density as a function of the ratio of change in DSM to thickness (equation from linear regression analysis)

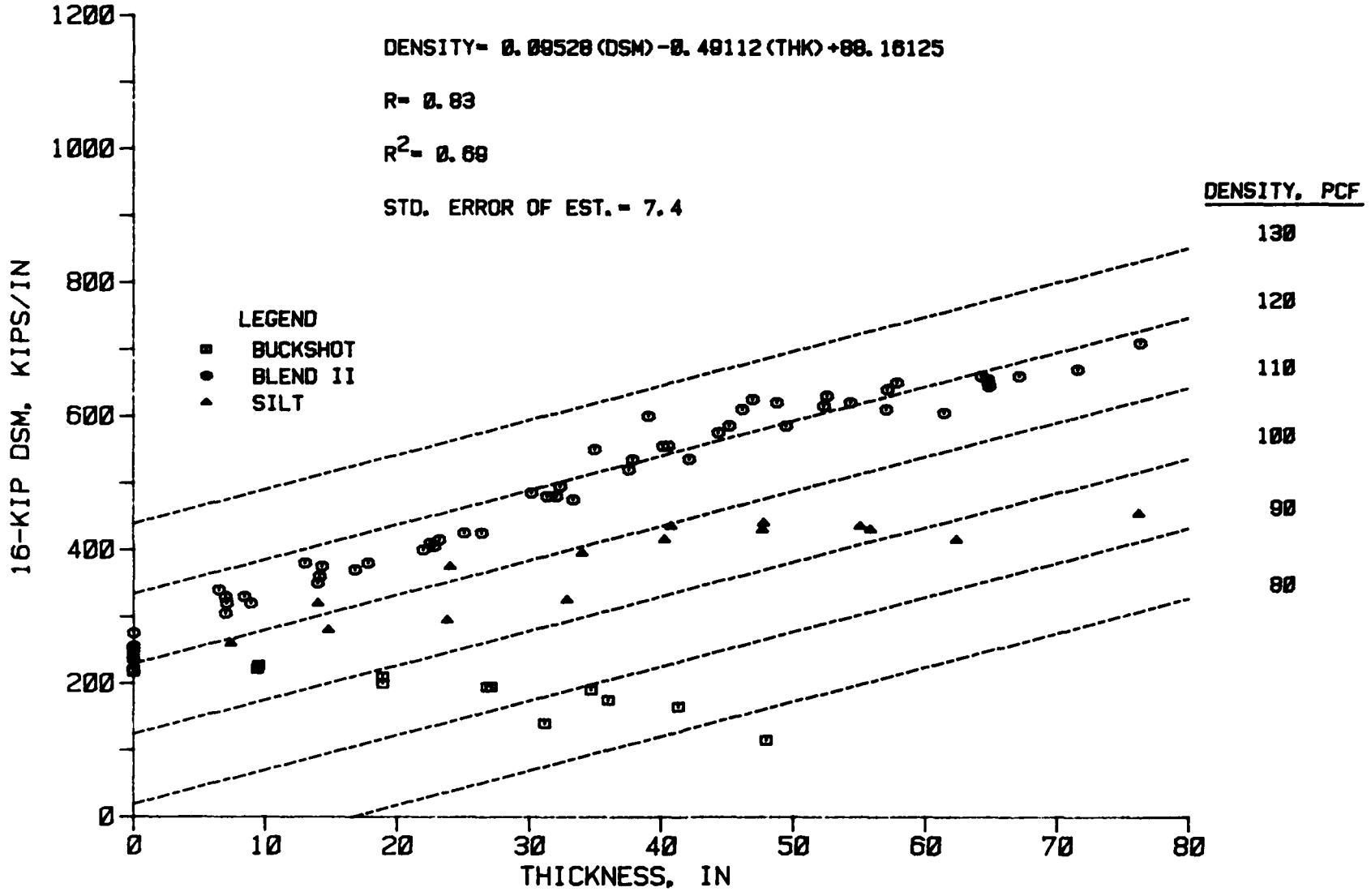

Figure 29. Predicted density as a function of DSM and thickness (equation from linear regression analysis)

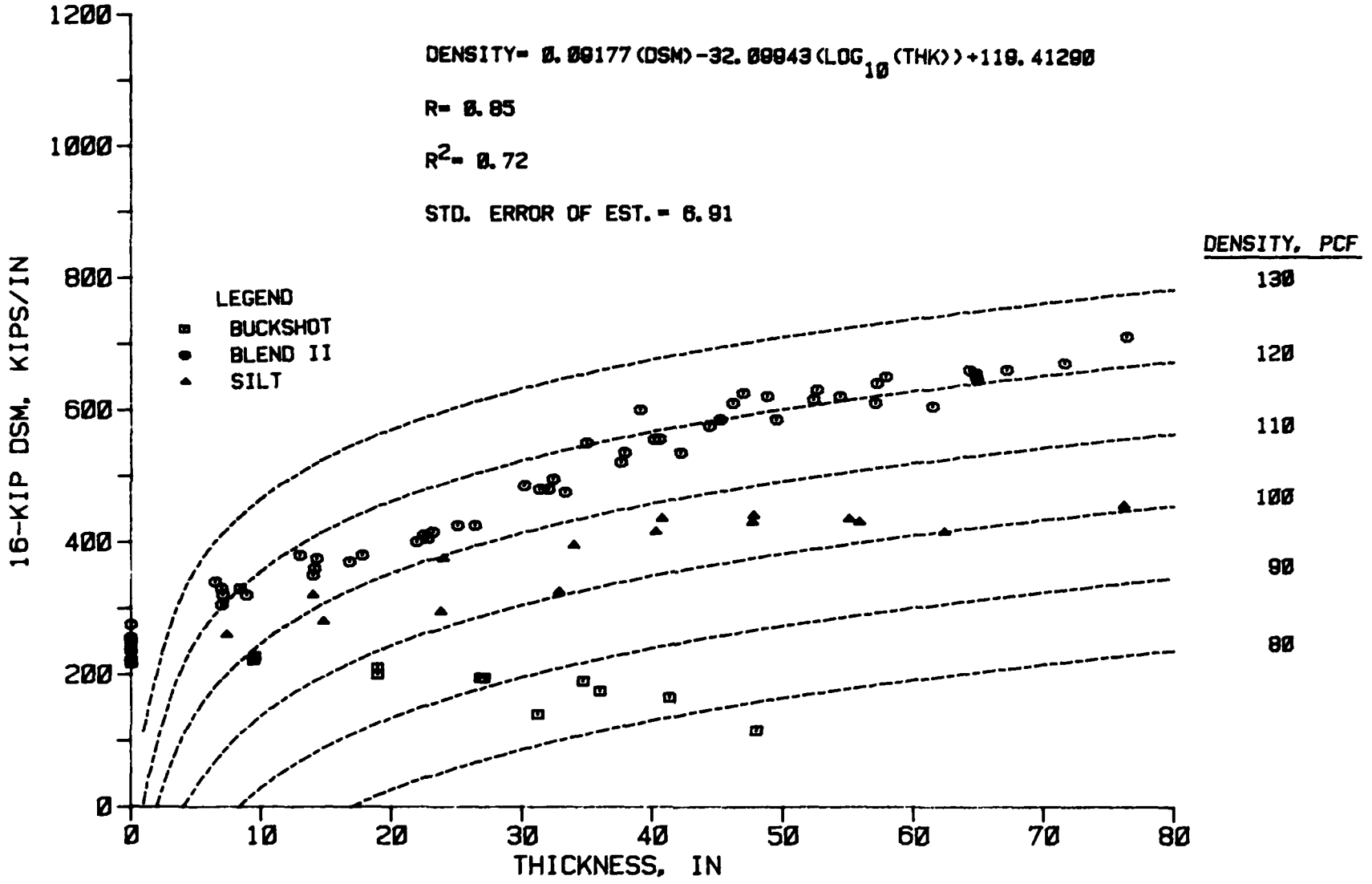

Figure 30. Predicted density as a function of DSM and LOG_{10} (THK) (equation from linear regression analysis)

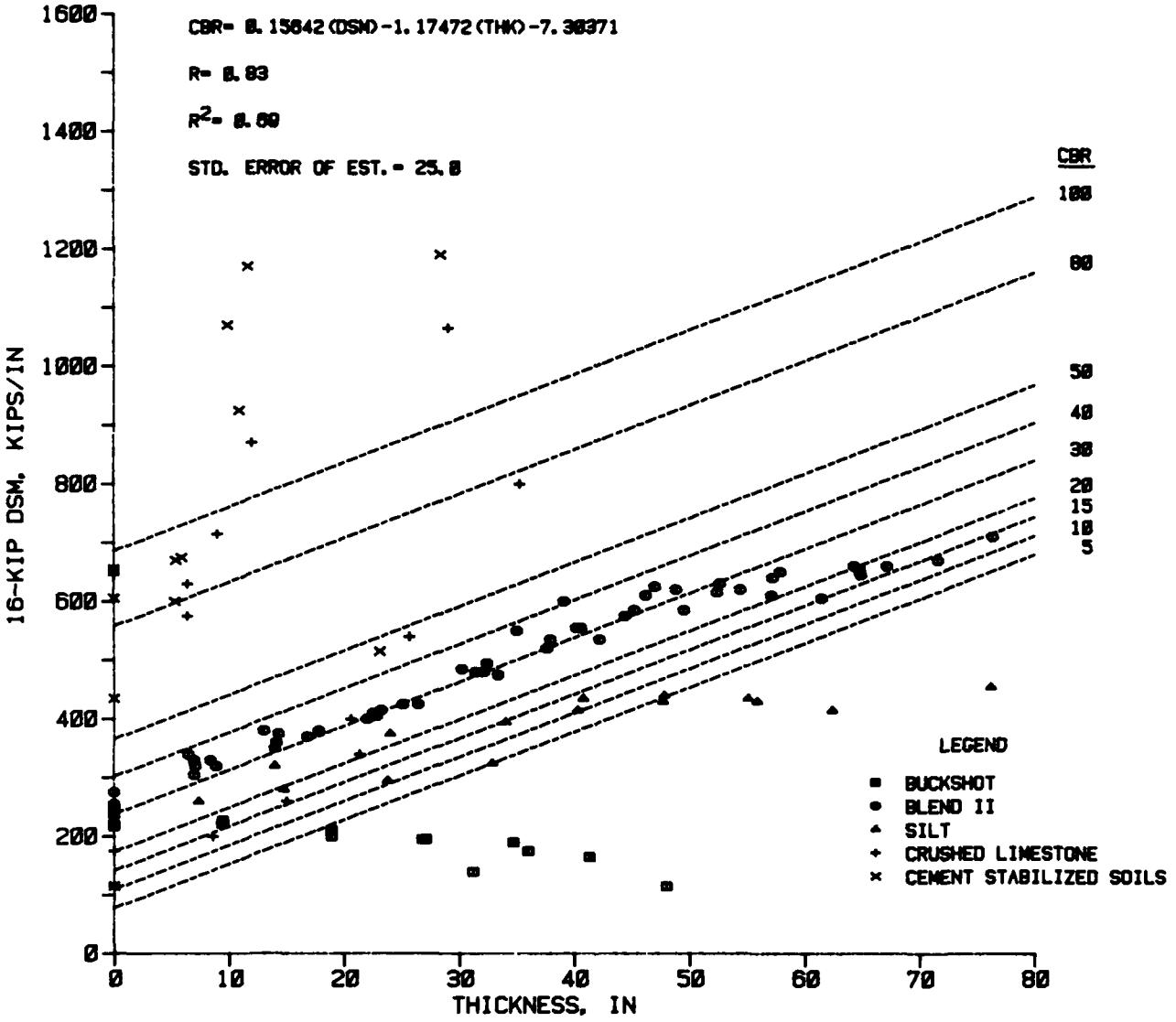

Figure 31. Predicted CBR as a function of DSM and thickness (equation from linear regression analysis)

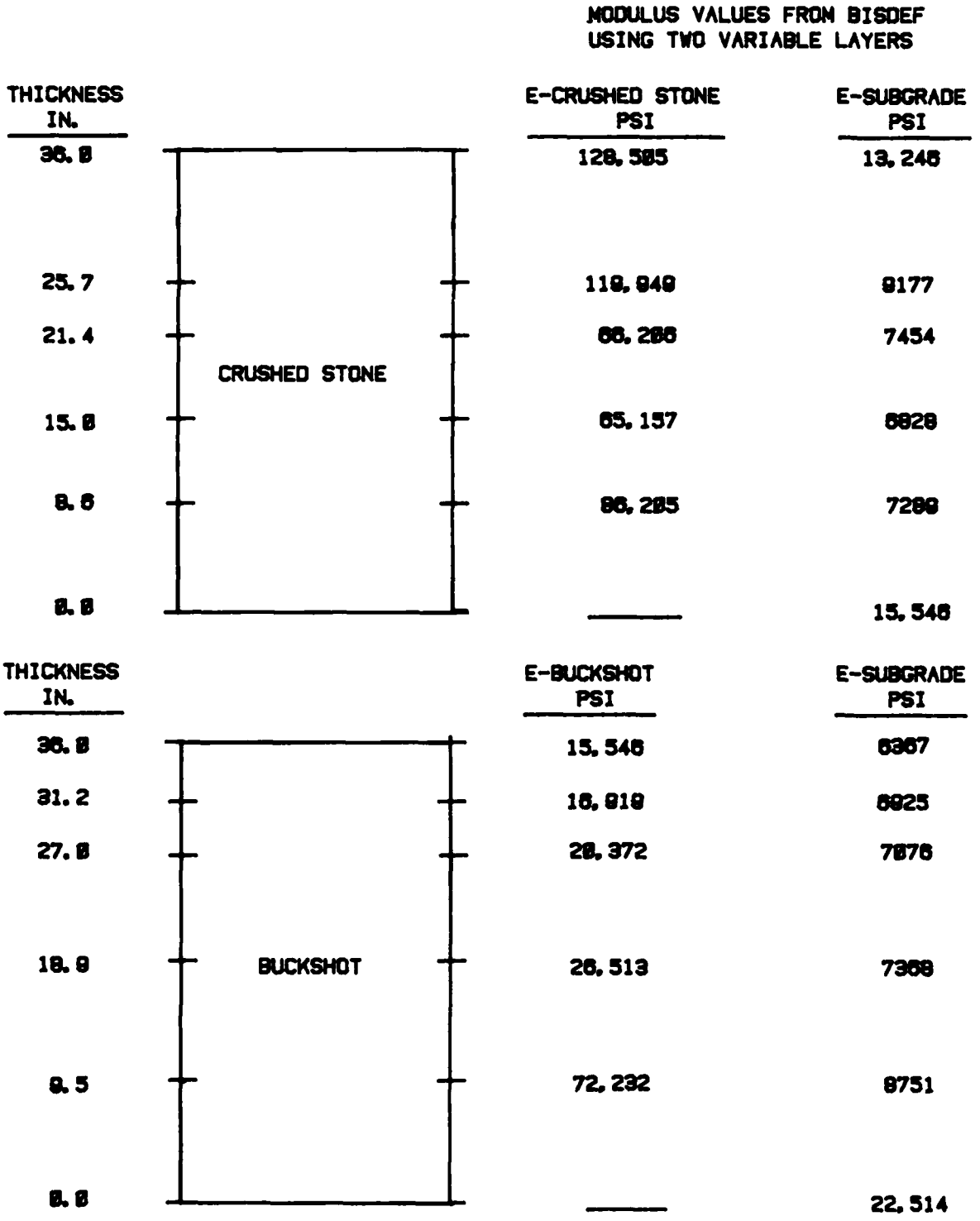

Figure 32. Computed modulus values for buckshot clay and crushed limestone from BISDEF (two-variable layers) and 16-kip deflection data

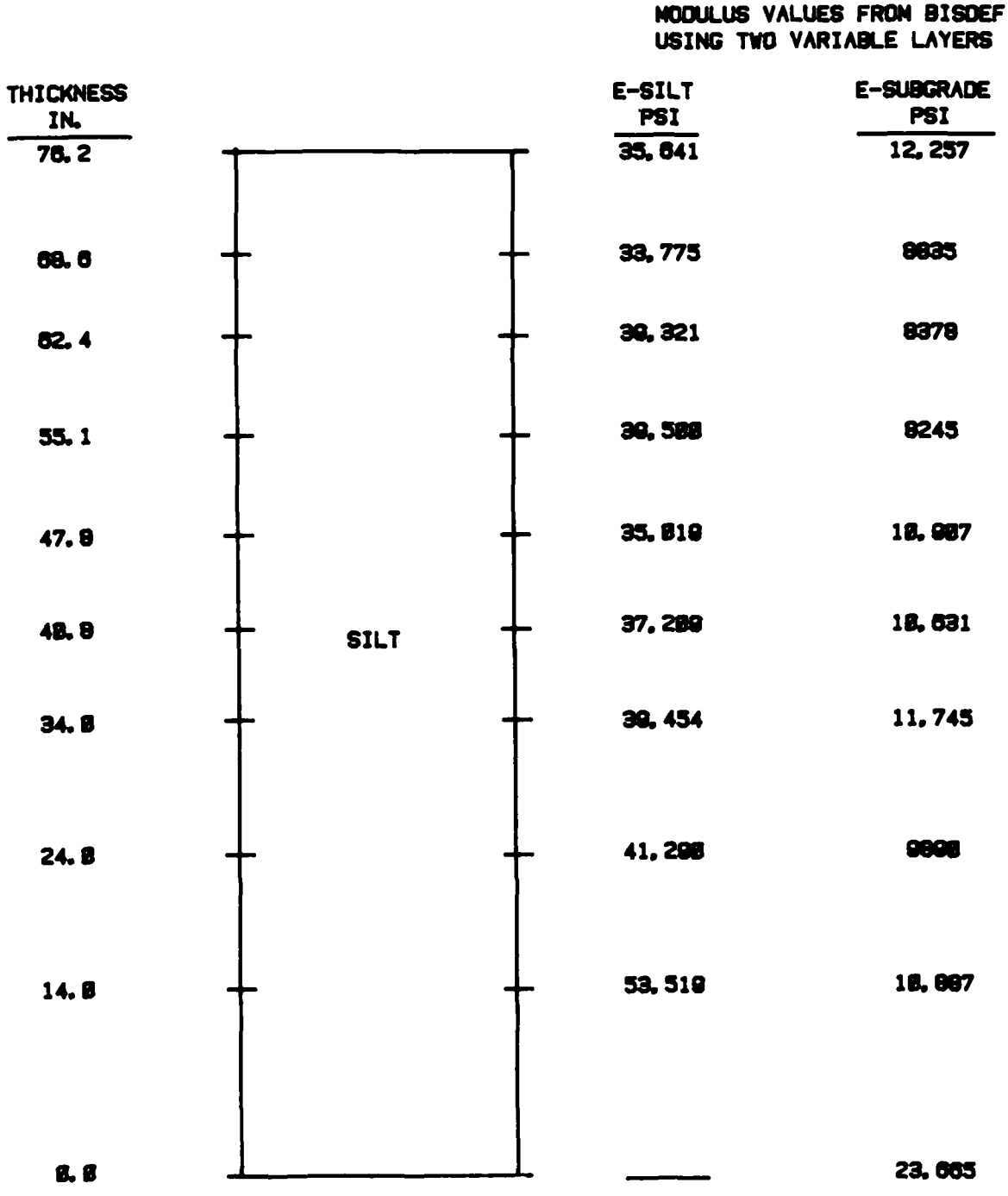

Figure 33. Computed modulus values for silt from BISDEF (two-variable layers) and 16-kip deflection data

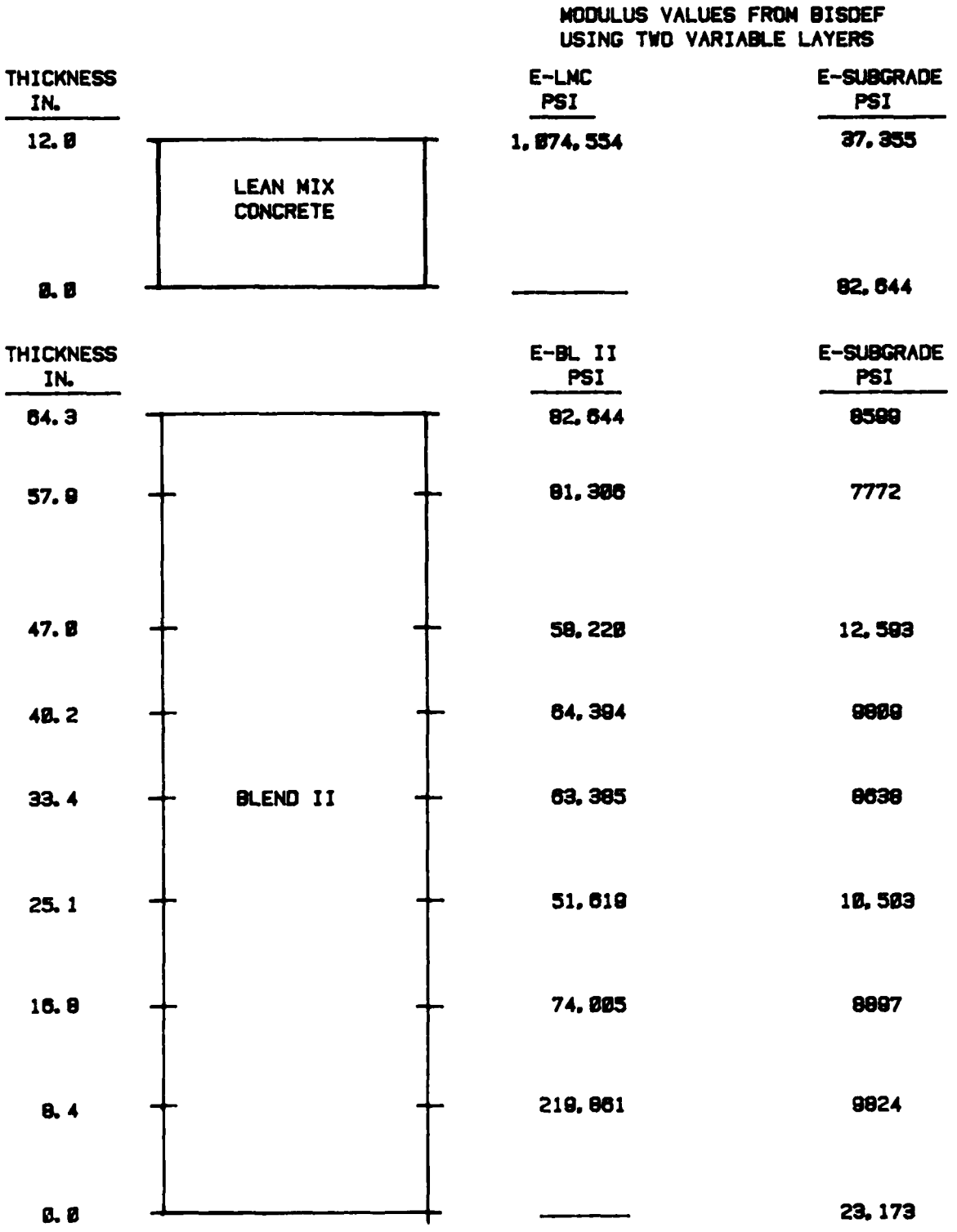

Figure 34. Computed modulus for Blend II and lean mix concrete from BISDEF (two-variable layers) and 16-kip deflection data

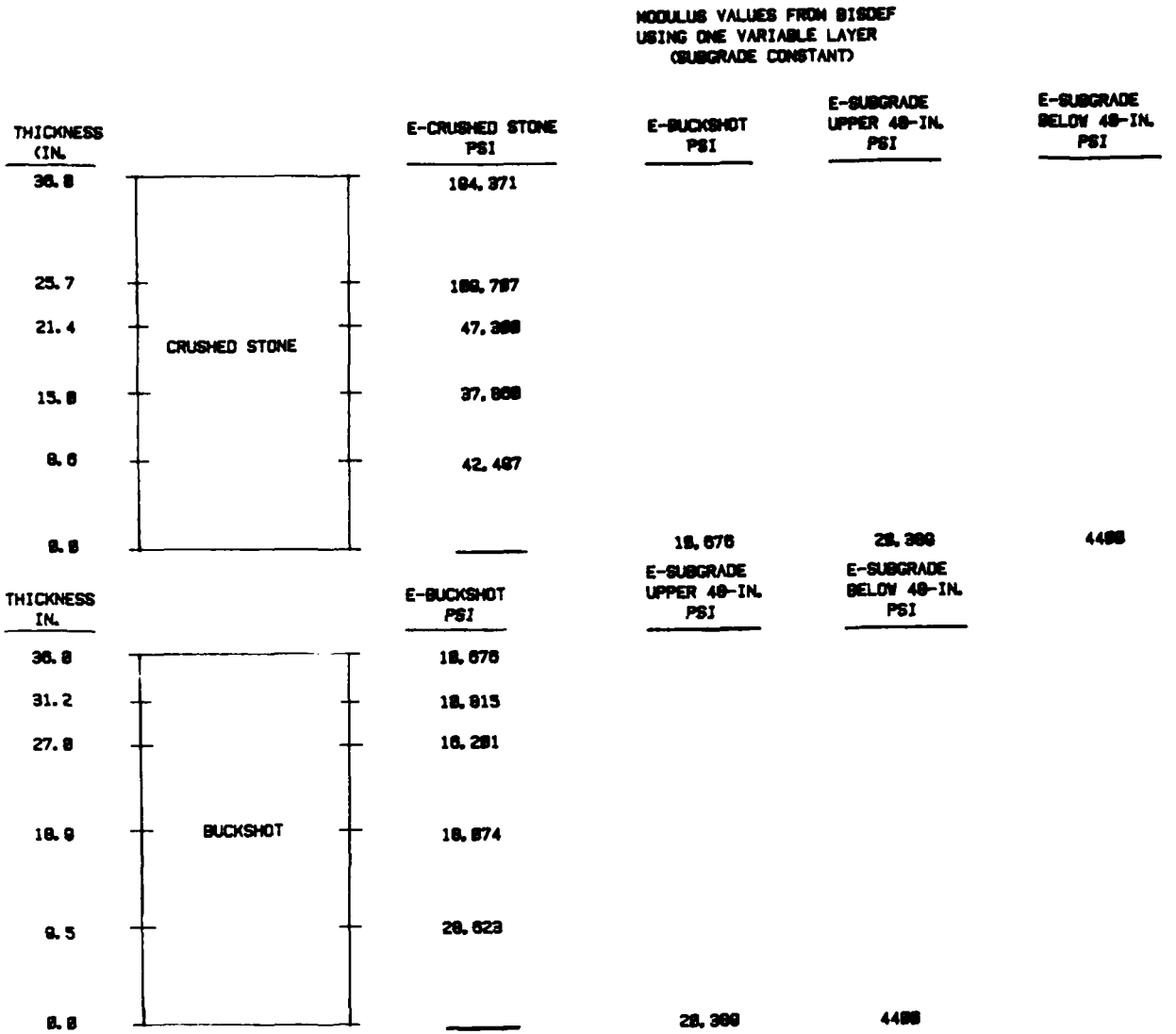

Figure 35. Computed modulus values for buckshot clay and crushed limestone from BISDEF (one-variable layer) and 16-kip deflection data

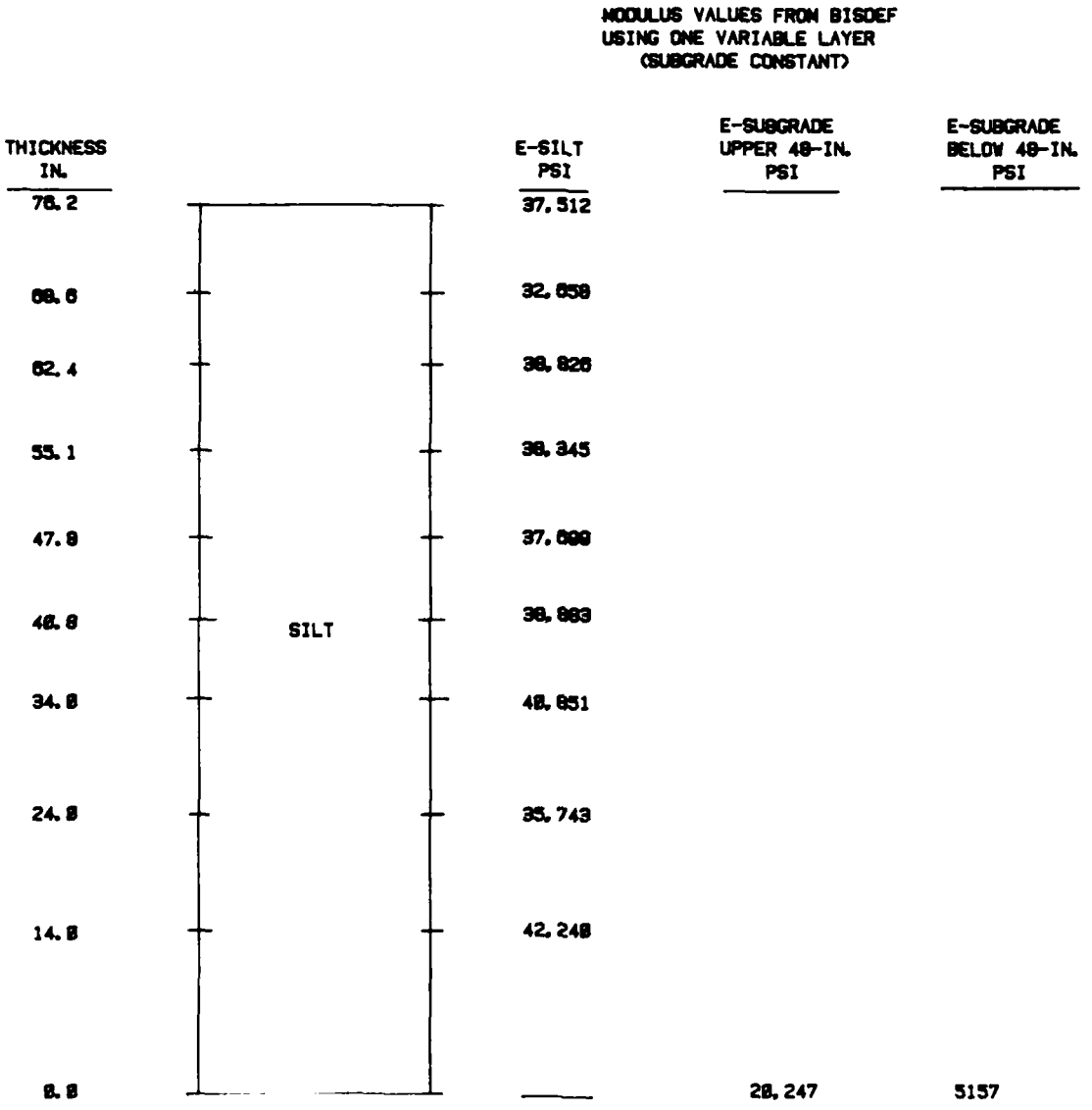

Figure 36. Computed modulus values for silt from BISDEF (one-variable layer) and 16-kip deflection data

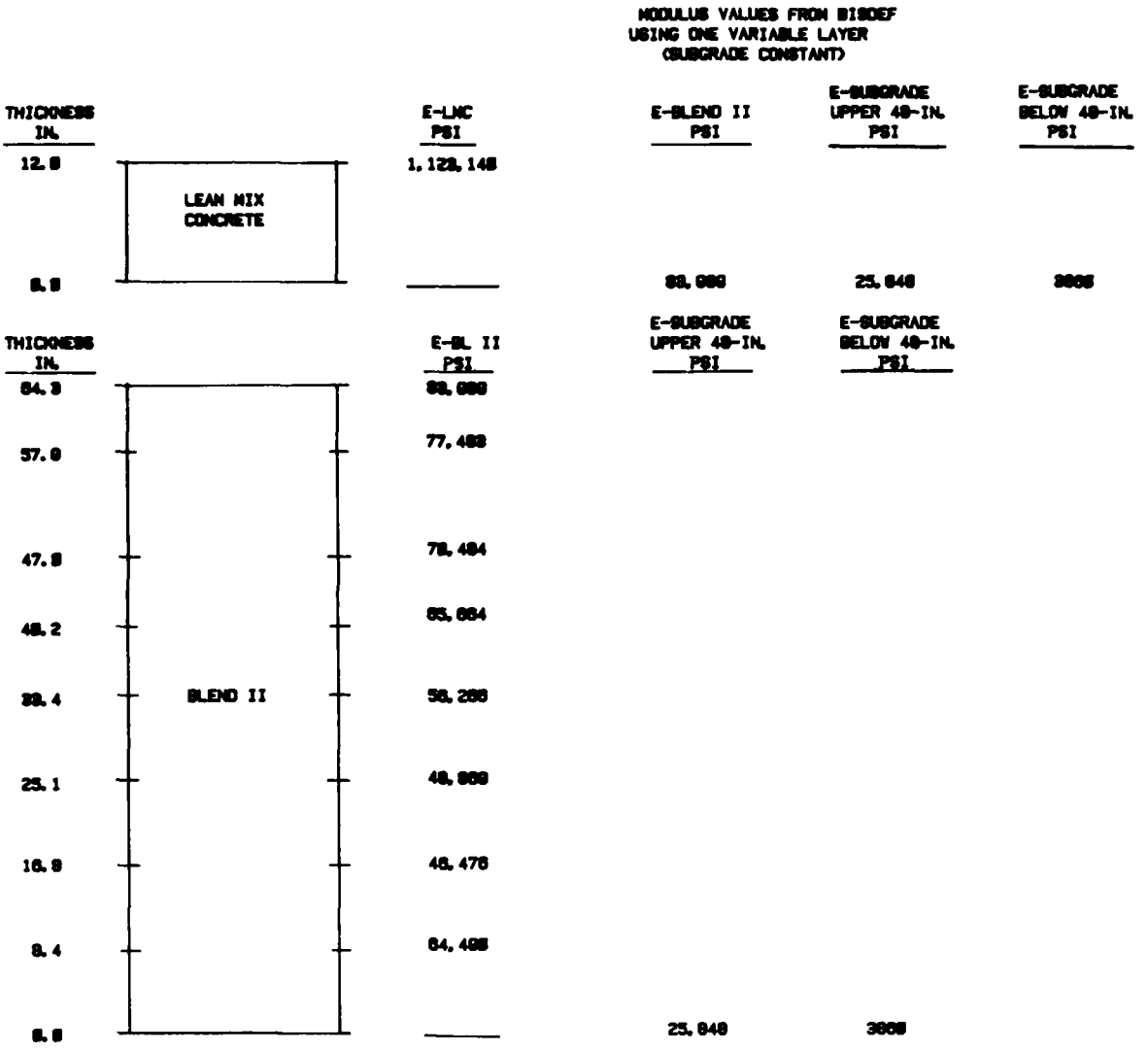

Figure 37. Computed modulus values for Blend II and lean mix concrete from BISDEF (one-variable layer) and 16-kip deflection data

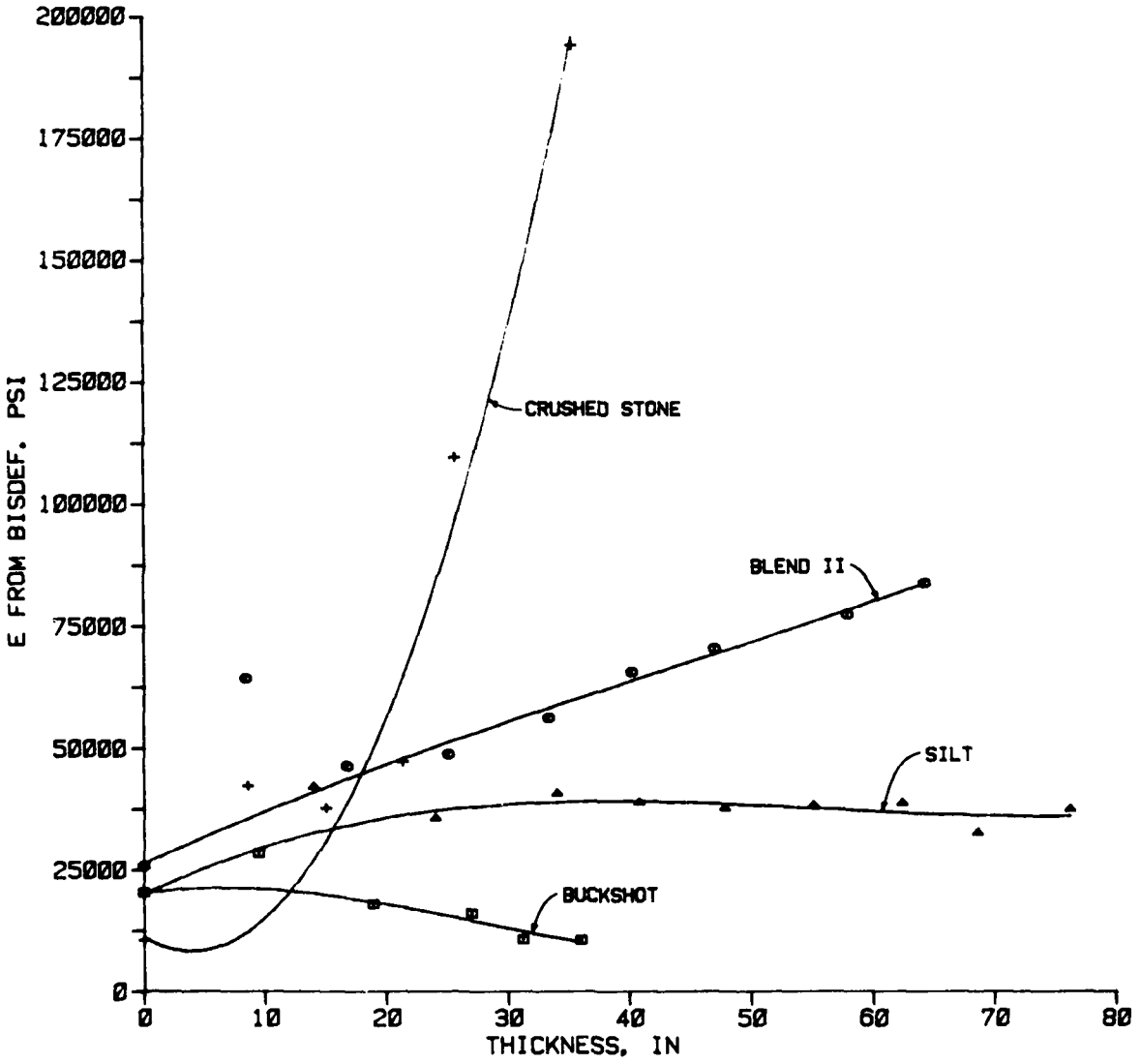

Figure 38. Modulus values determined from BISDEF using a two-variable layer system and 16-kip deflection data versus thickness

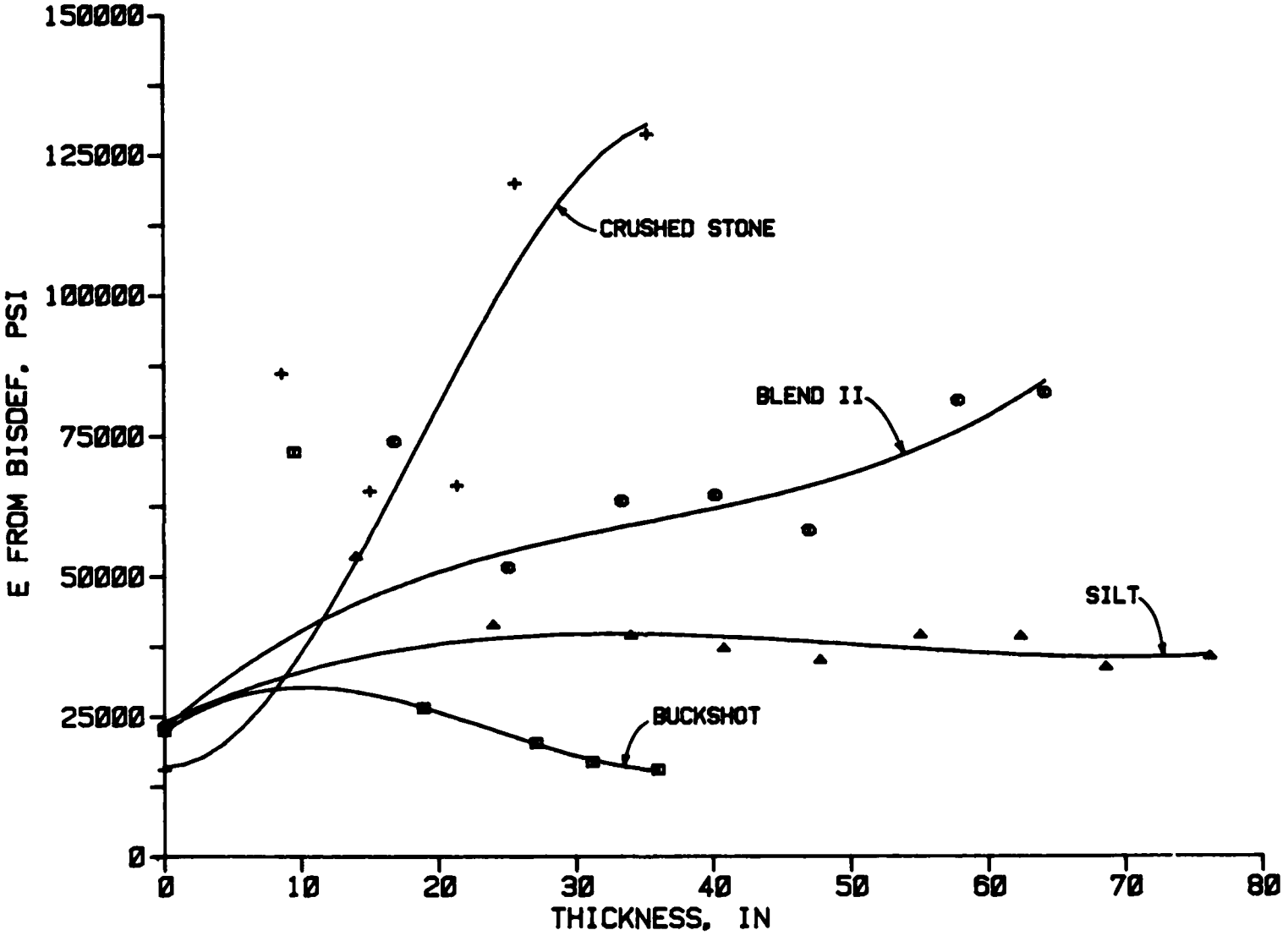

Figure 39. Modulus values determined from BISDEF using a one-variable layer system and 16-kip deflection data versus thickness

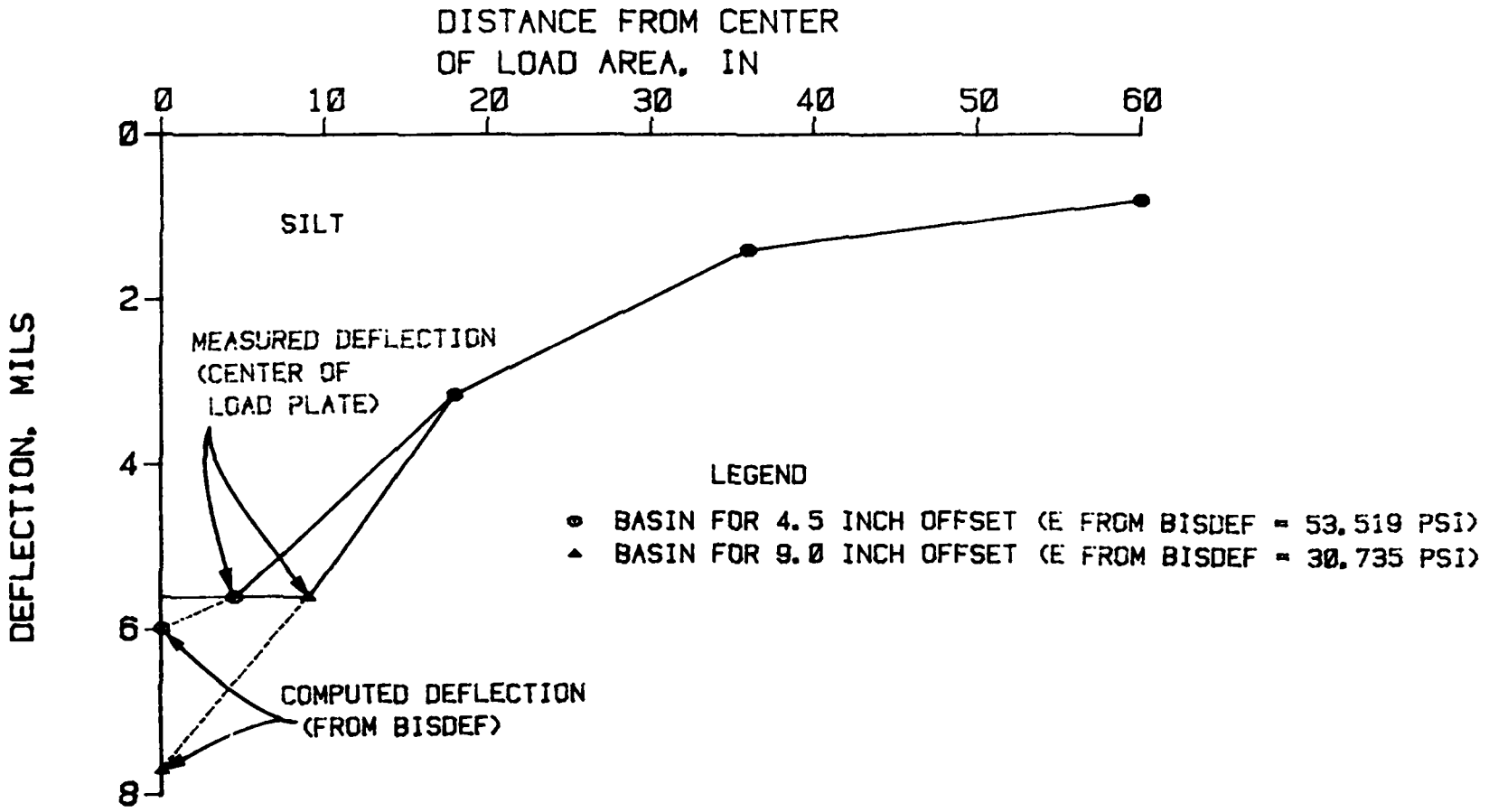

Figure 40. Actual deflection basin for 14.0 in. of silt with computed deflections at the center of the load area from BISDEF for one-half and one radius offsets of the measured plate deflection

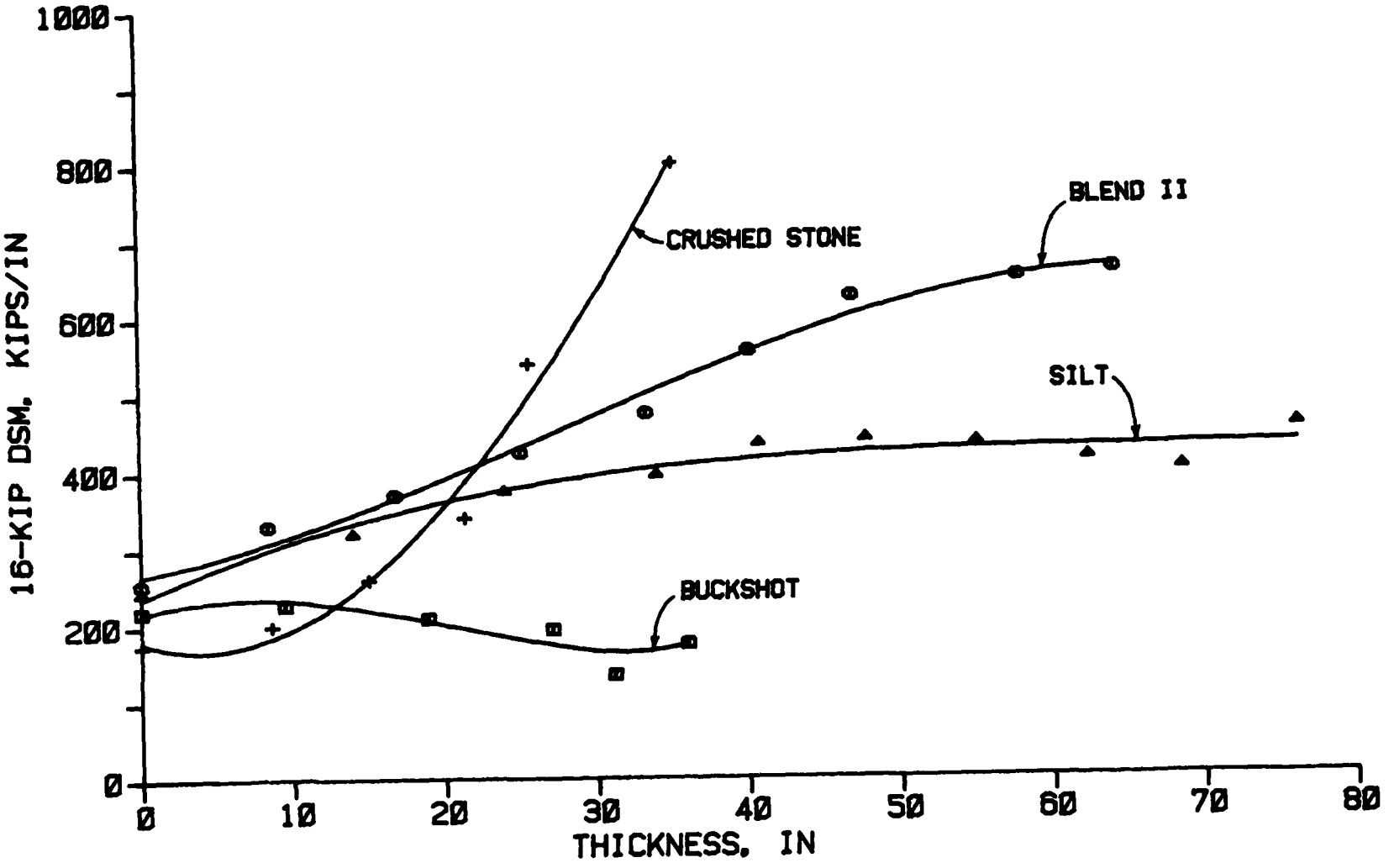

Figure 41. 16-kip DSM versus layer thickness for Items 1 and 5 (lane 1) and Item 3 (lane 2)

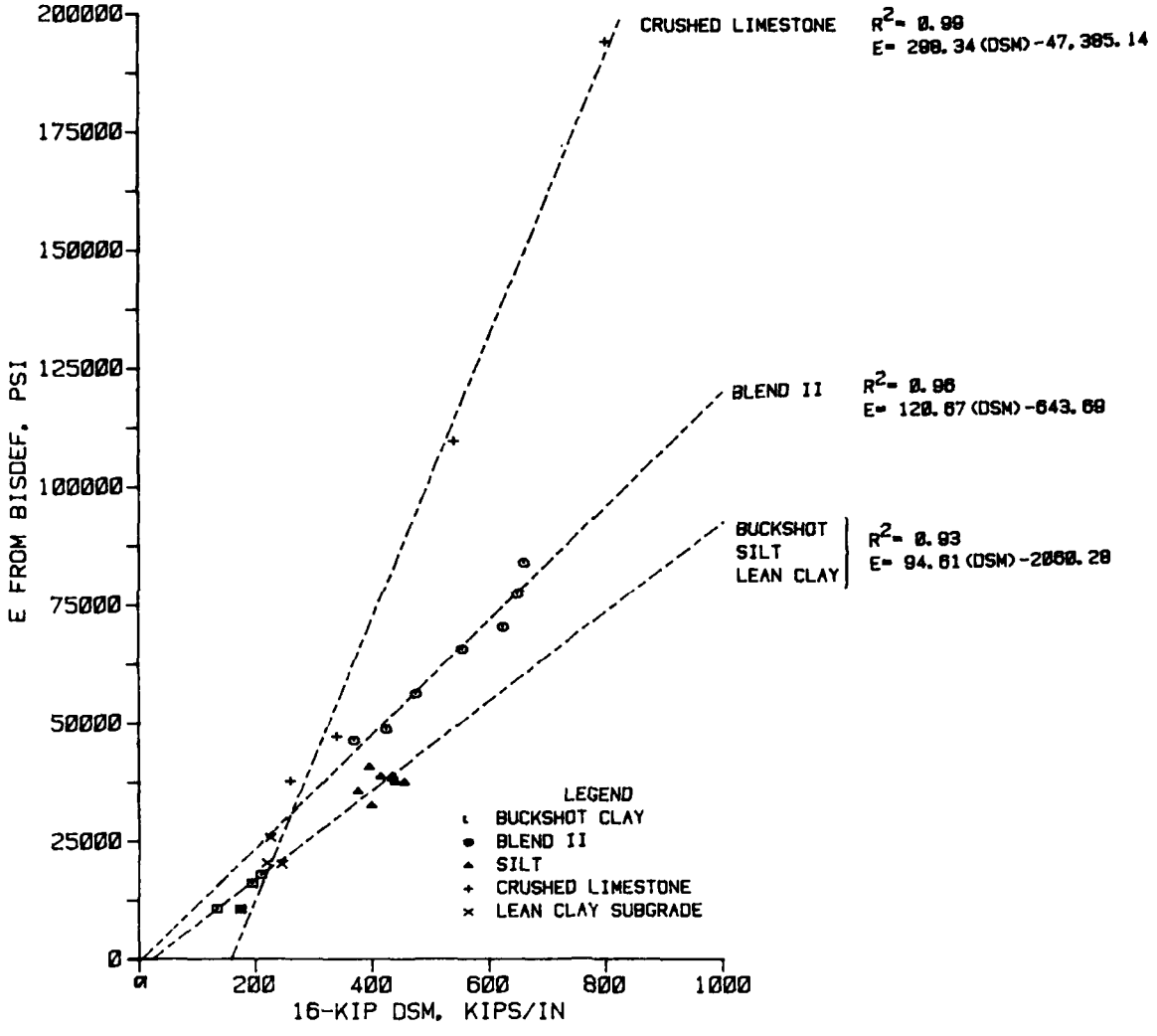

Figure 42. E from BISDEF (one-variable layer) versus 16-kip DSM

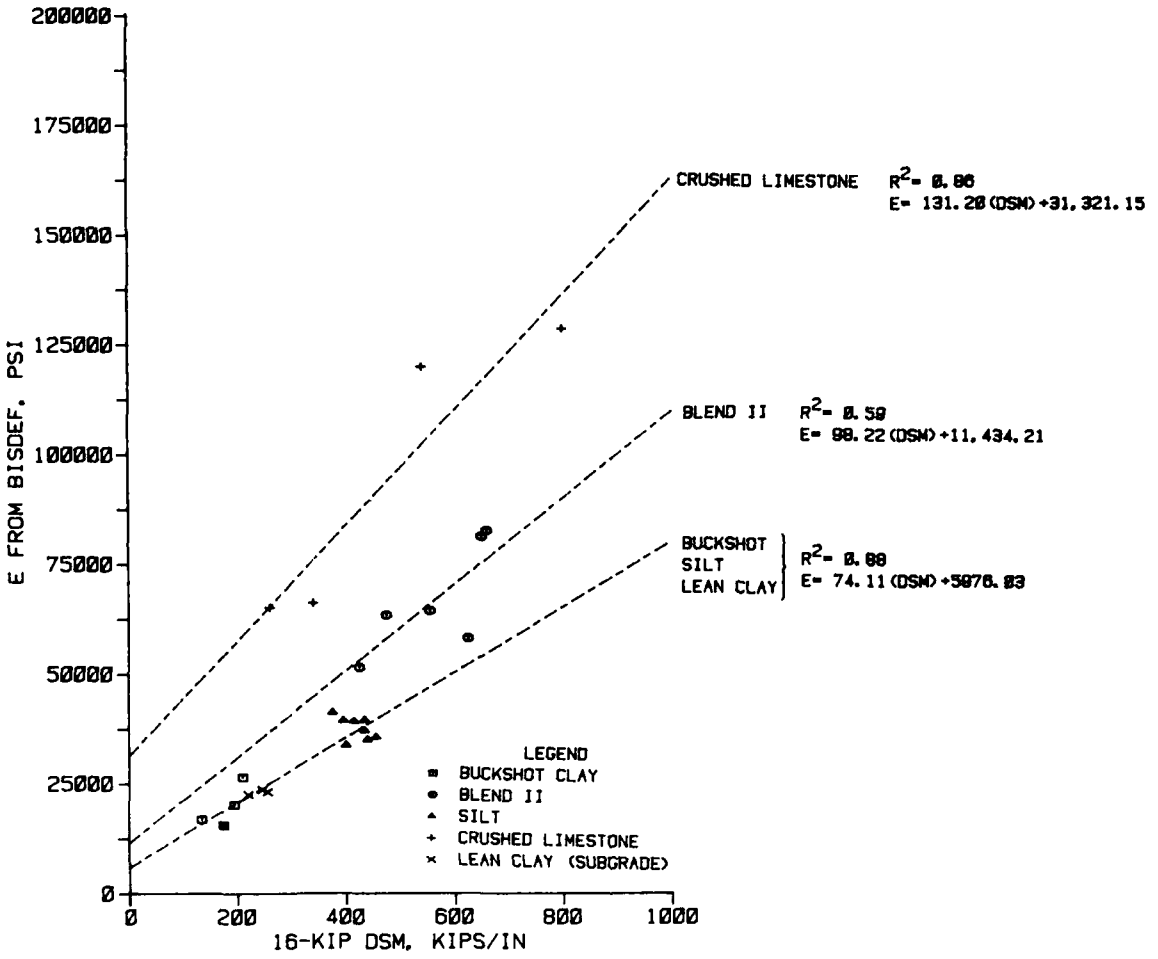

Figure 43. E from BISDEF (two-variable layers) versus 16-kip DSM

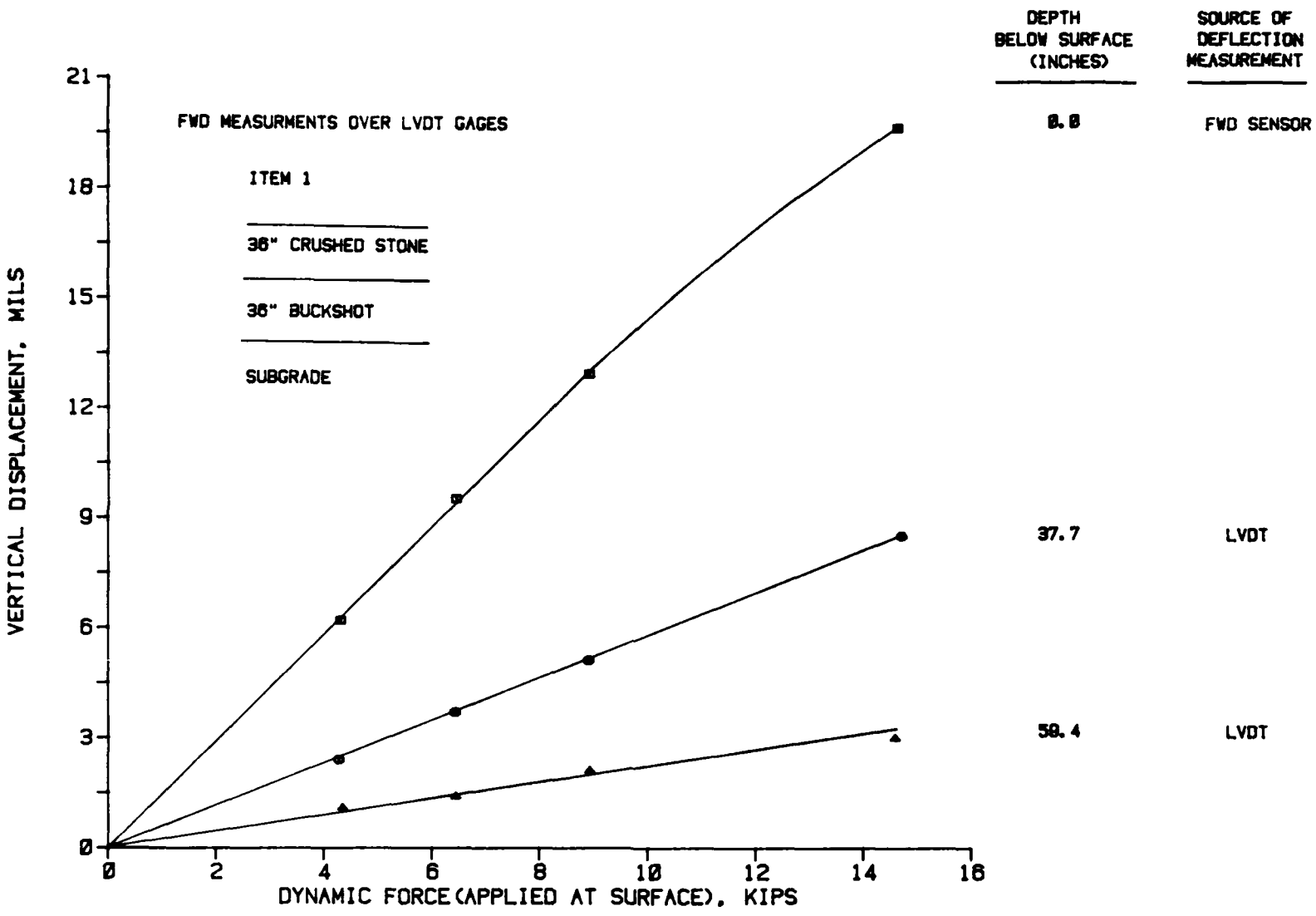

Figure 44. Measured displacements for a range of Falling Weight Deflectometer load levels (Item 1, lane 1)

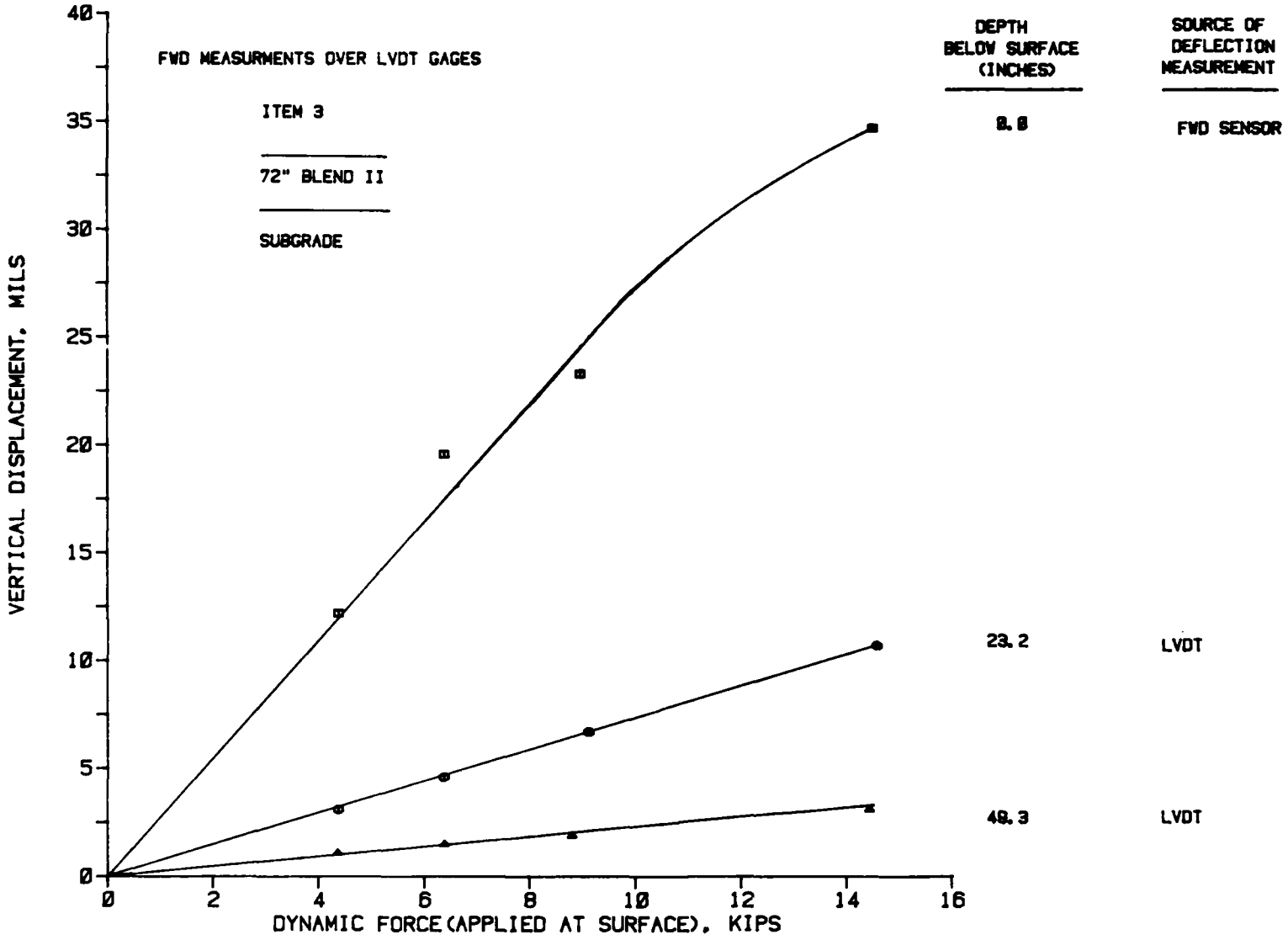

Figure 45. Measured displacements for a range of Falling Weight Deflectometer load levels (Item 3, lane 1)

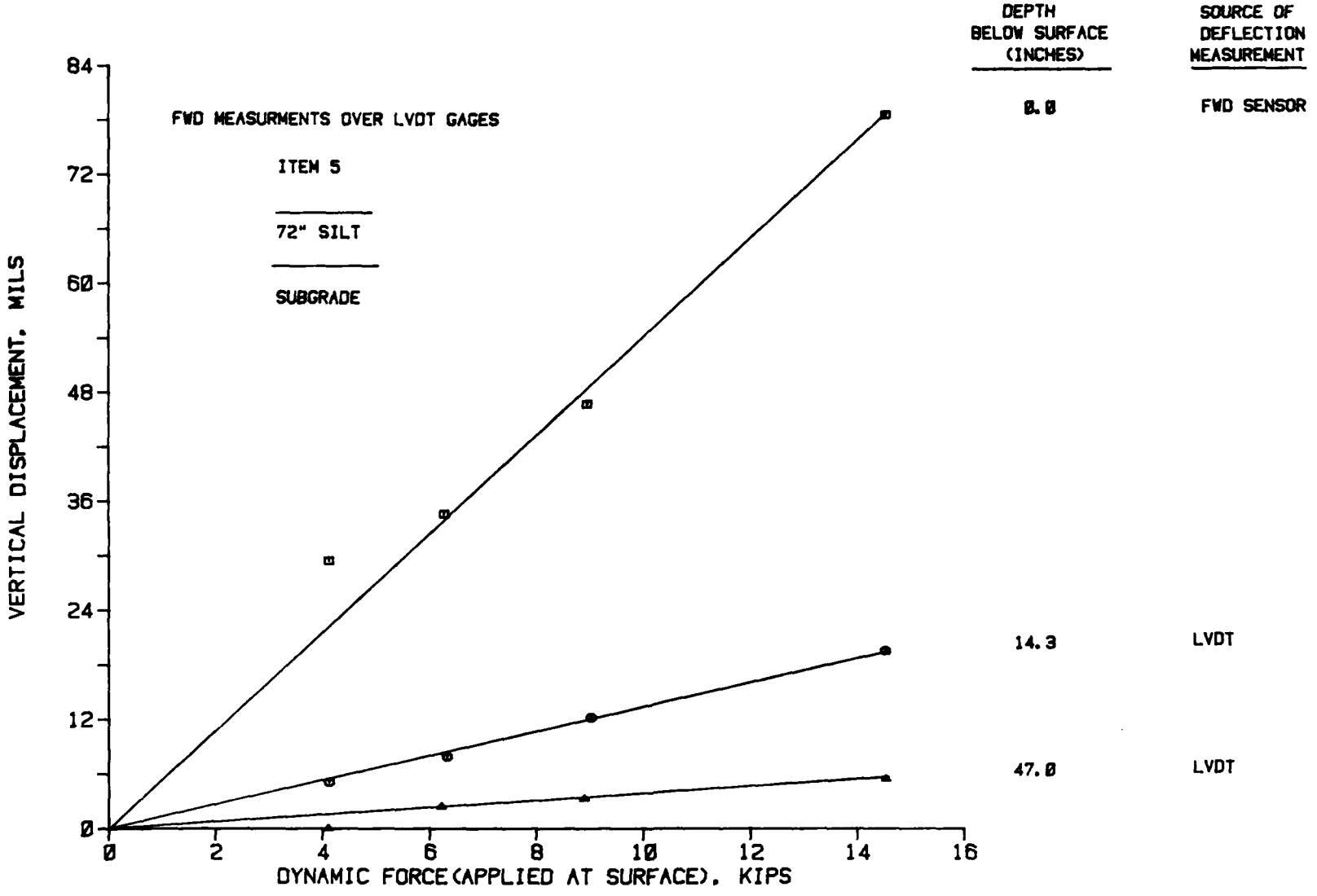

Figure 46. Measured displacements for a range of Falling Weight Deflectometer load levels (Item 5, lane 1)

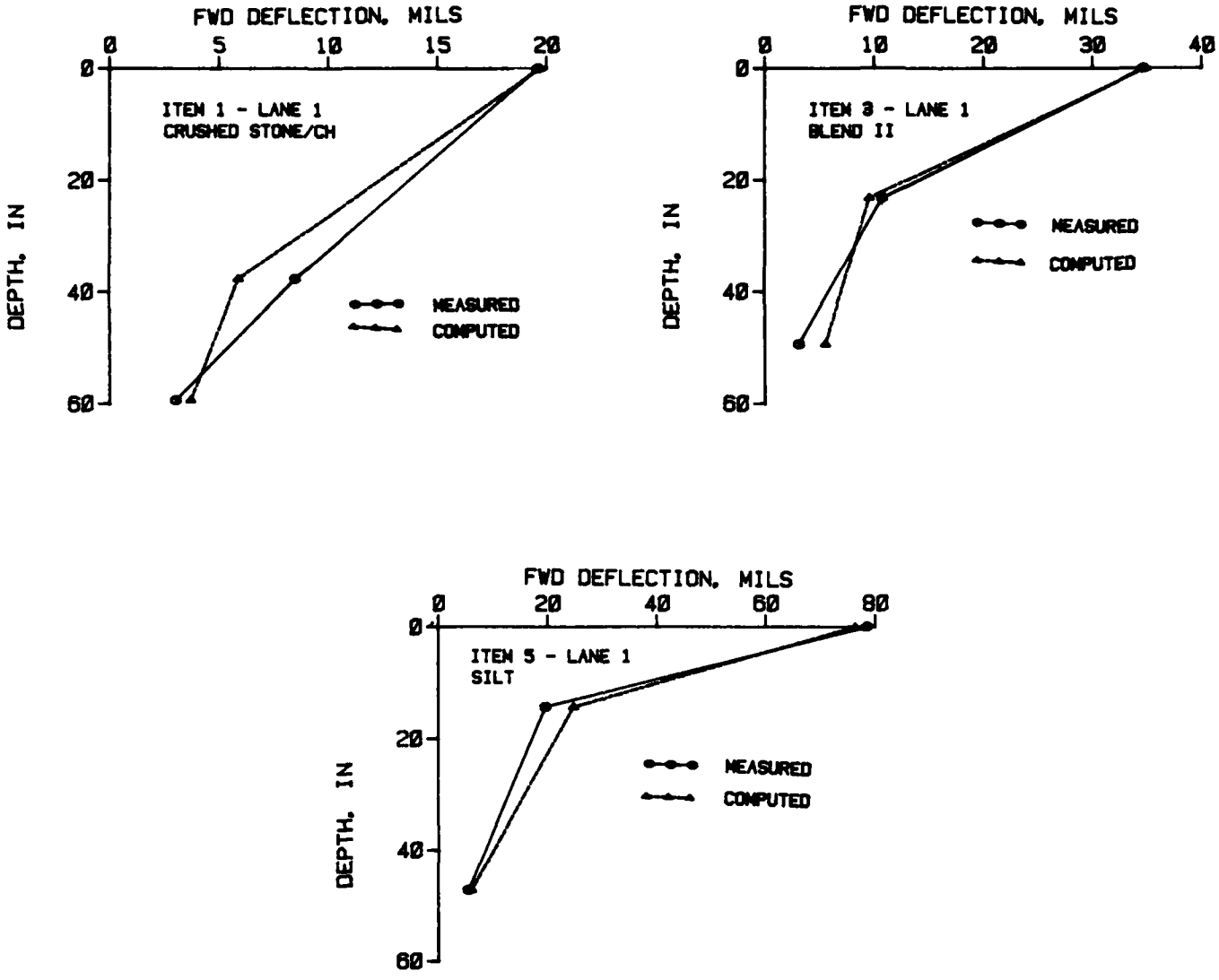

Figure 47. Comparison of measured displacements to displacements computed using a layered elastic approach

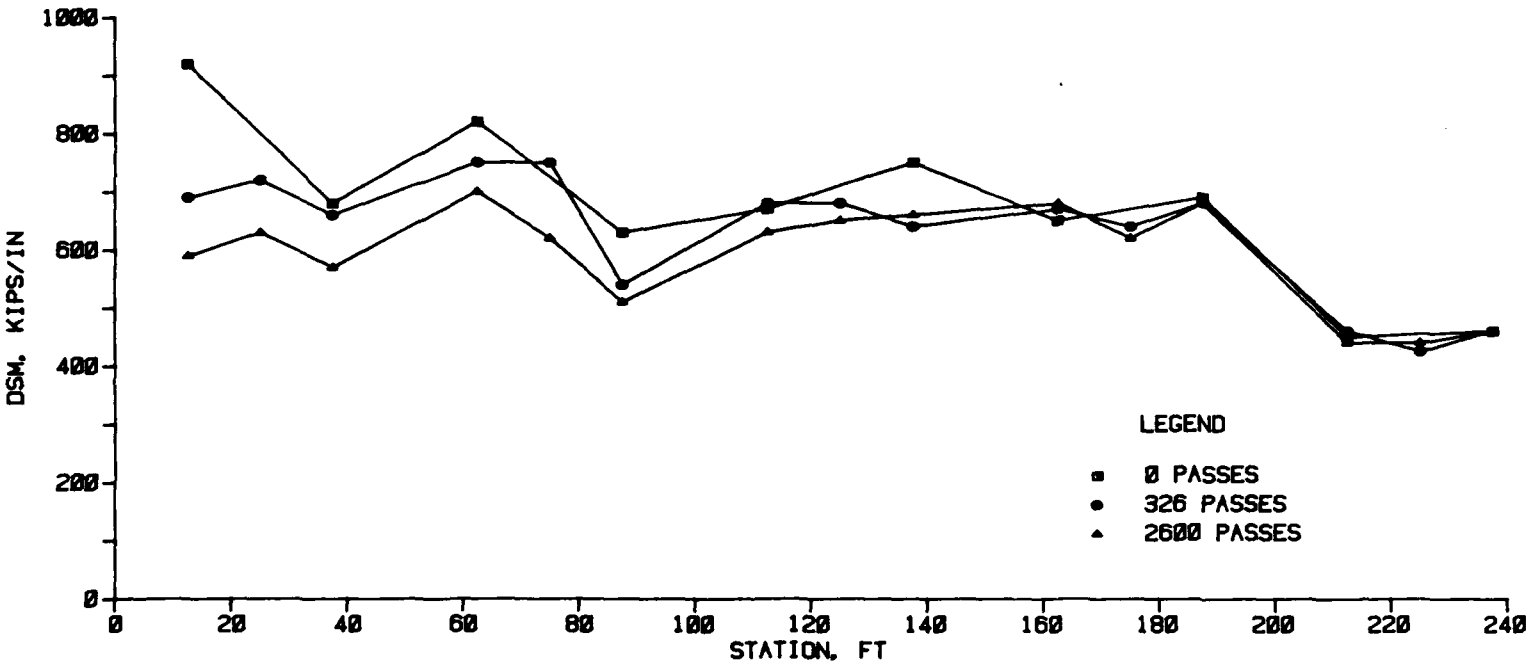

Figure 48. Nondestructive test results during traffic, WES 16-kip vibrator (lane 1)

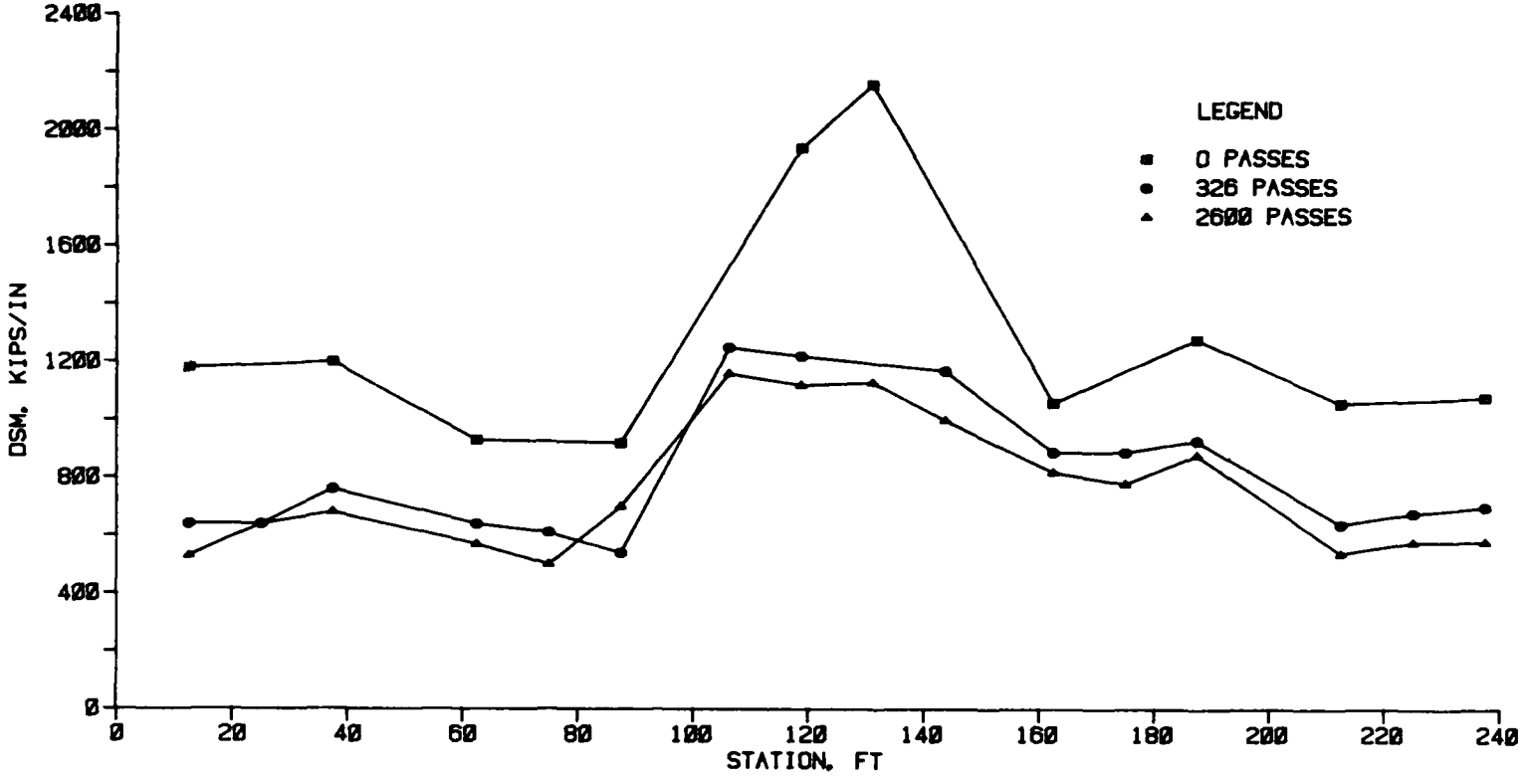

Figure 49. Nondestructive test results during traffic, WES 16-kip vibrator (lane 2)

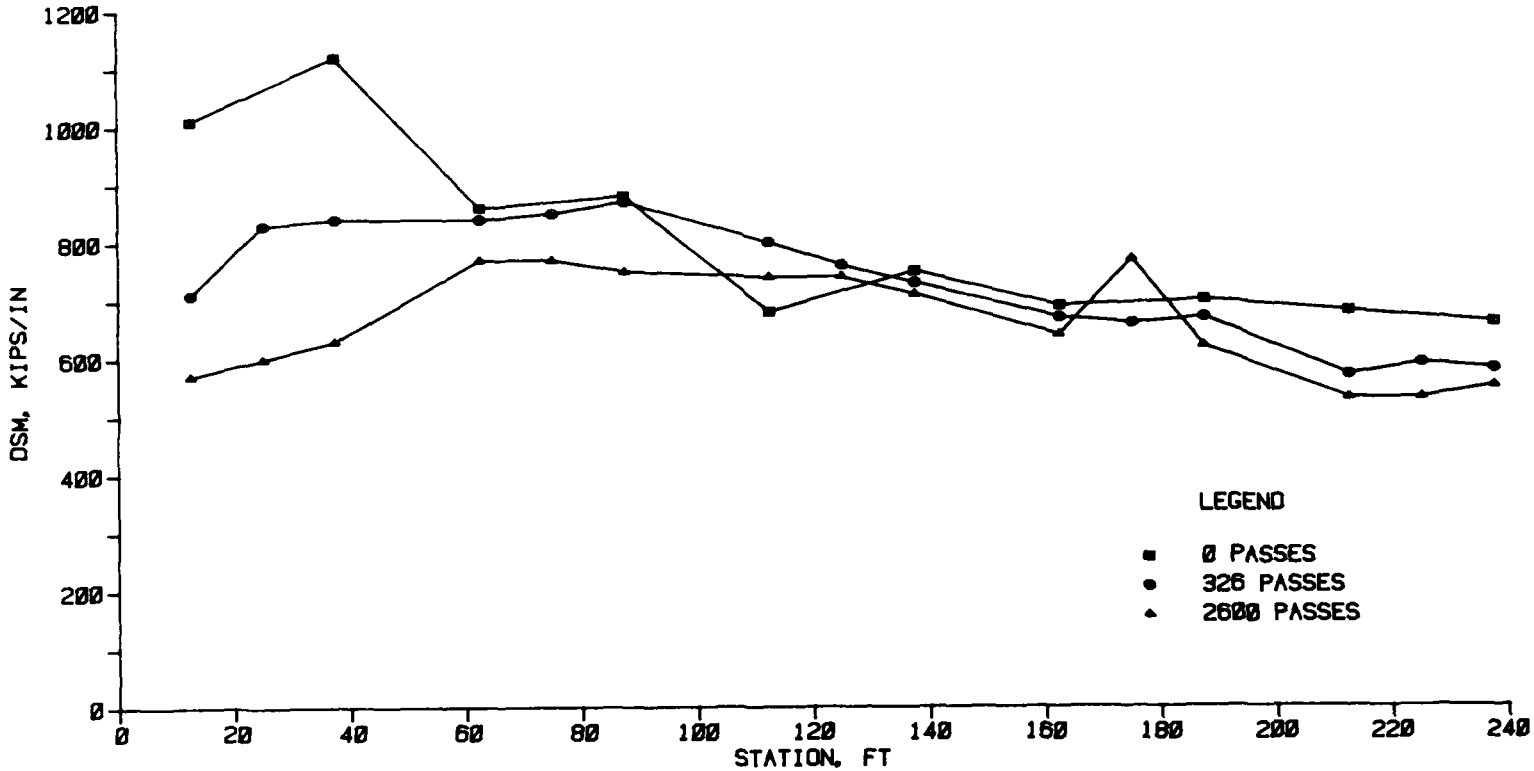

Figure 50. Nondestructive test results during traffic, WES 16-kip vibrator (lane 3)

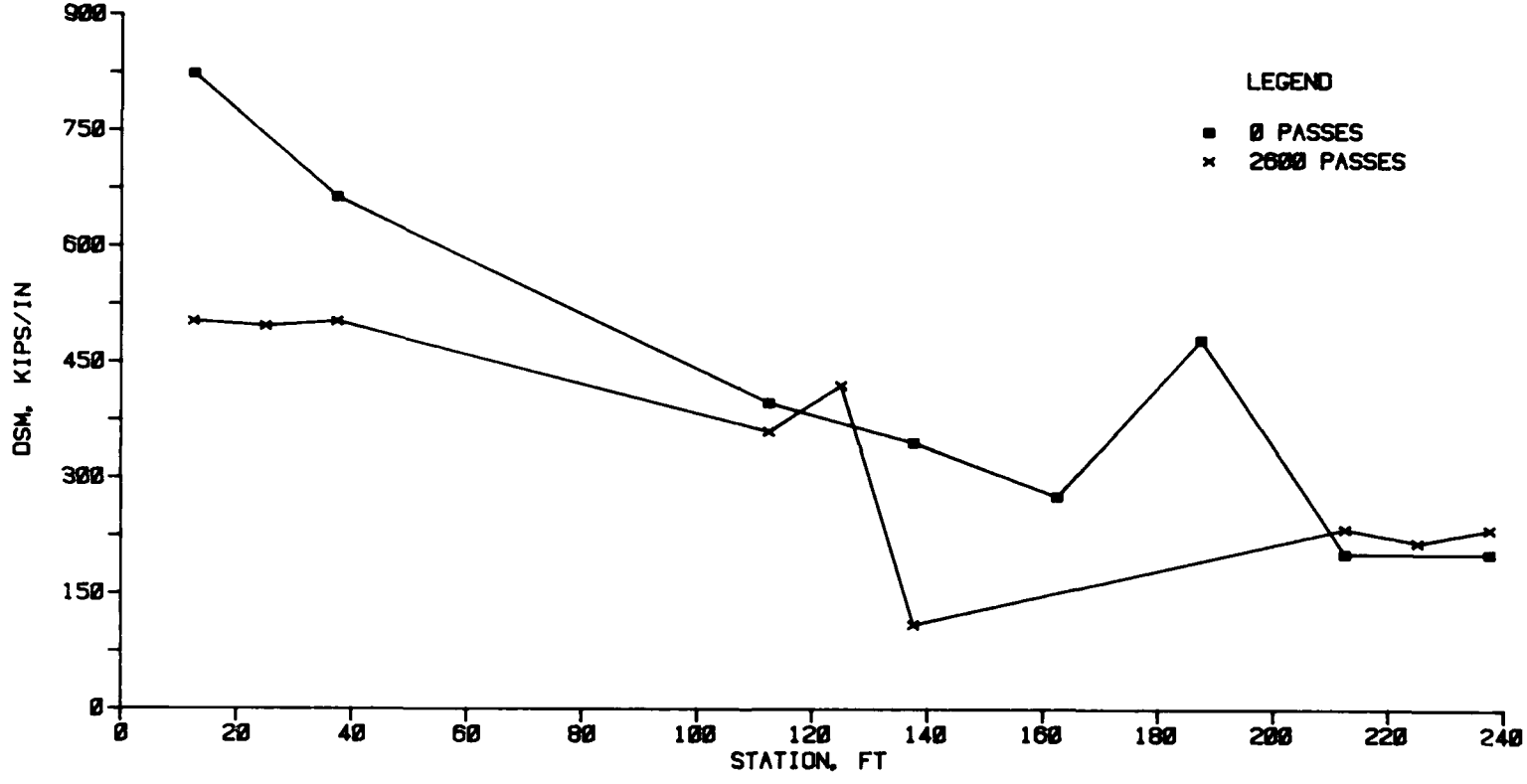

Figure 51. Nondestructive test results during traffic, Road Rater 2008 (lane 1)

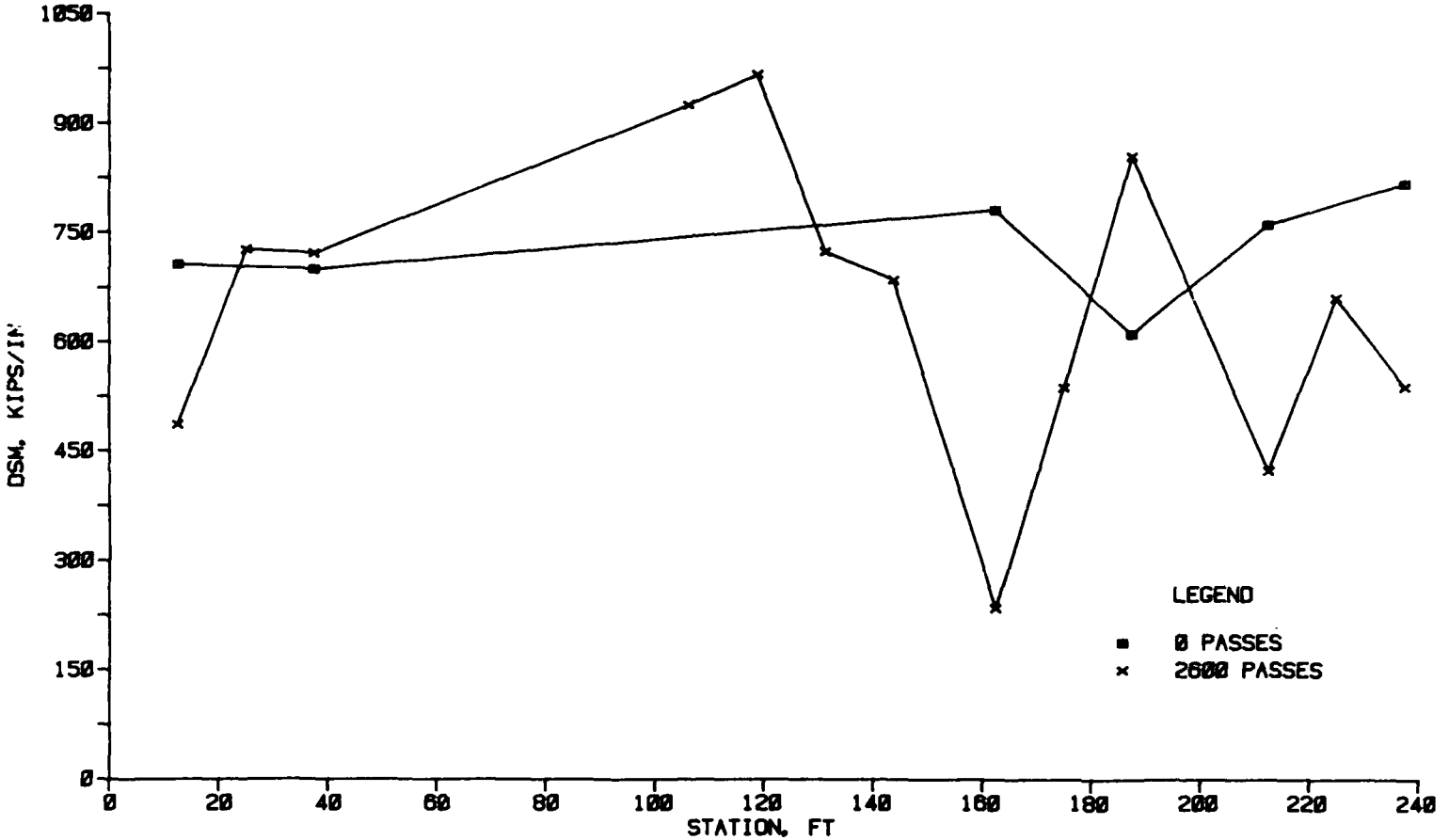

Figure 52. Nondestructive test results during traffic, Road Rater 2008 (lane 2)

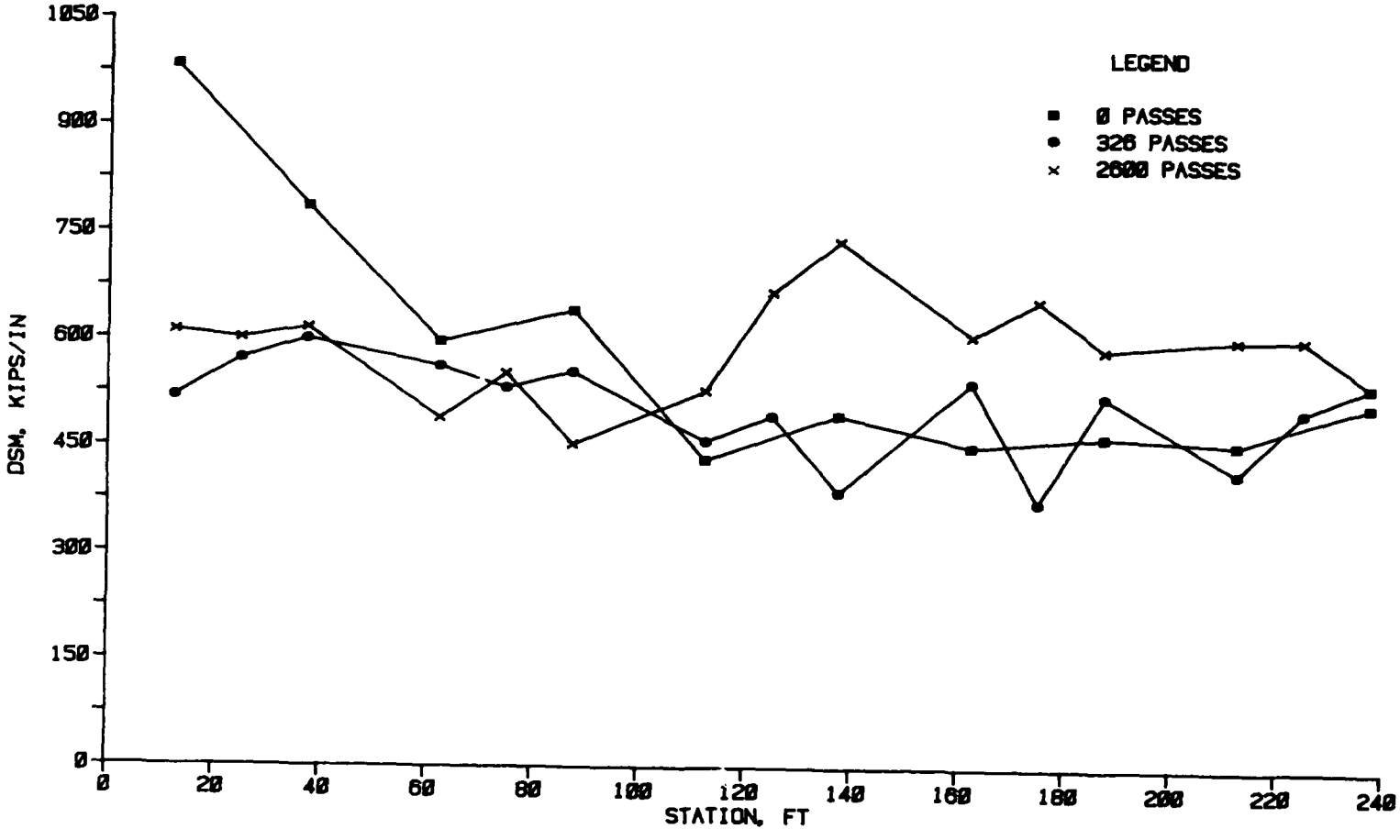

Figure 53. Nondestructive test results during traffic, Road Rater 2008 (lane 3)

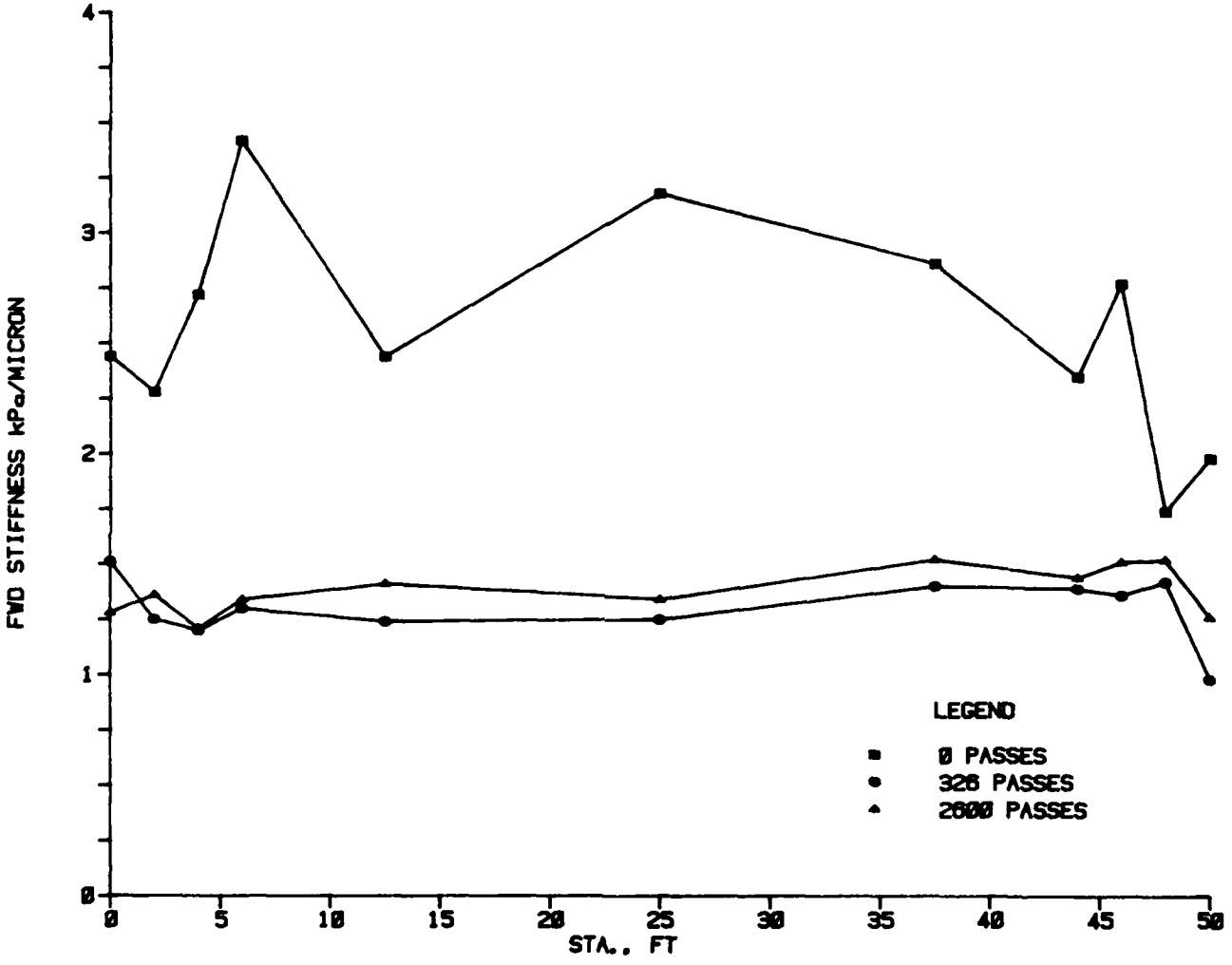

Figure 54. Nondestructive test results during traffic, Falling Weight Deflectometer (land 1, Item 1)

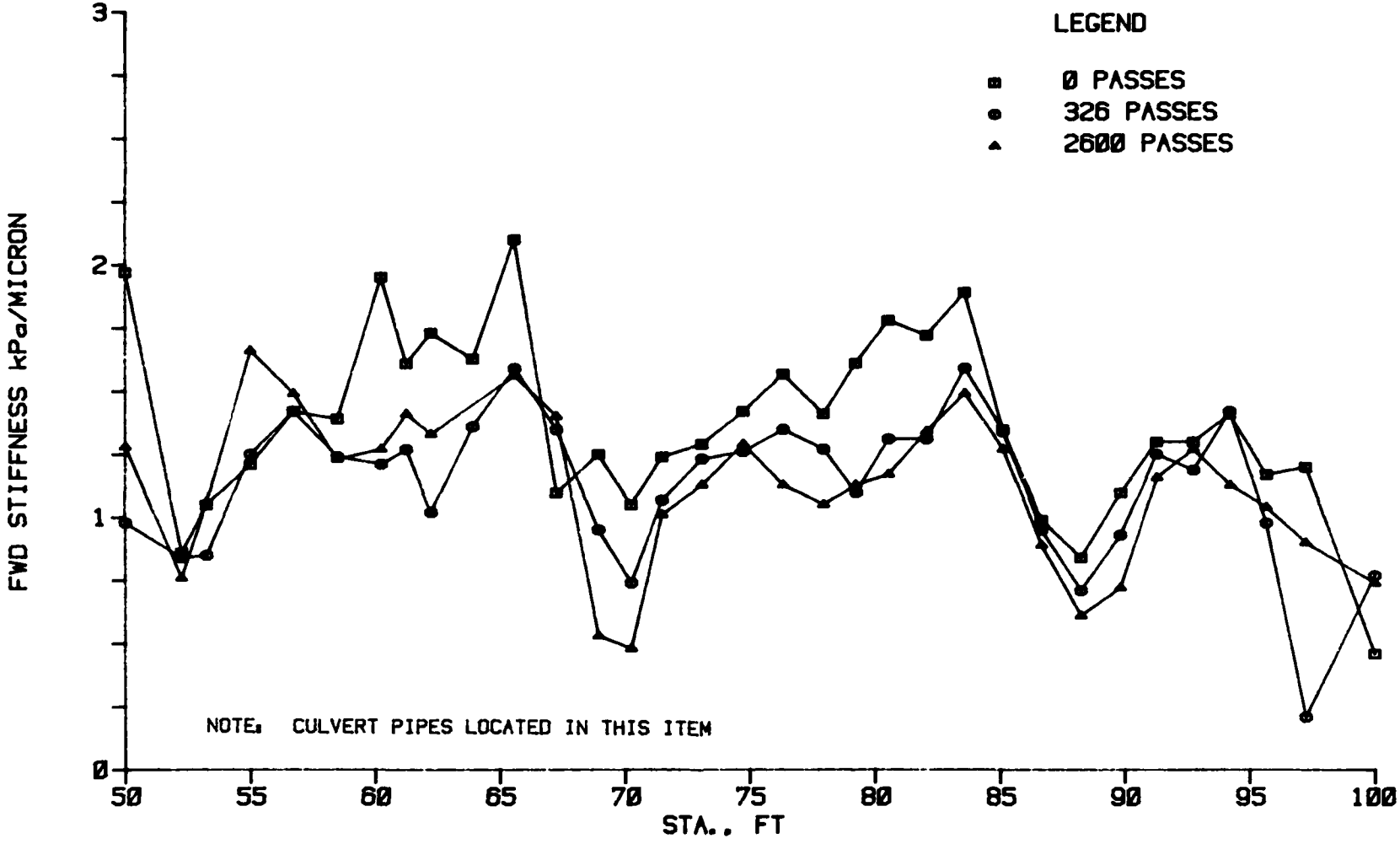

Figure 55. Nondestructive test results during traffic, Falling Weight Deflectometer (lane 1, Item 2)

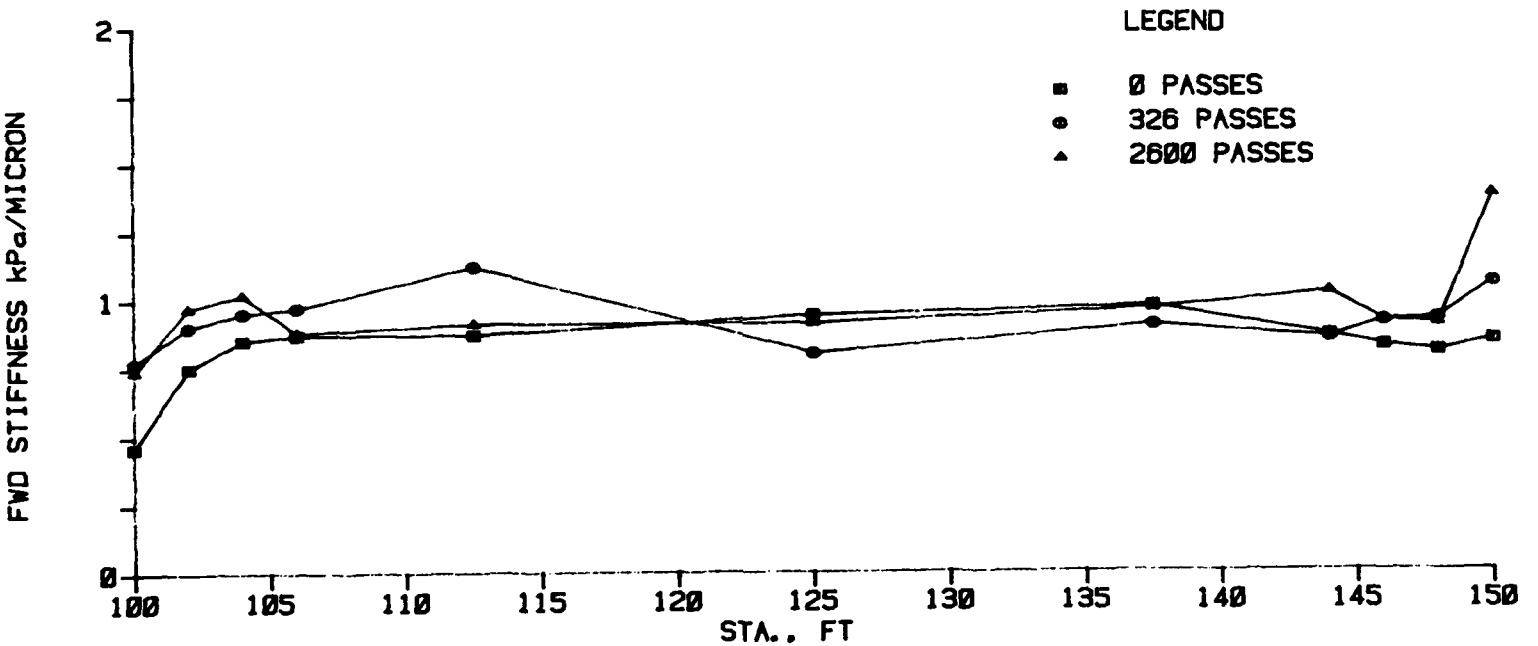

Figure 56. Nondestructive test results during traffic, Falling Weight Deflectometer (lane 1, Item 3)

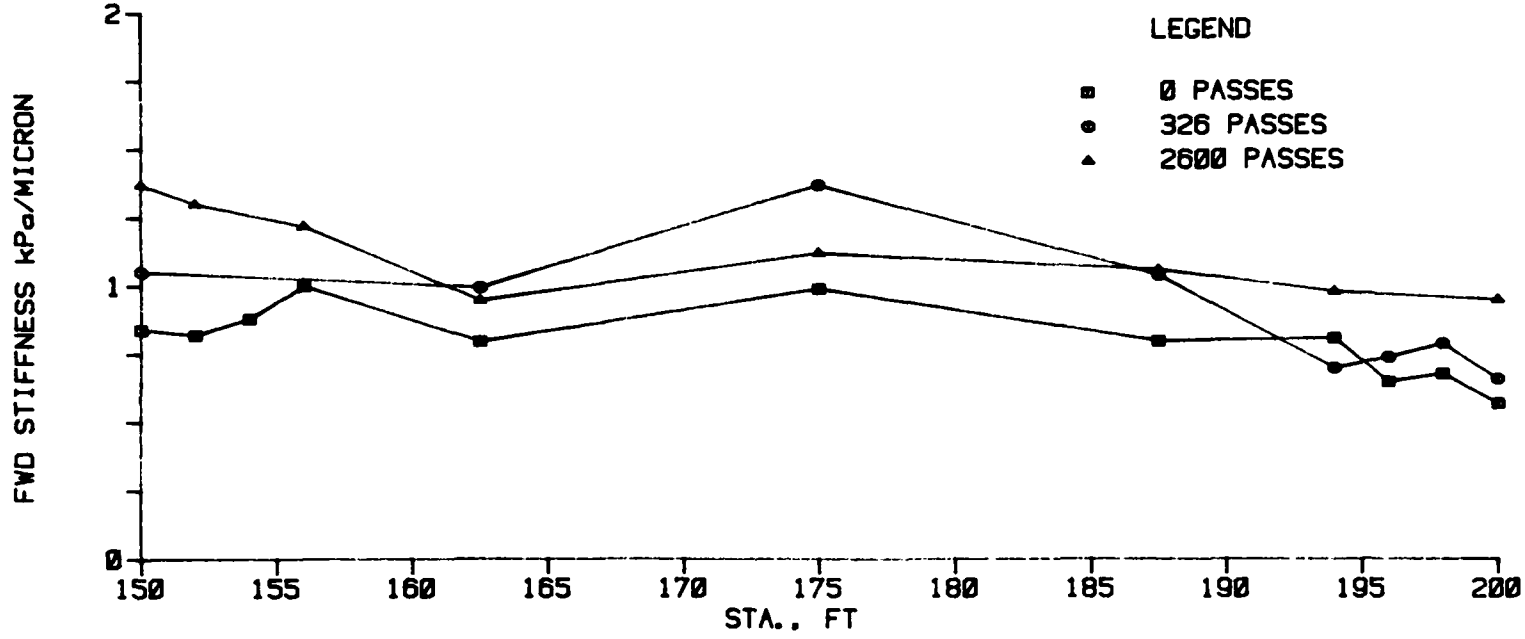

Figure 57. Nondestructive test results during traffic, Falling Weight Deflectometer (lane 1, Item 4)

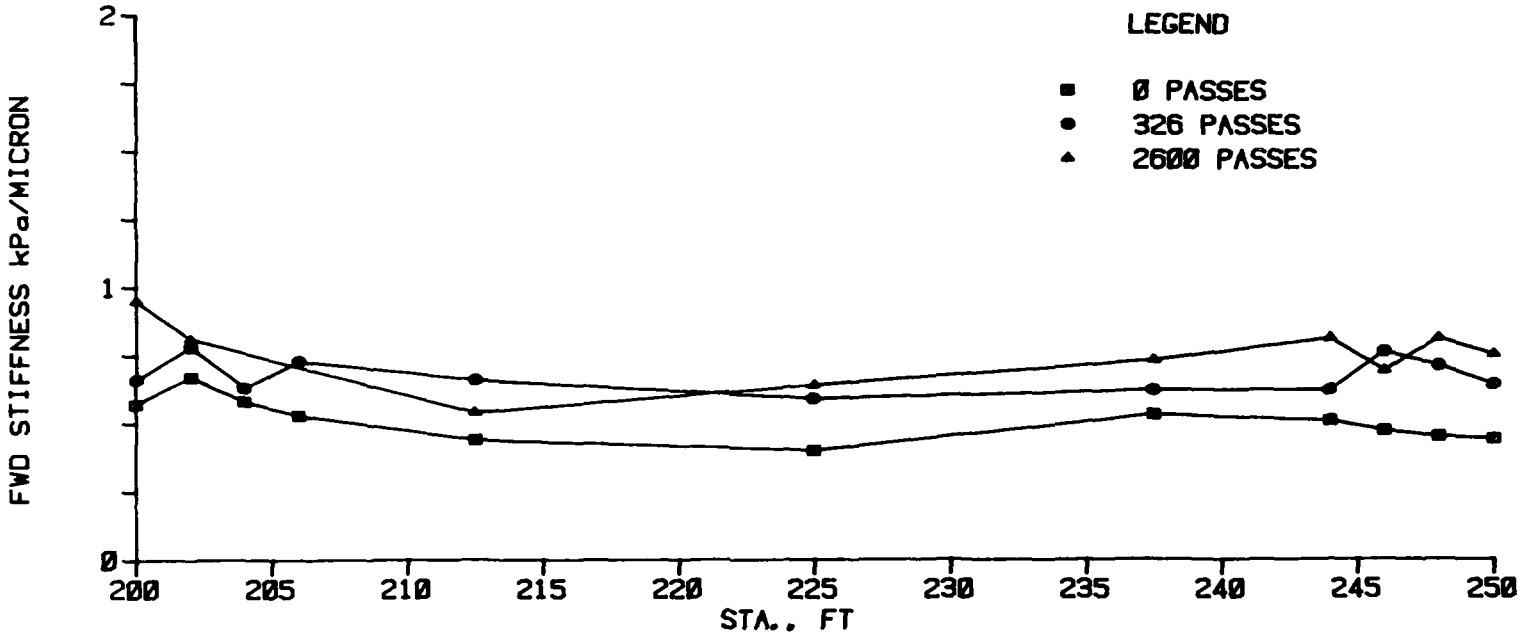

Figure 58. Nondestructive test results during traffic, Falling Weight Deflectometer (lane 1, Item 5)

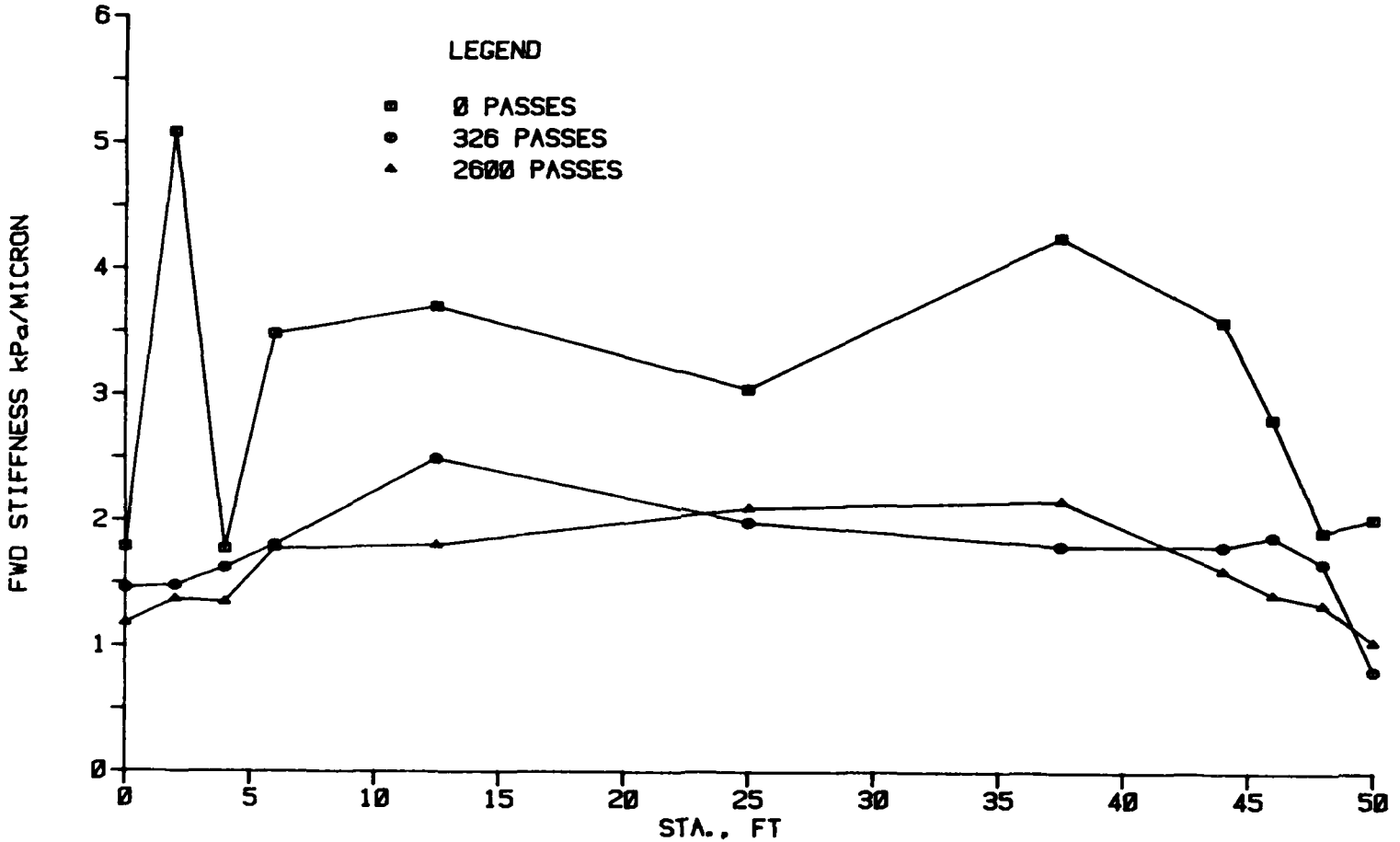

Figure 59. Nondestructive test results during traffic, Falling Weight Deflectometer (lane 2, Item 1)

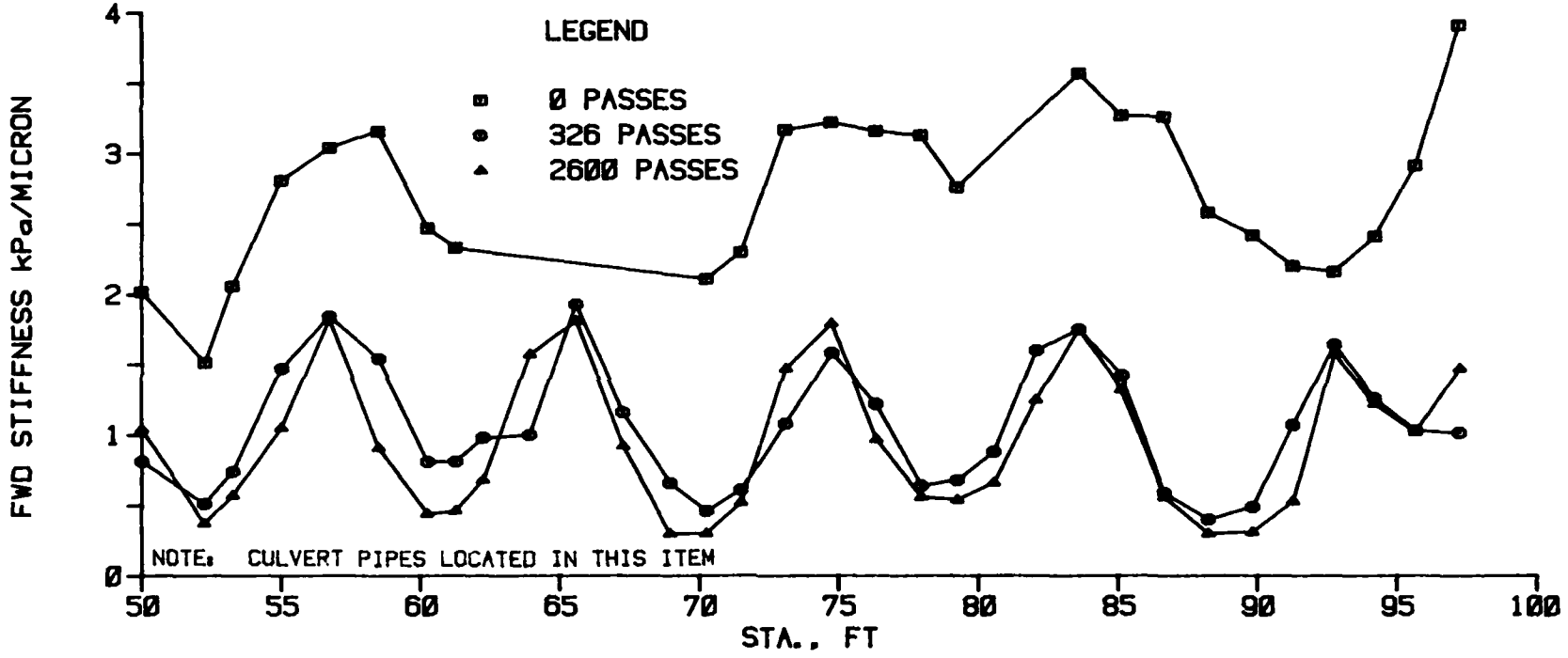

Figure 60. Nondestructive test results during traffic, Falling Weight Deflectometer (lane 2, Item 2)

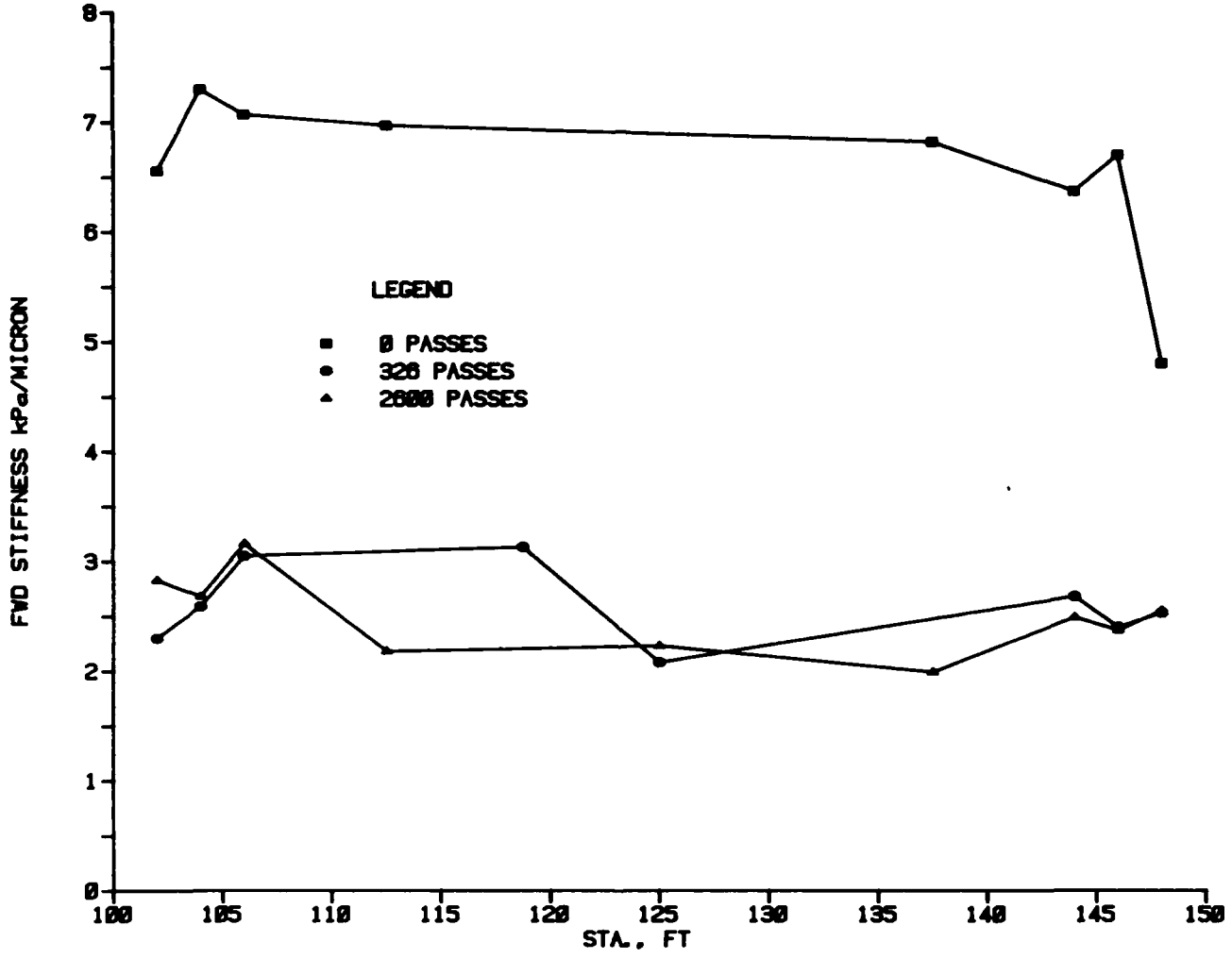

Figure 61. Nondestructive test results during traffic, Falling Weight Deflectometer (lane 2, Item 3)

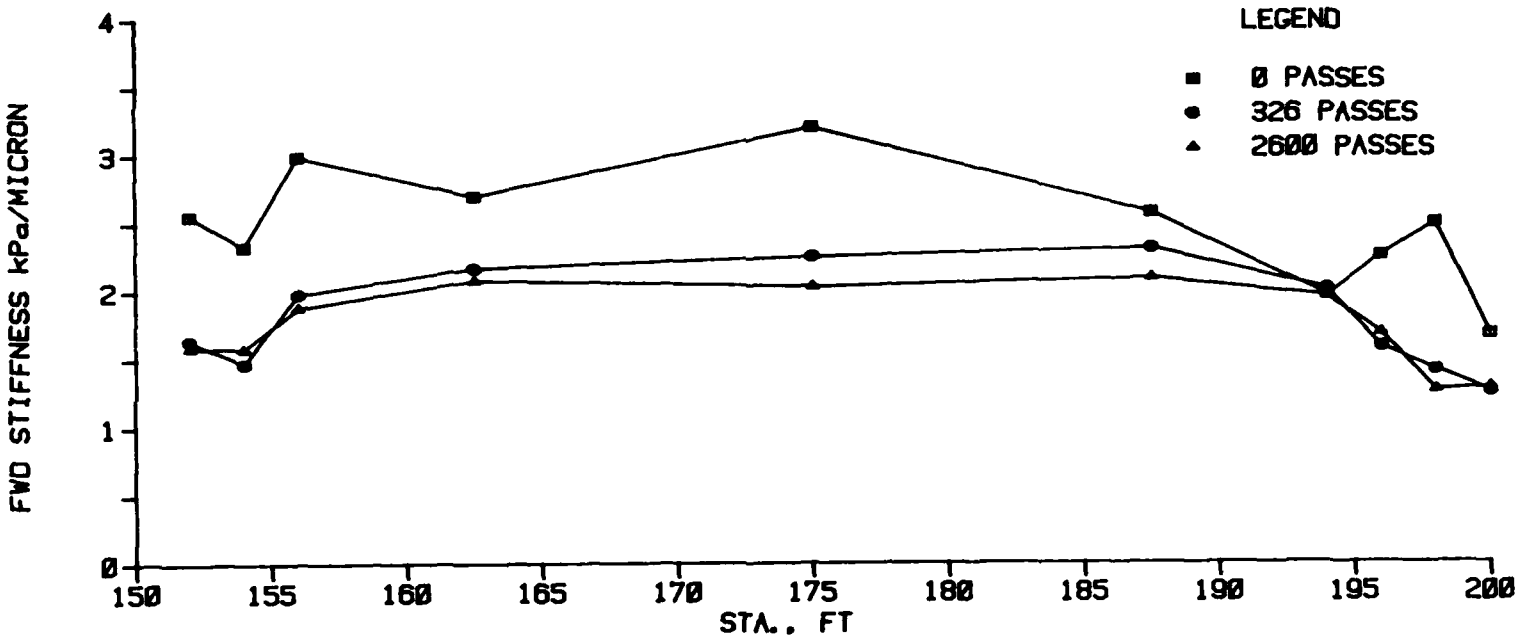

Figure 62. Nondestructive test results during traffic, Falling Weight Deflectometer (lane 2, Item 4)

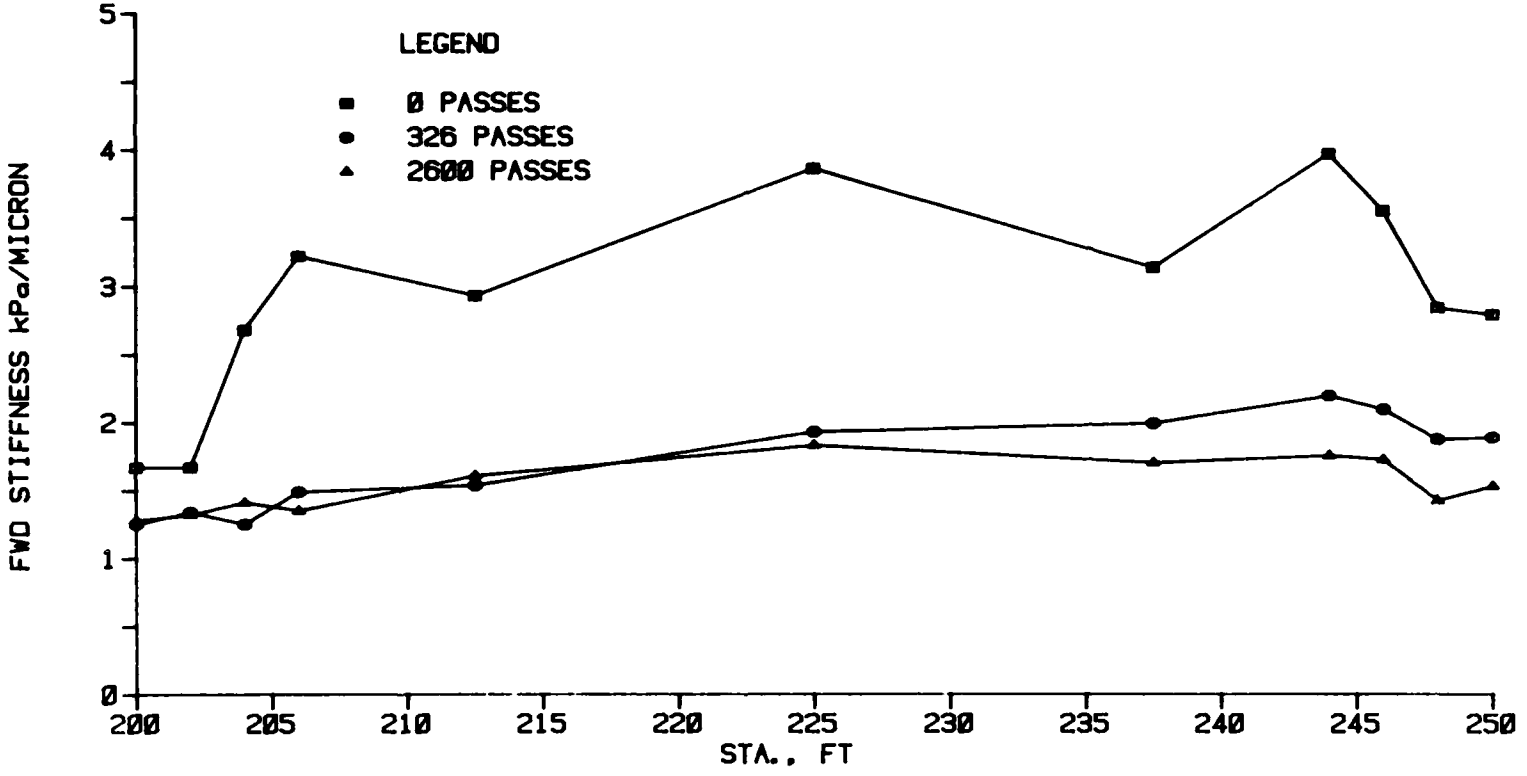

Figure 63. Nondestructive test results during traffic, Falling Weight Deflectometer (lane 2, Item 5)

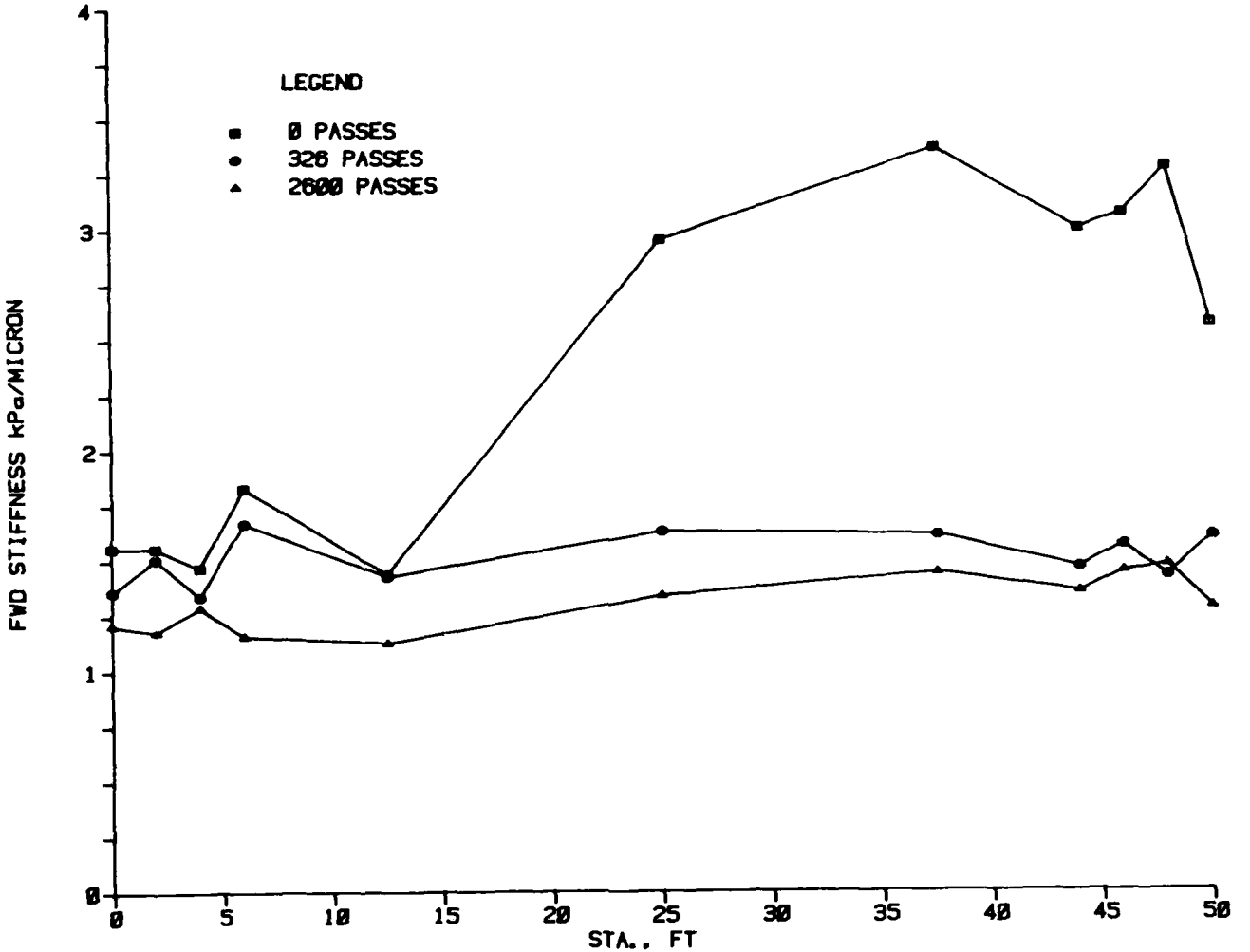

Figure 64. Nondestructive test results during traffic, Falling Weight Deflectometer (lane 3, Item 1)

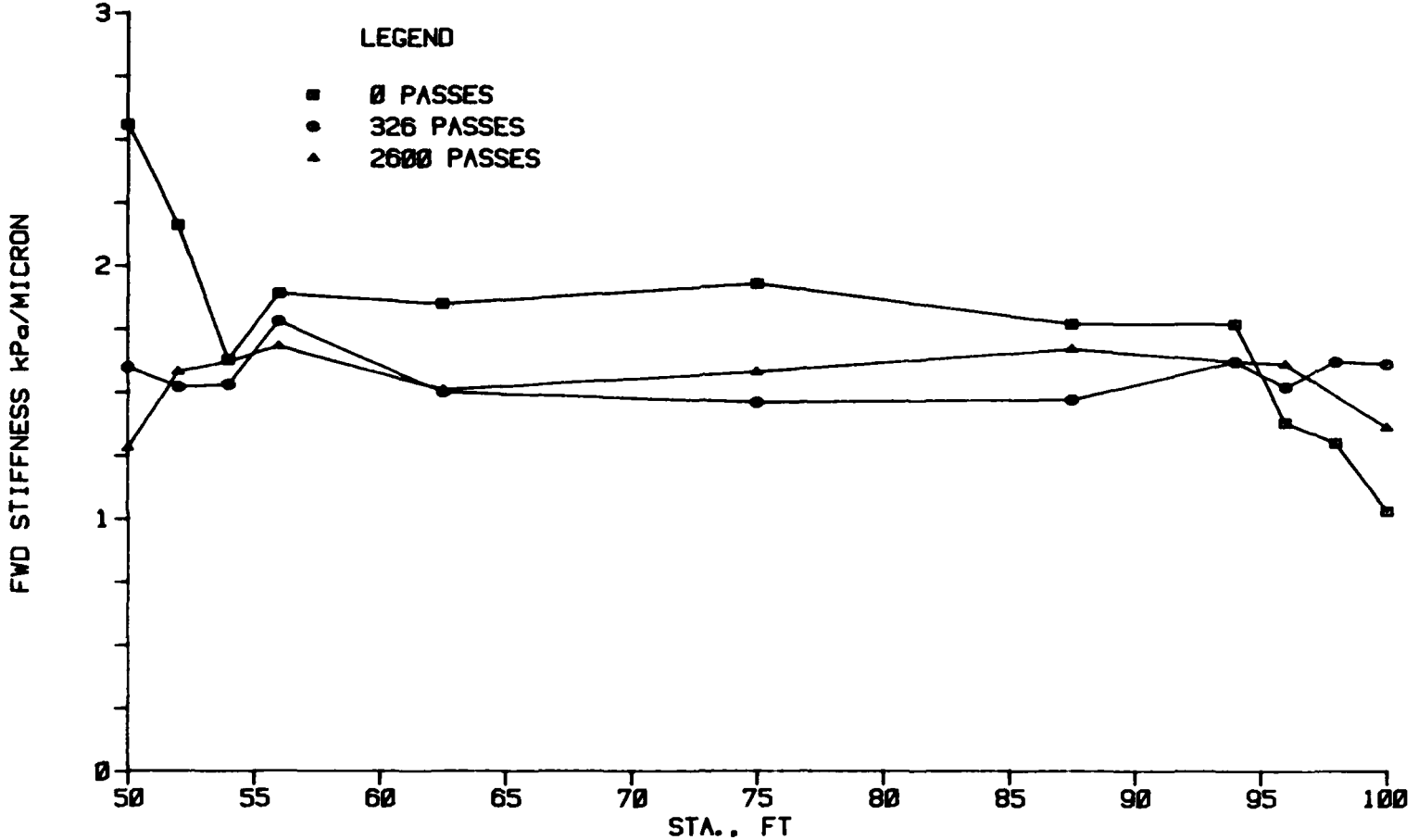

Figure 65. Nondestructive test results during traffic, Falling Weight Deflectometer (lane 3, Item 2)

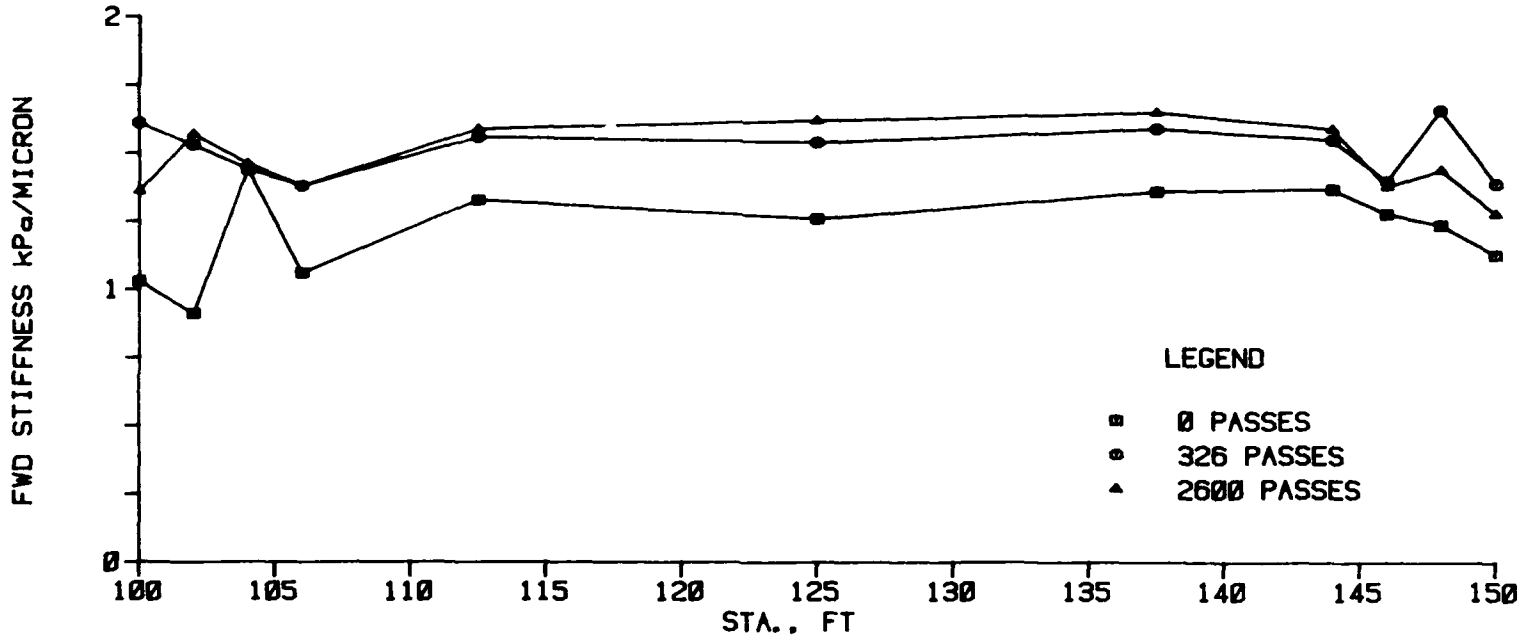

Figure 66. Nondestructive test results during traffic, Falling Weight Deflectometer (lane 3, Item 3)

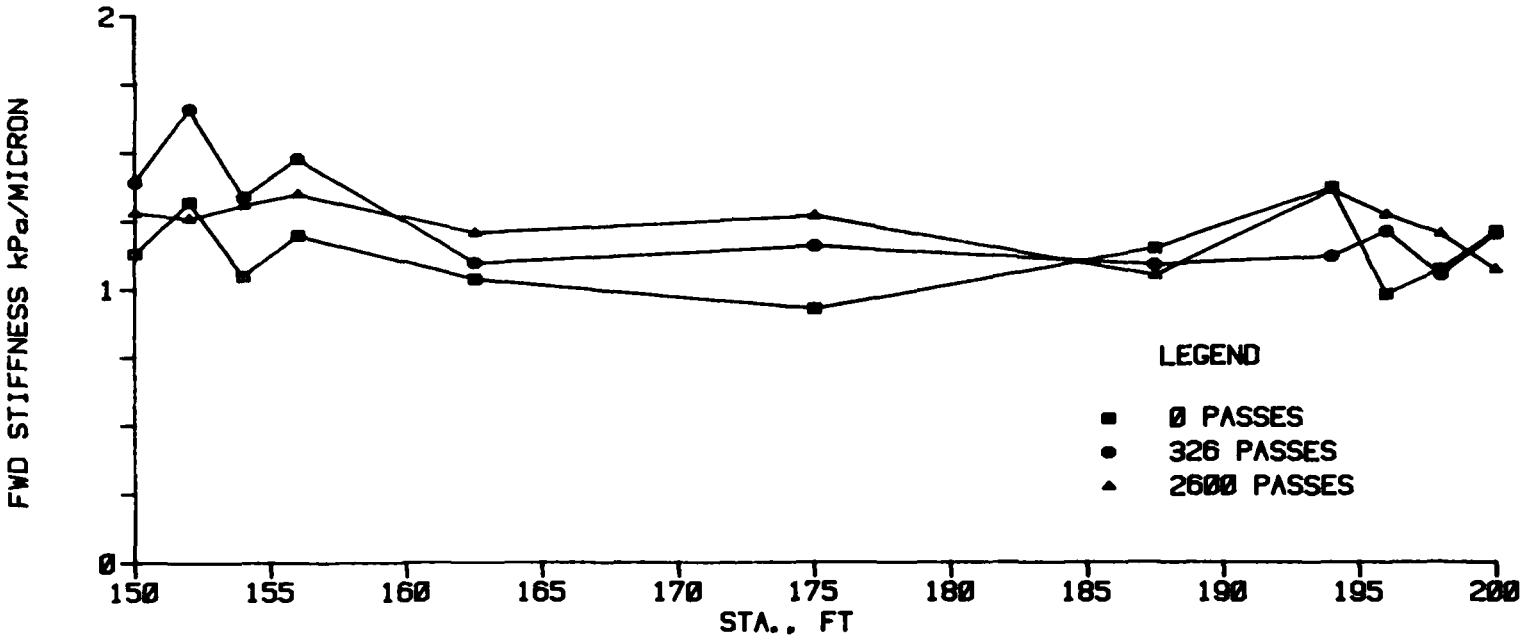

Figure 67. Nondestructive test results during traffic, Falling Weight Deflectometer (lane 3, Item 4)

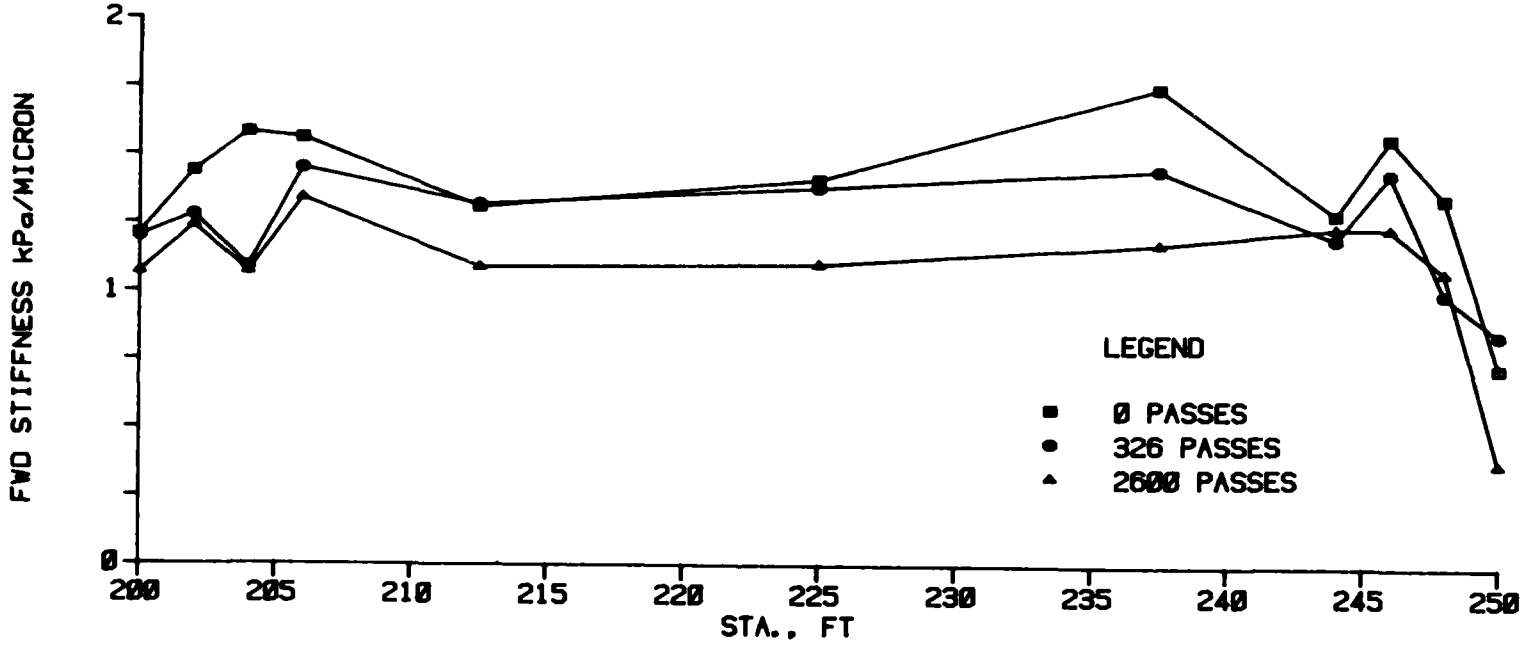

Figure 68. Nondestructive test results during traffic, Falling Weight Deflectometer (lane 3, Item 5)

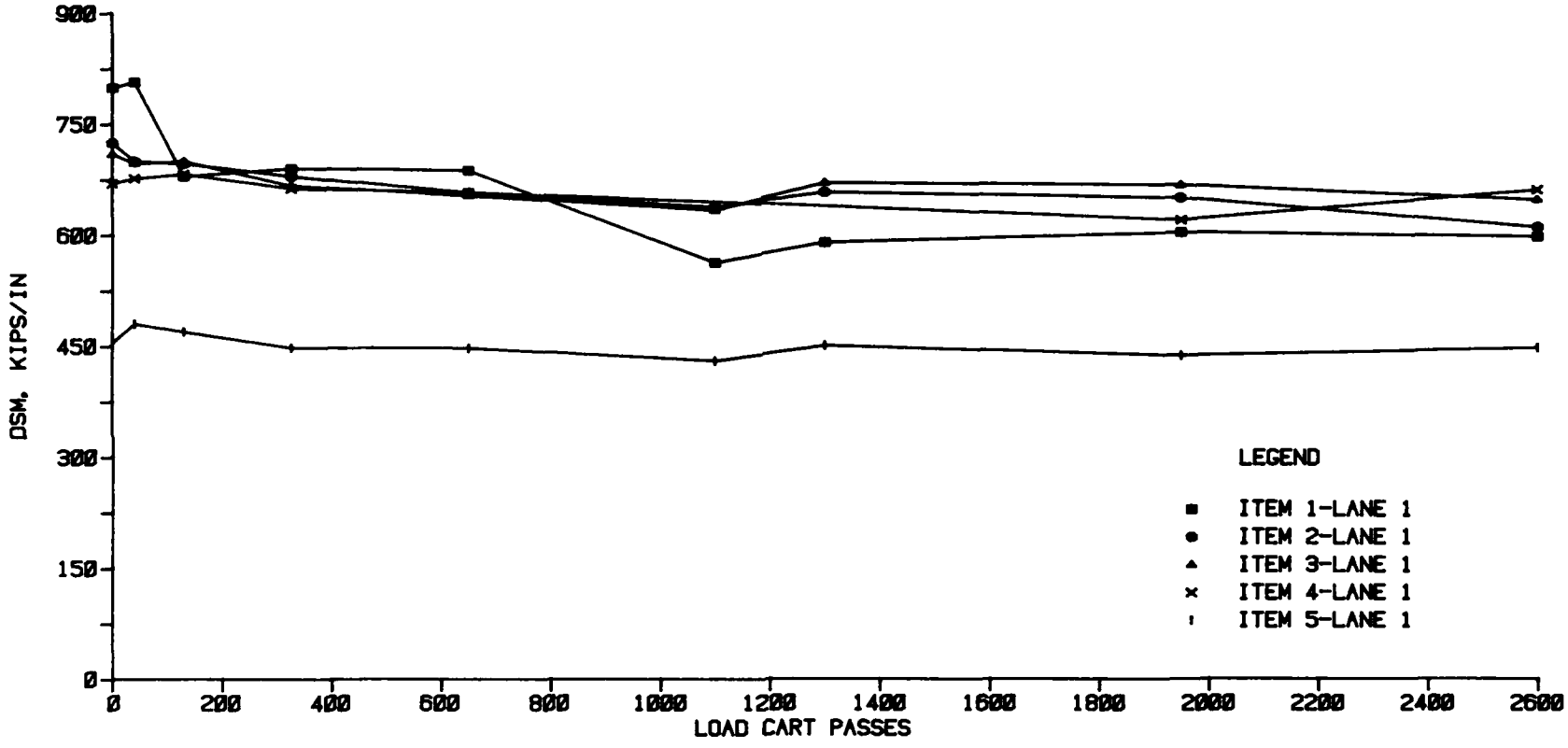

Figure 69. 16-kip DSM versus load cart passes (lane 1)

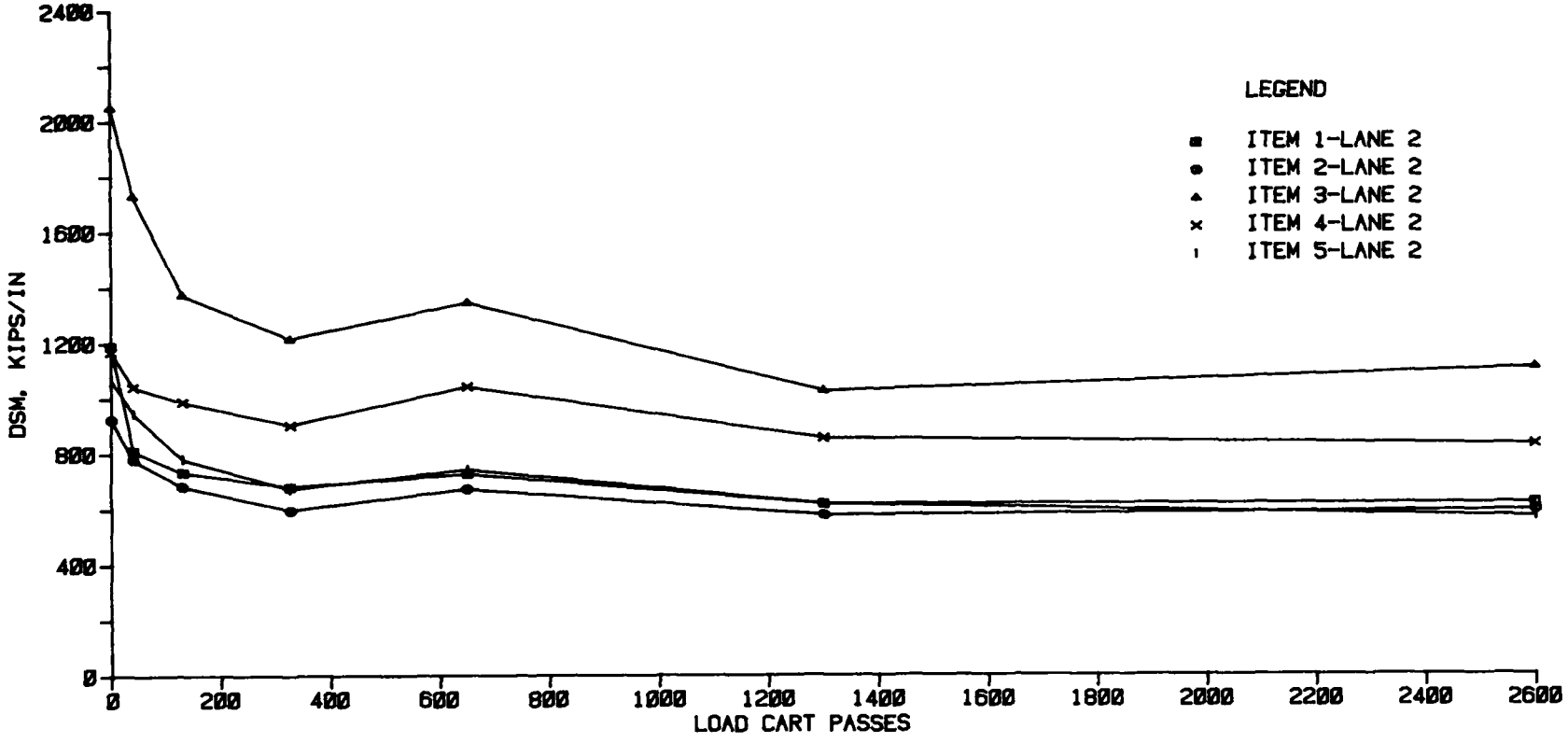

Figure 70. 16-kip DSM versus load cart passes (lane 2)

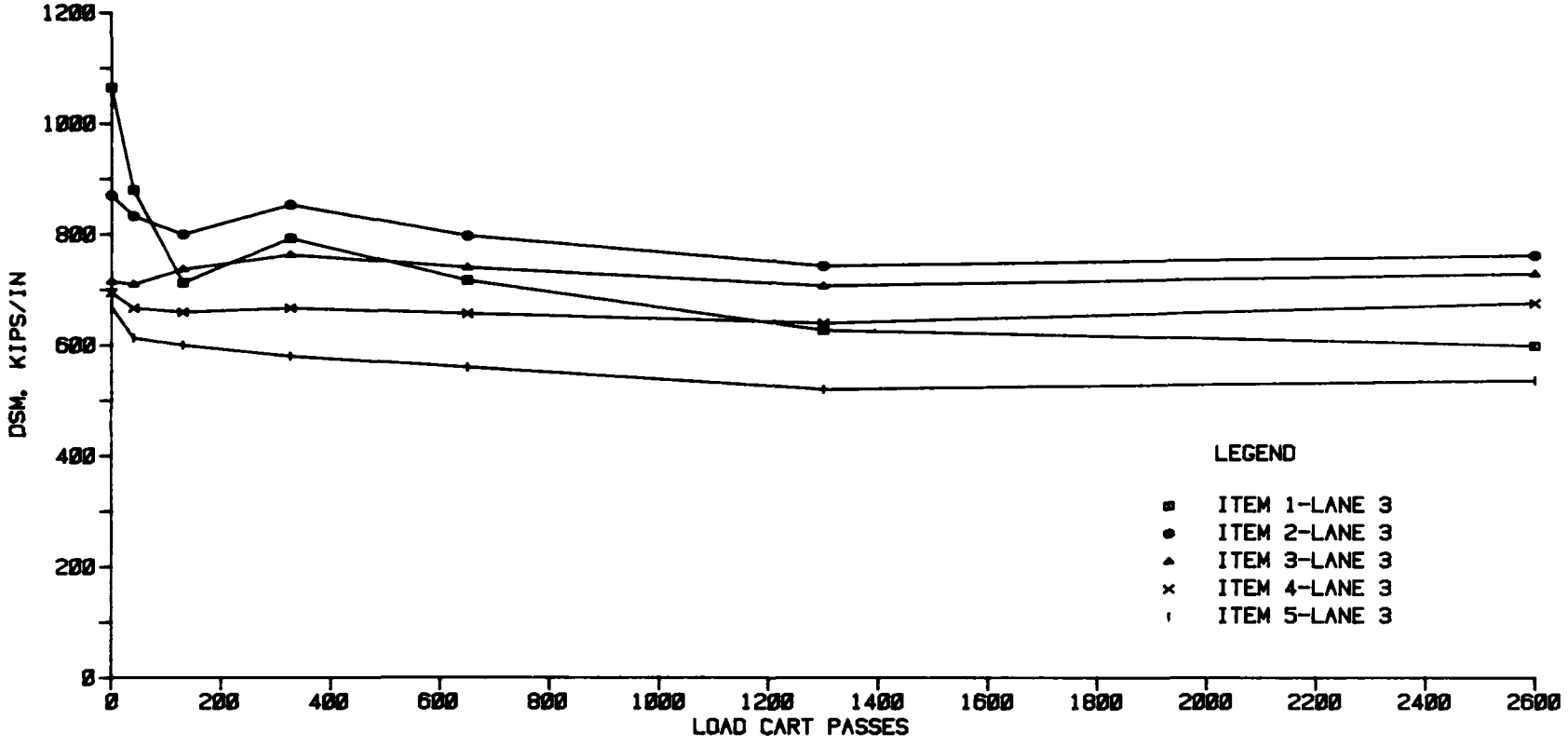

Figure 71. 16-kip DSM versus load cart passes (lane 3)

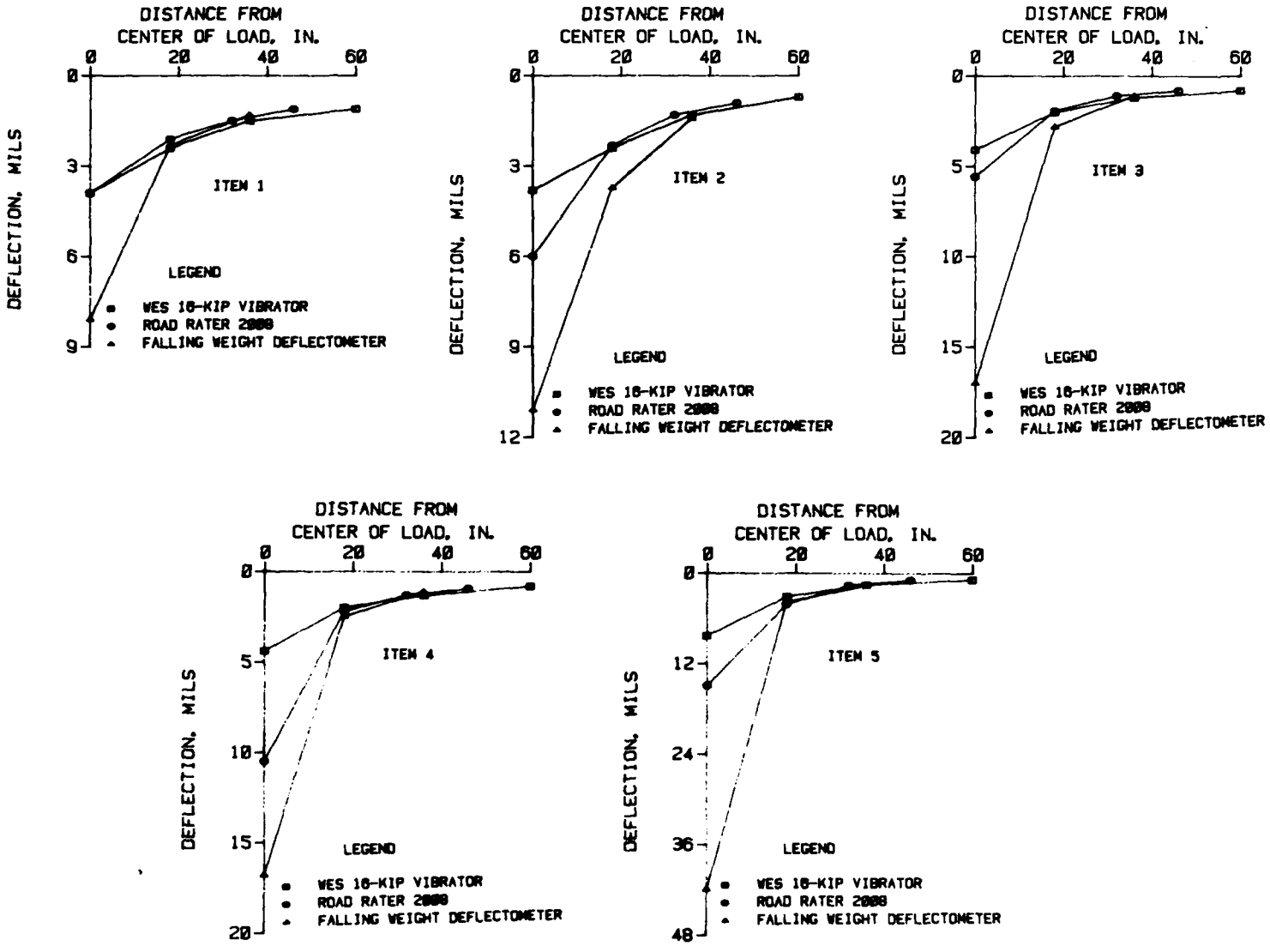

Figure 72. NDT deflection basins for lane 1 (just prior to traffic tests) normalized to a 5,000-lb force level

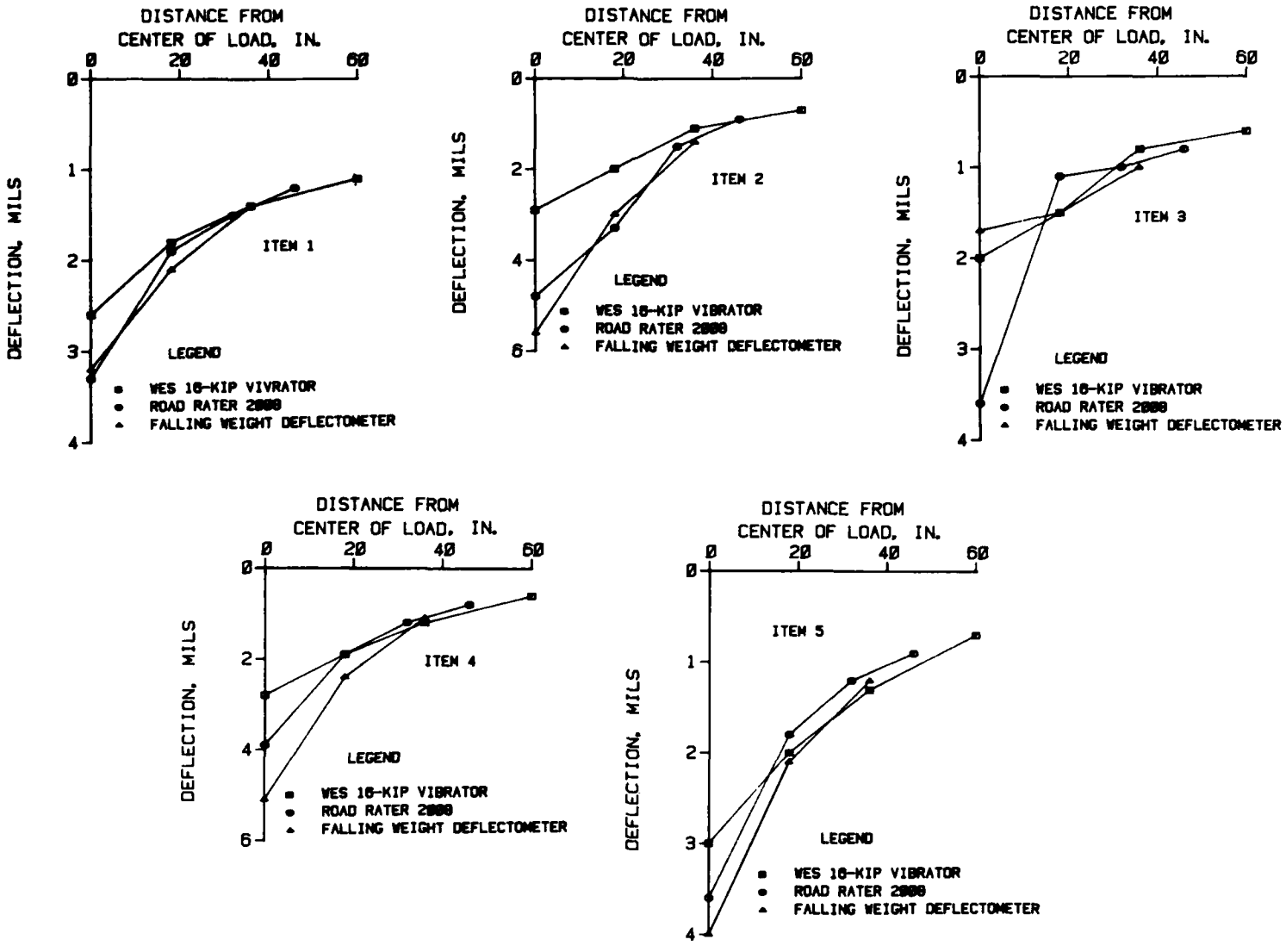

Figure 73. NDT deflection basins for lane 2 (just prior to traffic tests) normalized to a 5,000-lb force level

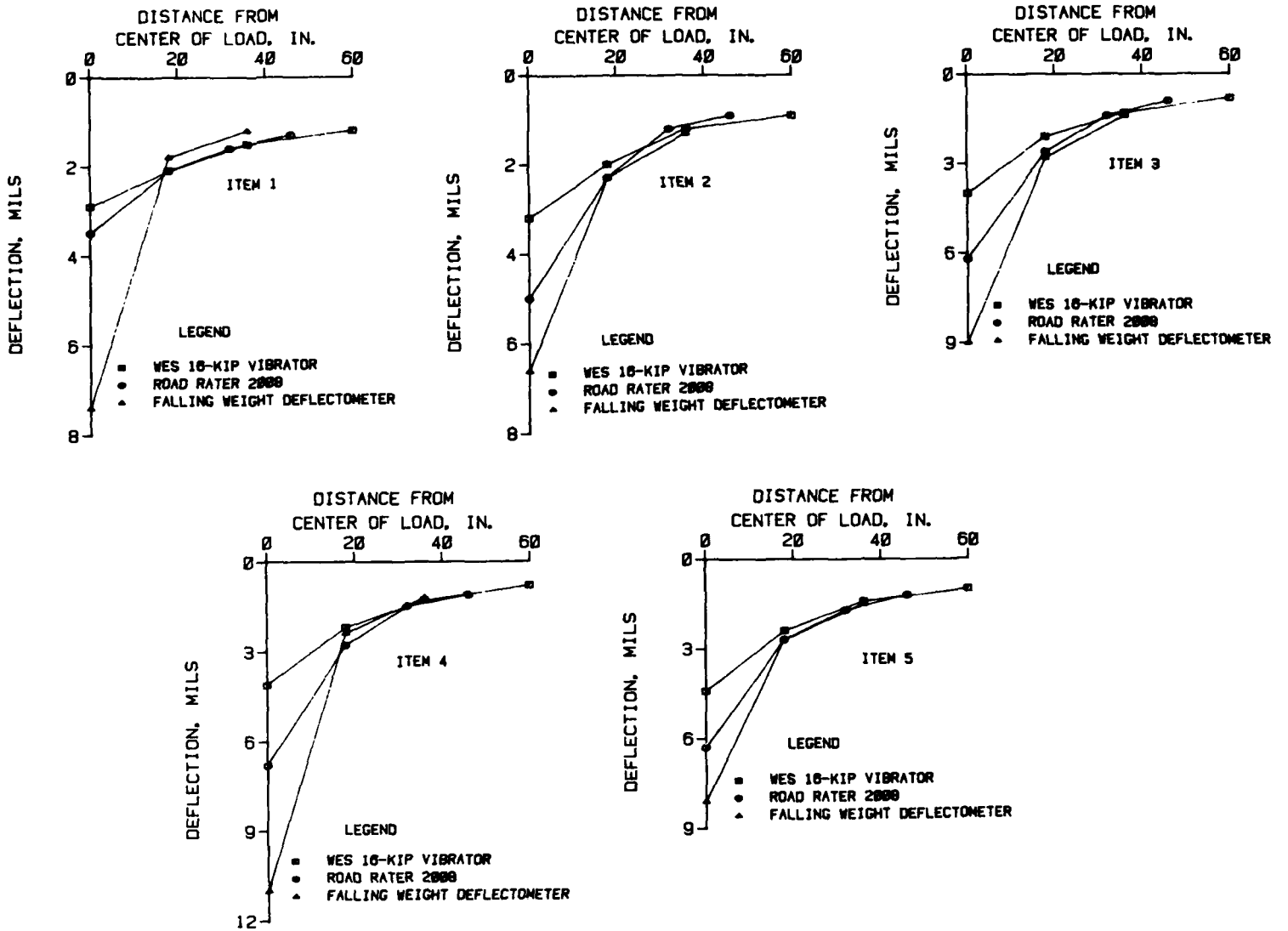

Figure 74. NDT deflection basins for lane 3 (just prior to traffic tests) normalized to a 5,000-lb force level

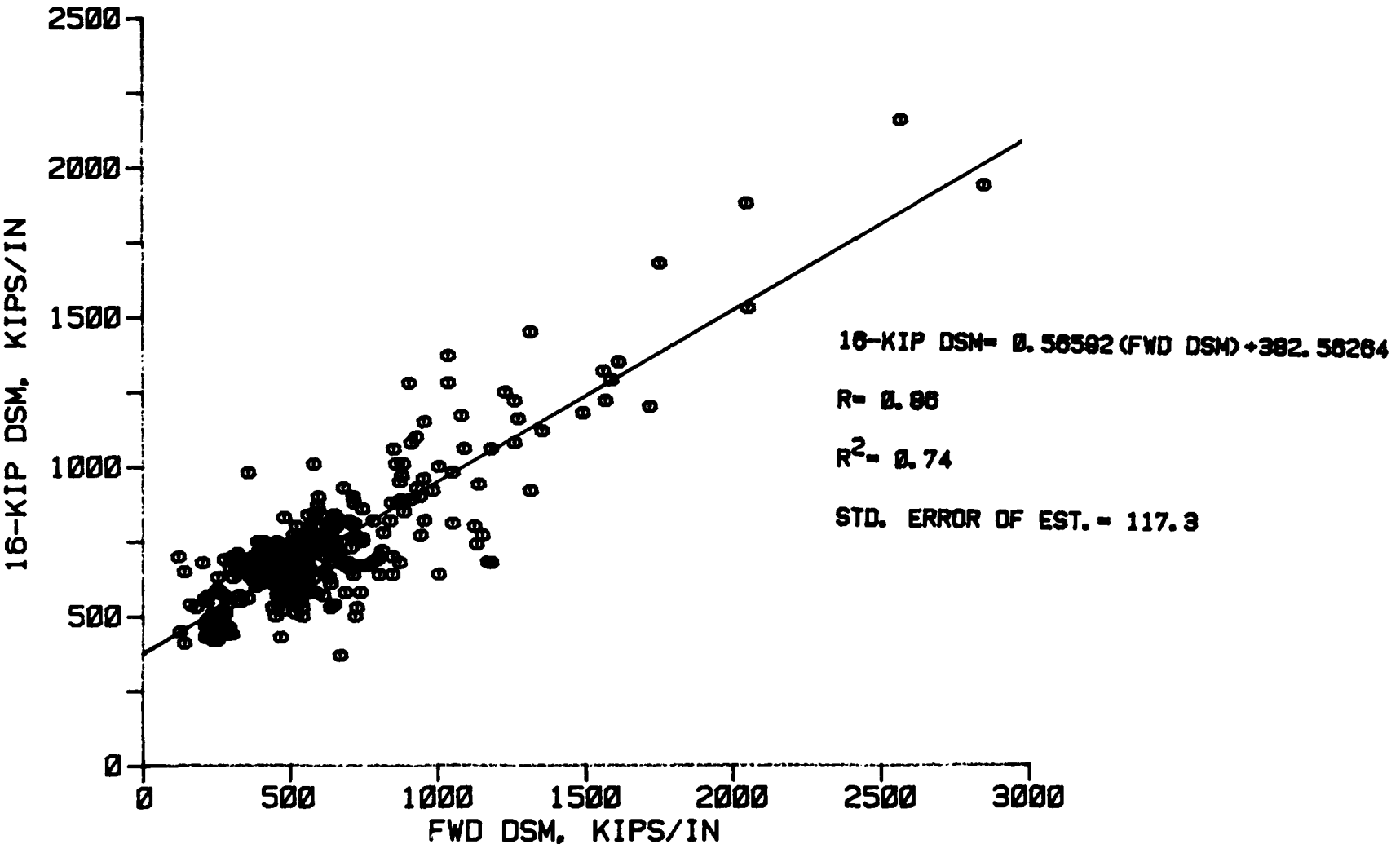

Figure 75. Comparison of 16-kip and falling weight deflectometer DSM's obtained during construction and traffic testing

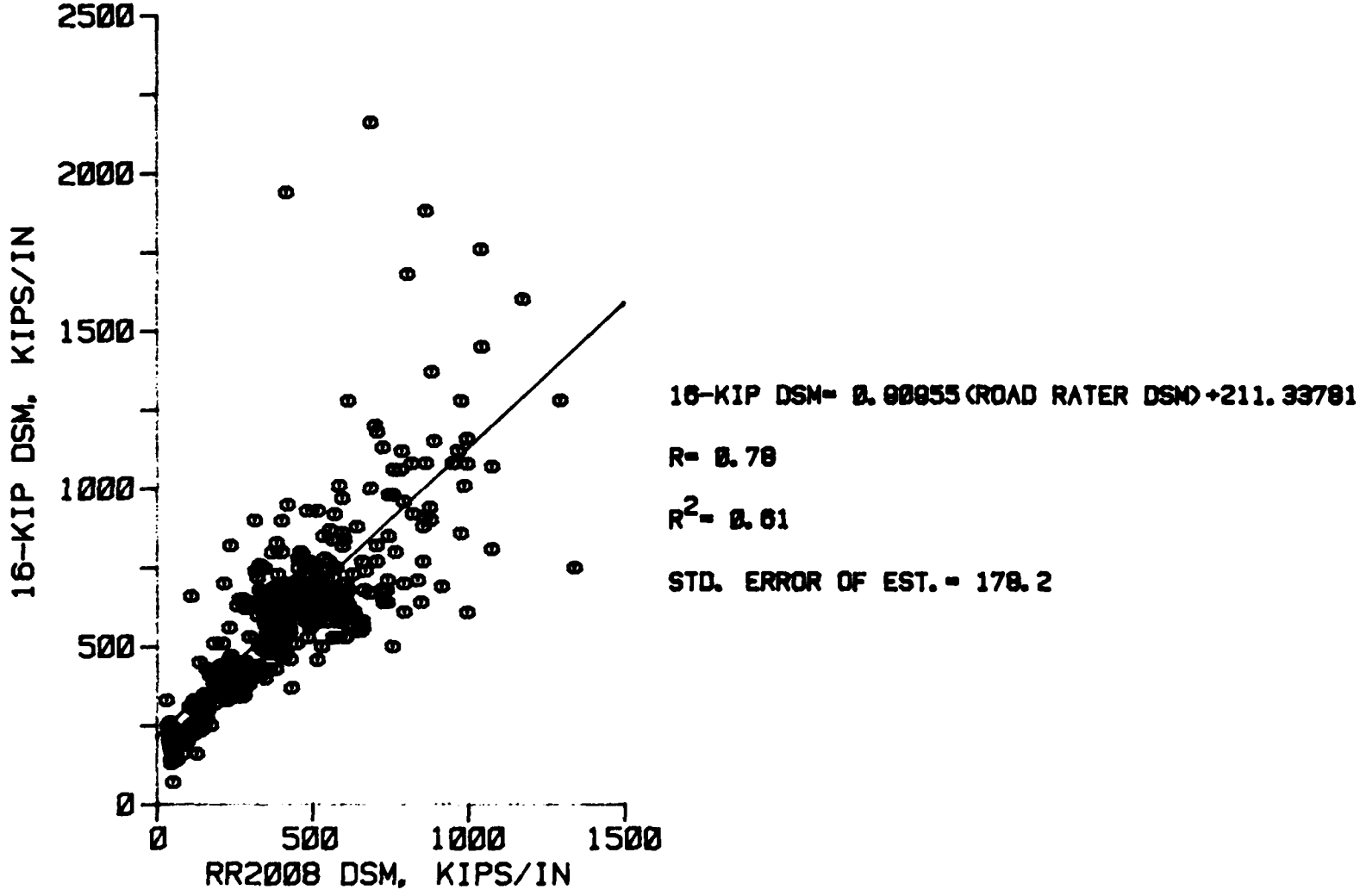

Figure 76. Comparison of 16-kip and road rater DSM's obtained during construction and traffic testing

END

FILMED

6-86

DTIC